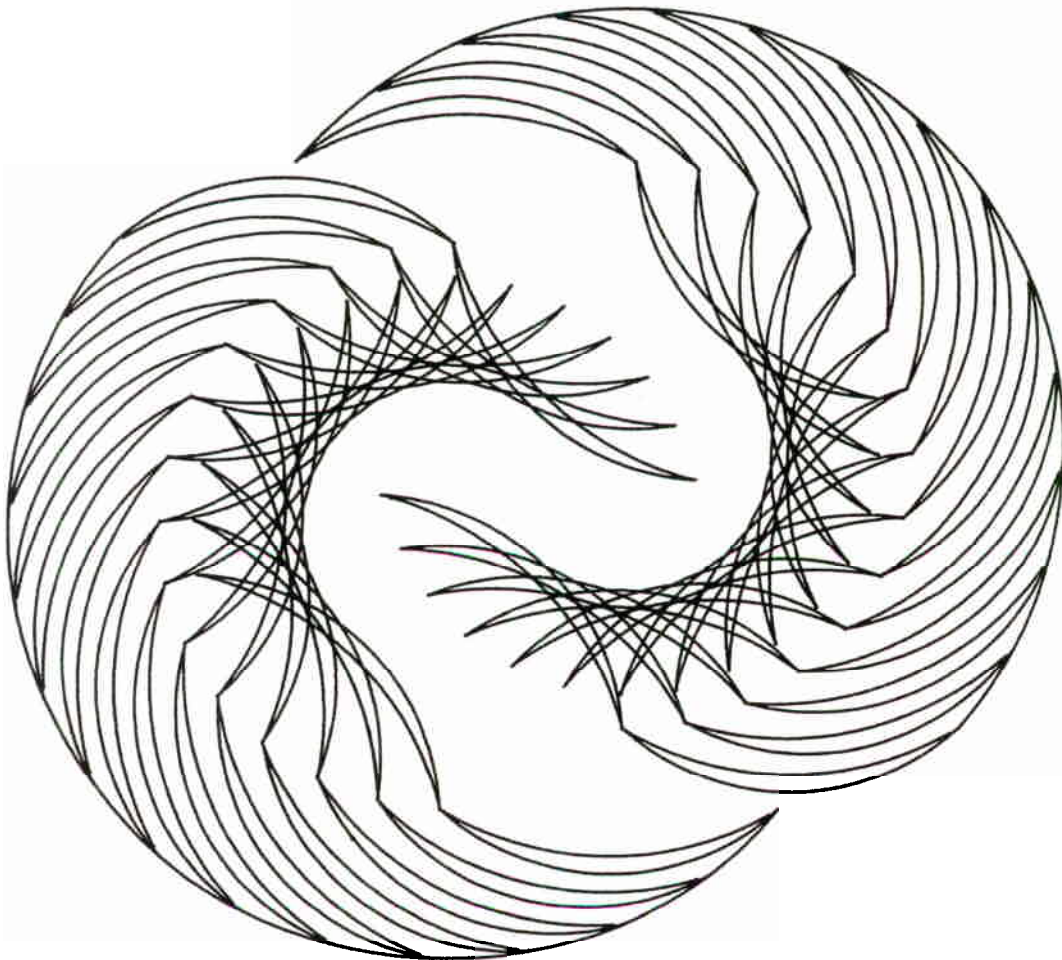


Session II

Targetry and Production

Moderators: R.J. Nickles, T.J. Ruth



The Wright brothers spent less than one thousand dollars to build their first airplane.

Session 2: Targetry and Production
Co-chairs: R.J. Nickles and T.J. Ruth

Introduction

The papers selected for oral presentation in this session were chosen to enhance discussion on topics that have a potential for a very broad impact on how radioisotopes are produced both in terms of efficiency and purity. Thus the topics related to beam dynamics, surface phenomenon, void formation and cryogenic targets were opened to presentation and discussion.

The papers dealing with the loss of production capacity that has been observed over the years and attributed to the effects of beam interaction with the target material. In the case of gaseous material it has long been felt that the dominant issue was thermal effects due to beam heating. The collaboration between the groups at Turku and Debrecen provided further evidence to this thought with their study of the beam dynamics within a gas target. Researchers at CTI presented a paper describing the how voids in liquid targets could be explained on the basis of charge build-up. In using a model based on an electrochemical cell a number of assumptions were called into question by the workshop participants. While the approach did not generate a ground swell of acceptance it did provide a format for clarifying what we do know about the hot atom interactions and dissipation of energy (heat and otherwise) which may result in a better understanding of the problem.

The papers on the compositions of surfaces in the materials from which we construct our targets illustrated the complexity of the problem at the microscopic level and sub-micromolar concentrations.

While more effort has been expended at extracting quantitative information to try and establish a scientific basis for how to best approach the production of radionuclides, the problems in interpreting these results remain. However, it is clear that the research presented here provides a basis upon which to design future experiments that will help solve the problems we encounter daily.

Study of Static and Dynamic Effects in Gas Targets

F. Tárkányi, S. Takács, S-J. Heselius*, O. Solin* and J. Bergman*

Institute of Nuclear Research of the Hungarian Academy of Sciences, Pf. 51, H-4001 Debrecen, Hungary

** Accelerator Laboratory, Åbo Akademi, SF-20500 Turku, Finland*

Introduction

Gas targets play key roles in different fields of science and technology. The penetration of energetic charged particles into high pressure gas targets has been studied by several groups to optimize the radionuclide and neutron production using thin and thick gas targets, as well as in the field of investigation of charged particles and neutron induced nuclear reactions (reviews: Wieland, 1984; Heselius, 1986; Solin, 1988). To study the interaction of charged particles with gaseous material several experimental methods have been developed on the basis of measurement of the activity of the produced radioisotopes, secondary neutrons, heat, charge, emitted light, change of density, temperature, refractory indexes etc. The obtained results were mainly interpreted qualitatively using different phenomenological models. Only a few groups made systematic study of the interaction of charged particle beams and gas targets and still many questions remain open.

This work was initiated by the optical study of gas targets made at Åbo Akademi, Turku, Finland, and by the experimental results of excitation functions and production yields obtained in Debrecen, using gas targets at horizontal and vertical irradiation arrangement. The high speed video technique and charge distribution measurement allowed us to study both the transient effects of the beam penetration into gaseous targets, and the final equilibrium states of the beam in the targets at horizontal and vertical beam lines. An effort was made to explain the results phenomenologically.

Shape of the beam in equilibrium state at horizontal and vertical irradiation positions

Heselius and his coworkers reported, that at high beam current density the shape of the beam appeared to be asymmetric in horizontal irradiation position due to an upward transport of the heated gas. The upward flow of the heated gas was checked also by measuring the activity distribution of the produced radioisotope on the inner wall of the target chamber [Solin, 1984].

In the present work we measured simultaneously with the emitted light the charge along the beam axes and integrated it at a given position at different angles to confirm the observed asymmetry of the horizontal beam. A target chamber equipped with a plexiglass window for optical study and with an isolated electrode for charge collection (see Fig. 1) was used. The charge was collected at four different angles in a plane perpendicular to the beam direction.

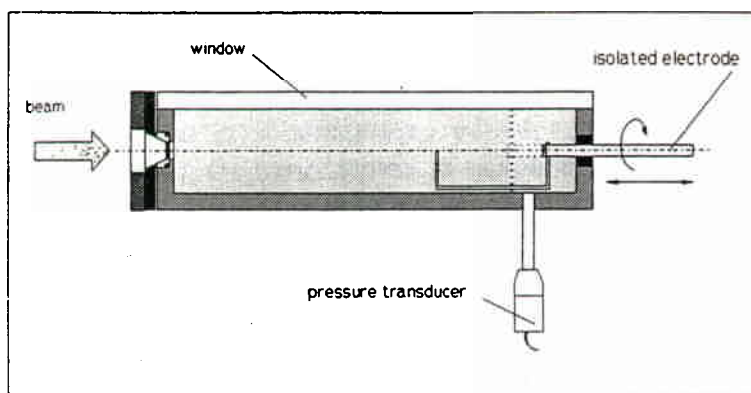


Figure 1 A target chamber equipped with plexiglass window for optical study and isolated electrodes for charge collection.

The integrated charge was measured both on the electrode and on the isolated target chamber. The electrode was rotated to different angles and different axial positions by remote controlled stepping motor and micropositioners. The measured charge distribution was found to be asymmetric in good agreement with the optical studies (see Fig. 2).

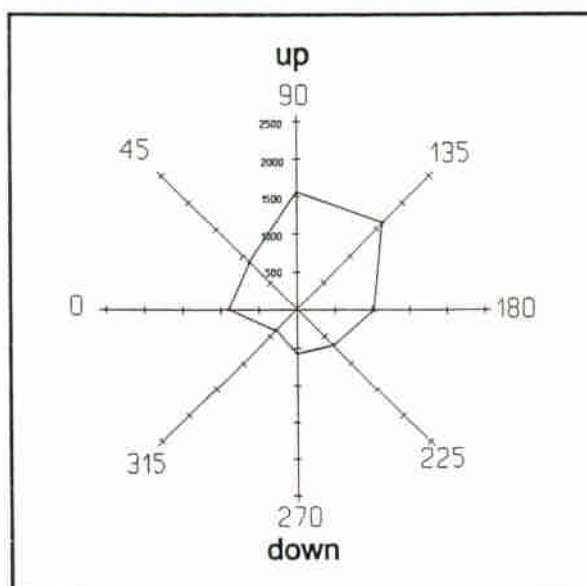


Figure 2. Charge distribution of a horizontal beam measured in a plane perpendicular to the beam axes.

We have investigated the effect of upward mass transport at a vertical irradiation position for the first time. The sketch of the vertical beam line in Debrecen is shown in Figure 3. The view of light emission following the interaction of a proton beam ($E_p=8$ MeV, $I_p=5.8$ μ A, $d=6$ mm in diameter) with a gaseous target filled with 7 bar initial pressure of Ar gas is shown in Figure

3. in comparison with the picture obtained at horizontal irradiation position under the same circumstances.

The symmetric distribution of the emitted light at vertical irradiation position is clearly seen in Figure 3. in accordance with the expectation, i. e. due to symmetric upward mass transport and symmetric density reduction in vertical irradiation position. The evolution of the observed equilibrium shapes in both irradiation arrangements is discussed in more detail below.

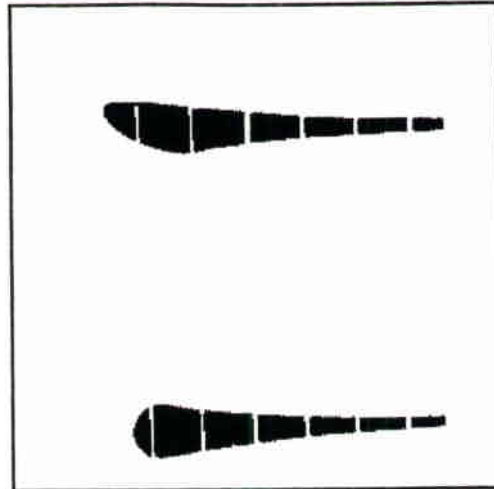


Figure 3. The view of horizontal and vertical beams of $E_p=8$ MeV, $I_p=5.8$ μ A of protons in 7 bar initial pressure of Ar.

Investigation of dynamic effects

It was noticed that the shape of the beam on the photograph taken during the very first impact of the beam was a little bit different from the shape of the beam on the photograph taken several seconds later. Taking into consideration that all the earlier investigations deal exclusively with the description of the steady state, i.e. after the equilibrium has been reached, we decided to study the transient effect in more details.

The transient effect of the first period of the interaction of charged particle beams with the target gas was investigated both at horizontal and vertical irradiation arrangement. The process was investigated by recording the emitted light with a videocamera. The recorded pictures were digitized and evaluated with commercial image processing programs. The penetration of the beam was followed continuously from the very first impact after opening the beamstop. The beam current and the target pressure were recorded simultaneously. Figures 4 and 5 present the views of light emission for the first 1 sec time period at horizontal and vertical beam arrangements respectively. From the detailed analysis of the records the following conclusion can be drawn.

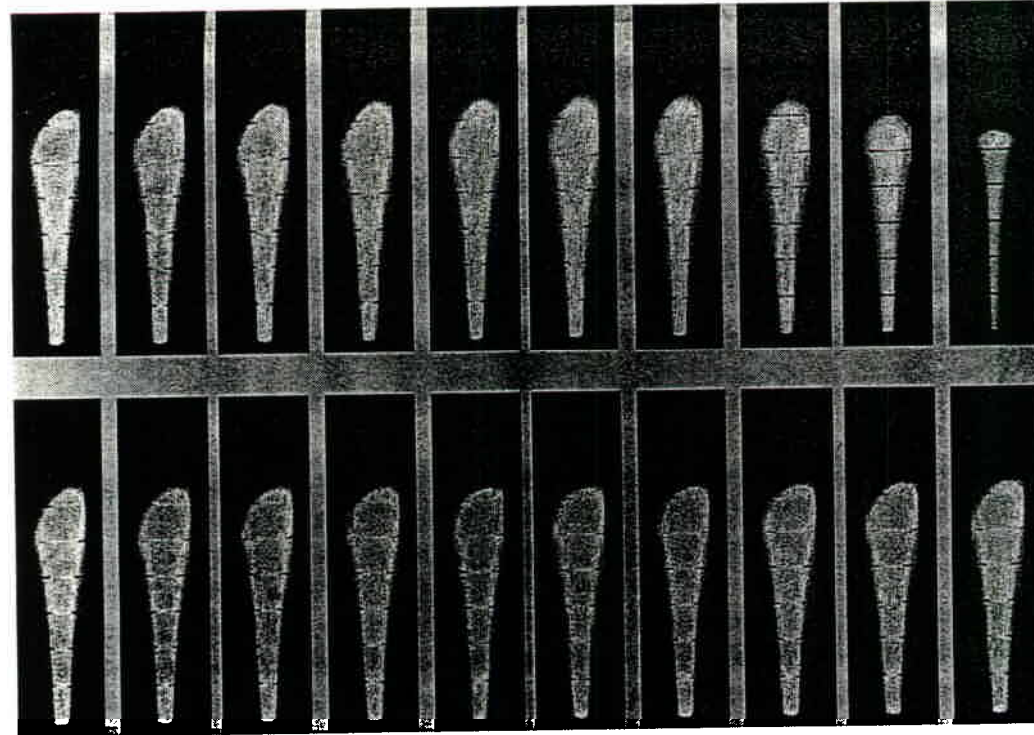


Fig. 4a

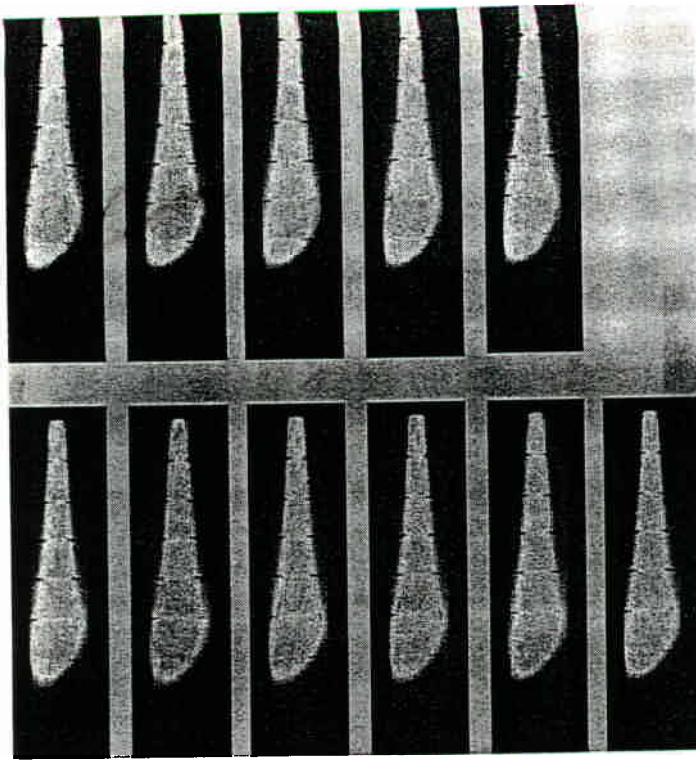


Fig. 4b

The views of light emitted during the first 2 sec. time period at horizontal beam arrangement $\Delta t=1/24$ sec (Fig. 4a) and $\Delta t=1/12$ sec (Fig. 4b).



Fig. 5b

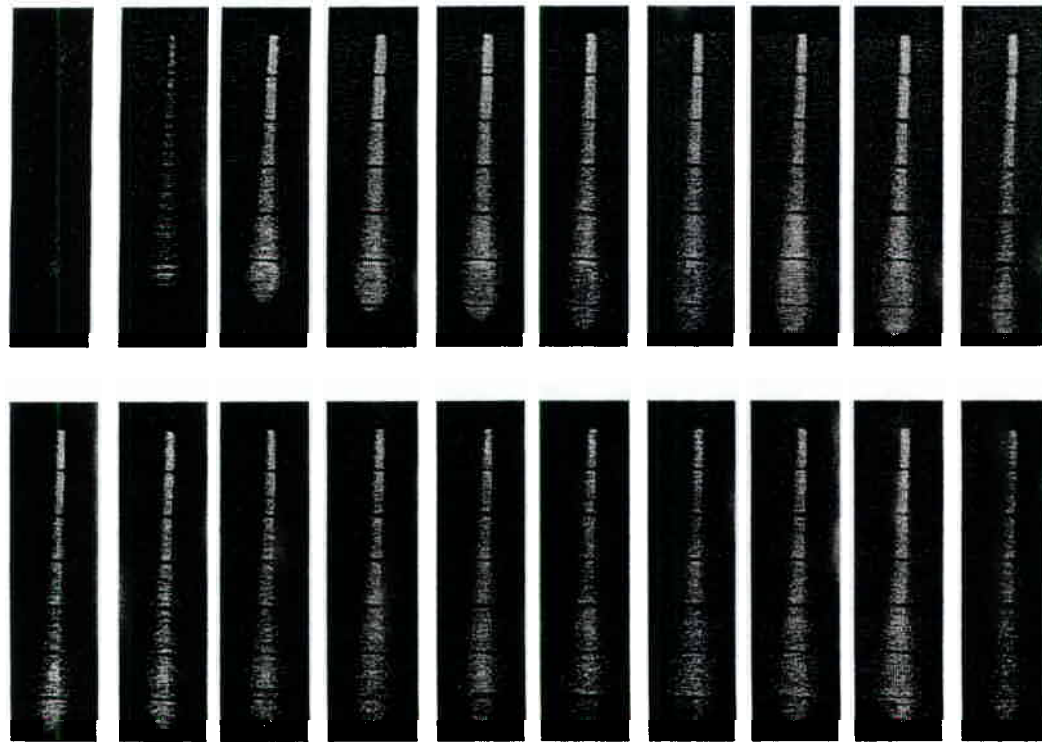


Fig. 5a

The views of light emitted during the first 2 sec. time period at vertical beam arrangement $\Delta t=1/24$ sec (Fig. 5a and Fig. 5b).

- ▶ The beam has a symmetric shape at the very beginning of the interaction and has short range in both irradiation geometry. Then the beam path gradually expands and reaches a maximum. After the maximum has been reached the path of the beam contracts back to a minimum length, which is longer than the absolute minimum at the beginning, then the range rises slowly and reaches an equilibrium state between the maximum and the minimum ranges.
- ▶ Not only the range, but the shape of the beam changes gradually especially in the last third part of the beam path in both irradiation geometries. In horizontal irradiation geometry the shape of the end of the beam varies from a rounded form to an asymmetric and at the same time the farthest point of the beam shifts upwards. In vertical irradiation geometry the early round shape changes to an arrow form and then takes up a round shape again.
- ▶ With measuring the pressure no oscillation was found. The time scale of the oscillations of the range was in seconds and the used pressure transducer was linear up to 3 kHz.

The optically observed range oscillation was verified and reproduced by charge measurement. The charge was collected simultaneously in the target chamber and on an isolated disc-shaped electrode as a function of position of the disc along the axes of the chamber. On the electrode first a maximum value was measured due to the beam oscillation, then a lower value after the beam reached the equilibrium state. The beam has produced a significant peak of current on the disk at a position far behind the maximum range point of the beam at equilibrium. Searching the reason of the observed oscillation we measured the beam build up in time on solid target. The beam current has reached its maximum during a much shorter period of time on solid target than the period of the oscillation in gaseous target, therefore, the observed oscillation effect cannot be explained by the finite speed of the beamstop, opening the way of the beam, consequently other physical effects may participate in the interaction of charged particle beams and gaseous materials.

Discussion

The observed phenomena can be followed and may be explained as follows.

At the very first moment of the interaction of charged particle beams with gaseous material the beam intensity and so the observed light emission is small. The beam shapes are symmetrical and round ended. Because of the used beamstop was not quick enough to open the whole beam at once, the intensity of the beam increased gradually and in the very first moment only a low intensity beam penetrated into a cold target gas which resulted a theoretical beam range and symmetrical shape. There was no time for building up of density gradient and for significant mass transport. Therefore, there was no practical difference between the shapes of the beams observed at horizontal and vertical beam irradiation position.

In the next moments the range is gradually expands. The shape of the end of the beam changes to an arrow shape at vertical irradiation geometry. At horizontal irradiation arrangement the asymmetry starts to appear, and consequently the place of the farthest point of the beam shifts upward. The density of the gas along the charged particle path is strongly reduced, especially in the central region of the beam (arrow shape), because of the heating and the charge repulsion effects. The effect of the upward thermal-gravitational mass transport starts to be important.

After reaching a maximum the range became smaller. At the end of the path of the beam

- in the Bragg region - where the energy loss and therefore the produced heat is large the density reduction is significant and the range becomes larger and longer. However a mass transport sets in toward the lower-temperature region, which results in an uneven density distribution. When the penetrated beam nearly fills the target chamber i.e. when the ballast volume is small the density in the first part of the target chamber significantly rises and, therefore, the range of the beam becomes smaller. When the ballast volume is large the effect of the strong density reduction at the beam end can cause only small oscillation.

The beam shape and the length of the beam is slowly, but gradually changes to reach the equilibrium. A thermal gradient develops between the gas heated up by the beam and the cold wall of the chamber, which resulting a mass-transport, and after a few second reaches a steady state.

In horizontal irradiation position, because of the upward thermal and downward density gradients, the upper part of the beam has larger ranges and an asymmetry builds up.

In vertical irradiation position the upward mass transport in the centre of the beam somewhat compensates the strong density reduction of the gas, therefore, the shape of the beam is round.

Conclusions

The asymmetric density reduction and shape of the beam in a gas target in a horizontal irradiation arrangement was checked and verified through the measurement of the charge distribution in the beam. The irradiation of thick gas targets at vertical beam line shows symmetrical beam shape. Investigating the temporal-spatial dependence of the penetrating charged particles a transient process has been found. The equilibrium state is reached through an oscillation process.

The density variation of the target gas under nonuniform heat production and gravitational effects as a function of time in and outside of the beam volume gives a possible explanation of the result. The assumption has to be confirmed by further experiments and with computer simulation.

As far as applications are concerned, the observed shapes at vertical and horizontal irradiation geometries may be of interest in construction of high intensity targets for isotope production and for nuclear data measurement.

References:

R. D. Wieland, D. J. Schlyer and A. P. Wolf, Charged particle penetration in gas targets designed for accelerator production of radionuclides used in nuclear medicine. *Int. J. Appl. Radiat. Isot.* 35 (1984) 387.

S.-J. Heselius, On the accelerator production of short-lived radionuclides. Studies of density reduction in gas targets. Academic dissertation, Abo Akademi, Abo, 1986

O. Solin, Interaction of high energy charged particles with gases. Academic dissertation, Abo Akademi, Abo, 1988.

O. Solin, S.-J. Heselius, P. Lindblom and P. Manngård; Production of ^{81}Rb from Kr - A target study, *J. Labelled Compd. Radiopharm.* 21 (1984) 1275.

Questions for paper 1, Study of static and dynamic effects in gas targets.

Speaker: Ferenc Tárkányi, Hungarian Academy of Sciences

The questioner is identified where possible and the answers are provided by the speaker unless otherwise indicated.

Question: John Clark, MRC Cyclotron Unit Hammersmith

In my experience, trying to measure current on electrodes inside targets to be irradiated it is really very tricky, because of the gas conduction. How did you overcome the leakage between the plasma, the electrode and the target body?

Answer:

We didn't. We cannot distinguish between the electrons and the protons.

Q: J. Clark

No, I mean when you run beam on a gas it gets highly ionized so that it is effectively a low resistance between electrode and the target vessel. I think most of us have experienced this problem.

Q: Jerry Nickles, University of Wisconsin

The input impedance of the electrometer you are using to measure current can be made to read that current read almost anything you like, if you properly or improperly bias it. Our experiences is that it is a very challenging measurement.

Answer:

Because we are not measuring with electrometers. We have a bigger distance measurement and we get closer, it makes no difference if I am measuring like in the experiments here is the beam now, when they have the foils and 3 mm from the end of the chambers. They also have measured the beam current. I don't see any problems with this one.

Because we are measuring the positive current here we are practically measuring all positive or negative is not important we are measuring from a long distance, there is a high current when it is starting of the irradiation and is disappearing when it is at equilibrium. Which it has to be something at the beginning which is not similar to equilibrium not important from the point of view of cause. However, from the point of view of the transient, there is no difference.

Comment: David Schlyer, BNL

When we measured the beam current in the gas targets, our measurements were across a gap at the back of the target which had a 300V bias on it. What we were doing was not trying to measure the current inside the target at all but just determining if the gas in that gap had been ionized which told us if the proton beam had made it to the back of the target.

Reply:

Yes, but you had a very big dark current which was hard to explain in your experiment also. When you irradiated with 20 μA and when the beam was stopping you had 60% behind the foil

and you can not explain it with the different nuclear reactions and not with the secondary electrons which means that the two chambers were connected.

Comment: D.Schlyer.

The beam was spread out due both to energy straggling which we all understand but the other is thermal effects. I think everything that we did, could be explained due to thermal effects happening inside the gas target. In fact we did some experiments when Sven-Johan (Heselius, Turku) was here where we put six thermocouples inside the target and measured the temperature distribution within the target and we found a temperature distribution pattern which matched a flow pattern similar to what you see here. I agree with basis here, we saw flow from the center around the outside and from the front of the target to the back of the target because of the Bragg peak and the gas heating underneath and moving to the cooler part of the target.

Reply:

I agree with Mr. Clark that it is very difficult to explain what we are measuring there, when the electrode is isolated. It is very complicated, because there is the direct electrons and because the beam time is shorter. There is in the charge collection, also is the transient. I agree with you that what is even there exactly, the question is how many percent is there from the beam because the beam is broadening and one part going to the wall, one part is going to the disk, but we can see that one, at the start of the beam, the range is longer or the charge and later it is short, which means that there is this transient. There is a high current at the start of the irradiation and it disappears when equilibrium is established. Which means there has to be something at the beginning which is not similar as an equilibrium and there is no absolute importance from that point of view. But from the point of view from the transient, there is no difference.

Comment: D. Schlyer -

My only point is that it might be possible to explain the transient due to circulation currents being set up in the target body. You might be able to see the same kind of behavior over the time course it takes to establish the flow pattern with the beam pulses.

Comment: R.J. Nickles

I would like to congratulate you on some very nice images, some pictures that one cannot possibly disbelieve, except when your looking at things visually, of course you are looking at light, and the light is not coming from the beam but from the secondary electron. The secondary electrons can be easily guided by stray magnetic fields. There was a question this morning about confining beams, the primary beam with magnetic fields. Has anybody done any confining of the secondaries, the actual intermediate, the link in the chain that is finally dumping the heat into the target gas. Has anybody tried using any axial magnetic fields to constrain them and to either guide hot electrons to the wall to slow down and minimize beam heating, or to make use of it in any way?

Reply:

Of course you are right. We already prepared our thinking about such experiment when the beam is asymmetric, which is problematic in this case when you measure this gap current and because it is changing and you see the upper end of the beam when it is very asymmetric, this

method. Sometimes it is very long this asymmetric path, sometimes it is very short, therefore it is very complicated. We were thinking when we would like to use that method some way to put back this beam with a very strong magnetic field. It is not very complicated to put it back because the end of the beam or half of the beam is stopping 5 or 6 MeV. Which means that it is possible 5 or 6 MeV to try with a very strong magnetic field because the heat is very high when somebody has a high intensity target, 4 kW then it is very difficult to put a superconducting magnet and to take out the heat inside. Therefore some alloy such as SmCo could be used to make a strong magnet (over) a short distance and try to move or not move the end of the beam to focus it or for focussing or not focussing the secondary electrons.

Question.

What was the maximum beam current you carried out these experiments?

Answer.

It was 10 μ A. But it was passed through a 6 mm by 5 mm collimator. The normal gas target has a 1 cm collimator which means the experiments had four times more density, equivalent to 40 μ A in current density.

Comment : Nigel Stevenson, TRIUMF

There is a finite element analysis program that has become available called COSMOS-M. The new modules can simulate volume heating and can simulate convection current in a gas. It might be able to quantize what you are seeing qualitatively.

Reply:

We know this program exists. The computer companies display nice graphics describing gas dynamics and fluid dynamic programs. However, we have to write the programs because the commercial ones are very expensive.

Formation of Voids in a Liquid Target due to Charge Deposition

Behrouz Amini, Ronald Nutt, David C. Patton, and Gerald Bida
CTI, Inc. 810 Innovation Drive, Knoxville, TN 37932-2571

Abstract

A new phenomenon which can occur in a liquid target as a result of charged particle (proton) irradiation is introduced. This phenomena is based on the fact that charge carriers in a liquid target are solely ions.

Proton irradiation of a liquid target inherently causes positive charge deposition directly into the target material. To prevent charge buildup in the target material, the charge must be carried out by ions to the conducting walls. However, high collision rates of ions with background molecules impede charge transfer from the target material to the target walls. Localised positive charge buildup occurs allowing electrostatic pressure to overcome the gravitational pressure, leading to formation of voids. The electric field which is generated due to charge buildup can also cause a local breakdown of water molecules, and subsequently enhanced radiolysis. These and other phenomena which can occur due to charge buildup generally degrade the target yields, however, in some cases, they can contribute to increased heat transfer by conduction. Conditions for the formation of voids, enhanced radiolysis, and the required electric fields are also presented.

Introduction:

To describe the phenomenon and its potential effects referred to in the above abstract we first raise a question, and then answer the question by referring to known facts. These facts form the foundation of the phenomenon to be described. The question is: what are the charge carriers in water, ions or electrons?

Although the answer to this question might seem very clear, let us consider a simple experiment. This simple experiment will help us for later comparison and perhaps give more insight to the issues to be discussed.

Assume that we wish to plate a metallic spoon with copper. To do this we tie the spoon with a wire, connect the wire to the negative electrode of a battery; and immerse the spoon in a copper sulfate solution. The positive electrode of the battery is connected to a copper bar and the bar is also immersed in the solution. We then close the circuit to plate the spoon. The amount of copper transferred to the spoon can be calculated by considering

the fact that each ionized copper atom (Cu^{++}) carries two units of charge, and when it reaches the spoon it sticks to the spoon during the charge transfer. We conclude from this experiment that positive and negative ions, Cu^{++} and SO_4^{--} are the sole carriers of charge in a copper sulfate solution. This conclusion is a restatement of what is well known.¹ In direct relation to this fact it is also known that electrons cannot carry the charge in a copper sulfate solution or in water. This is despite the fact that there is a finite electric field in the solution which is generated by the battery.

The fact that ions rather than electrons are the only charge carriers in a liquid like water can be seen by performing the above experiment with pure water. The very small current which can be measured with pure water is due to charge carriers resulting from the breakdown of a very small portion of H_2O molecules into H^+ and OH^- .

The motion of Cu^{++} and SO_4^{--} in the solution discussed above is described by 3-dimensional diffusion equations with a mean-free-path (λ) of intermolecular spacing of only a few angstroms. The motion of charge carriers is basically random walk which due to a very large collision frequency is only influenced slightly by the electric field.

Now we consider an electrically isolated sphere bombarded by a $20 \mu\text{A}$ beam of 10 MeV protons. We assume that the protons penetrate the sphere and stay in the sphere. Subsequently, the voltage of the sphere will initially go up and reach a maximum of 10 MV. Beyond this point the sphere rejects the protons through the electric field generated by the accumulation of charge. We want to know how fast the voltage of the sphere will increase. If we assume that the diameter of the sphere is 1 cm we then find, by simple calculations, that it only takes about 30 msec before the sphere's voltage raises to its maximum value. The only point we would like to make from this experiment is that when there is a local charge accumulation the voltage of that region increases very rapidly.

Irradiation of ^{18}O Water with a Proton Beam

We now consider the main issue of interest; irradiation of ^{18}O or ^{16}O water with protons. The target material is thick (deep target) so that the incoming protons will stop in the water. The situation is depicted in Figure (1). The target receives a net charge during the bombardment. Ions carrying the excess charge have to reach the wall to discharge. This is the only way of transferring the charge to the target wall. However, the ions' collisional rate (ν) with the background molecules is very high. This will impede the charge transfer to the wall and subsequently, at any given time, the target will have a net charge. This net charge accumulation occurs in a fraction of msec from the start of the target bombardment, and will remain in the target until the end of the target bombardment.² Excluding the short transient effect during which the net charge accumulates, the average current carried by the ions to the walls is equal to the beam current. Presence of the net charge will generate a self-consistent electric field which tends to drive the charge carriers to the wall. In the

experiment with copper sulfate the battery generates the electric field and there is no net charge in the solution. Here, the electric field is generated by the net charge which in turns applies forces in the direction of the target walls to the charge carriers.

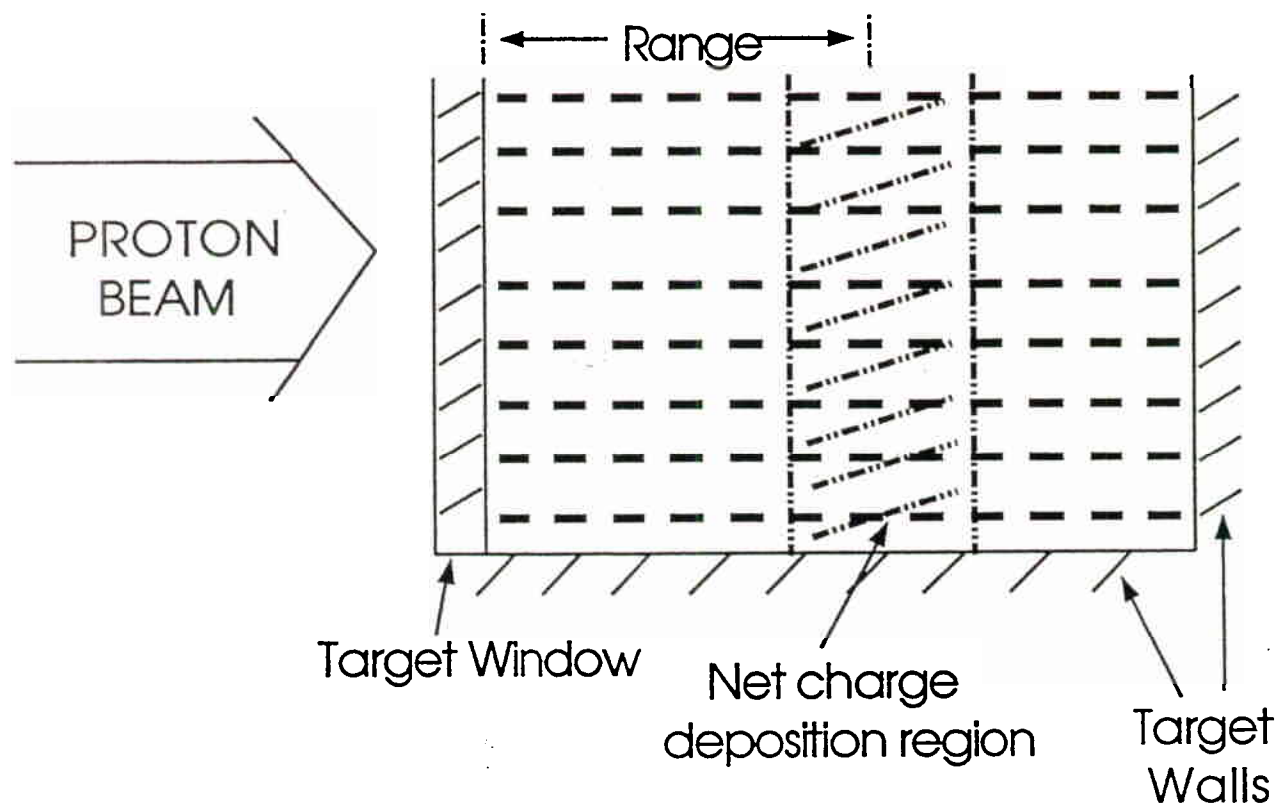


Fig. 1 Schematic of target bombardment.

Collisional Frequency of Charge Carriers

The reason for a high collisional rate is the small intermolecular spacing. Typically, intermolecular distances are a few angstroms. We may use a simplified equation to estimate the collisional frequency ν . Using

$$\frac{1}{2}mv^2 = \frac{3}{2}KT \quad (1)$$

we obtain $v = (3KT/m)^{1/2}$, and by

$$\nu = \frac{1}{\tau} = \frac{v}{d} \quad (2)$$

where d is the intermolecular spacing, we obtain that $\nu = (3KT/m)^{1/2}/d$. With $m=18$ amu, $T=300$ K, and $d \simeq 3\text{\AA}$, we obtain $\nu \simeq 4 \times 10^{12} \text{ sec}^{-1}$. We observe from this estimation that collisional frequency ν is very large. This means, as shown in the following section, that to generate even a small average drift velocity one needs a very large electric field.

Equation of Motion of a Charge Carrier

Let us now obtain an equation of motion for an ion using a simplified one dimensional analysis. We have

$$m \frac{dv_+}{dt} \simeq eE - m\nu v_+ \quad (3)$$

where v_+ is the ion velocity and e and E are the charge and electric field, respectively. In a steady-state the left-hand side of the above equation is zero. We then obtain the ion mean-drift-velocity v_+ from above. Accordingly, $v_+ \simeq (eE/m\nu)^{1/2}$. We observe from this relation that due to high collisional frequency rate ν , the electric field has to be large in order to maintain a reasonable value for v_+ . By "reasonable value" we mean a nonvanishing value. However, a large electric field, as explained shortly, can lead to formation of voids, local violent breakdown of water molecules which results in enhanced radiolysis, and other effects which in general decrease the activation yield.

Enhanced Radiolysis

Electrons which are freed from the water molecules through the incoming proton collisions can gain energy by the electric field and subsequently ionize water molecules by collision. This ionization of water molecules is very effective particularly in the presence of small bubbles or voids which always exist in the target. In such circumstances the electrons can gain enough energy to ionize water molecules. The magnitude of the electric field for the local breakdown of the water molecules can be calculated as follows.

$$\int eE \cdot dl = \epsilon \simeq \text{ionization energy of water} \quad (4)$$

which gives, $Ed \simeq \epsilon$ in eV. Here d is the distance that an electron travels under the influence of the electric field to gain an energy of ϵ . Thus d should be larger than the collisional mean-free-path of the electron. This requirement holds easily inside a void. For $\epsilon \simeq 4 - 5$ eV,

and $d \simeq 4 - 5\mu m$, we find $E \simeq 1kV/cm$. This is the value of the electric field for the local breakdown of the water. The magnitude of the electric field, which is really very small, suggests that the local breakdown of the water is very likely to occur. The result is enhanced radiolysis and a poor target yield.

Electric Field Values for the Formation of Voids

Since the target water has a net positive charge there is a repelling force in the water which tends to break the water apart. Let us approximate this repelling force as two charge sheets with the same charge density σ . The voids will form when

$$\frac{1}{2}\sigma E + P_{void} \simeq P_o \quad (5)$$

where $\sigma E/2$ is the electrostatic pressure, P_{void} is the pressure of the void, and P_o is the applied pressure in the target. Note that P_{void} is the saturation pressure of water at the target temperature. σ and E are related through $\sigma = 2\epsilon_o E$. Using this relation and solving the above equation for E we obtain that

$$E \simeq \frac{(P_o - P_{void})^{1/2}}{\epsilon_o^{1/2}} \quad (6)$$

This is the magnitude of the electric field for formation of voids in terms of target pressure and target temperature which defines P_{void} .

It is well known that voids will also form due to poor heat transfer which results in boiling the target water. The equation derived is based on poor charge transfer alone. Both of these effects which result in formation of voids support each other. For instance, due to repelling forces among the water molecules, the target water can boil at a lower temperature than it otherwise might.

Deposition of Impurities to the Target Body and Windows

A charged molecule is more likely to form a chemical bond than a neutral molecule. This is simply due to strong Coulomb interaction of a charged particle with the surrounding molecules. Impurity ions, which can also contribute to the charge transfer from the target to the target body and windows, can make a chemical bond with the target body and windows during the charge transfer, or can be simply adsorbed by the target wall.

The thin film of impurity which can form on the target wall is generally a dielectric material. This will further impede the charge transfer from the target. The result is degradation of target yield as a function of time. Note that such target degradation, which is well known, cannot be attributed to poor heat transfer. The film is too thin to make a noticeable change

in the heat transfer. However, even a very thin film of a dielectric material impedes the charge transfer.

How to Avoid the Problem

The effects discussed in the last three sections are symptoms of a target with a yield below the expected yield. This is in agreement with experiments. A low yield target has generally one or all of the symptoms discussed in the last three sections. It is also known that poor heat transfer from the target which results in boiling the target reduces the target yield. However, when the beam current is low neither poor heat nor poor charge transfer can reduce the target yield.

The cross section of ^{18}O activation as a function of proton energy has been reported in the literature.³ The activation threshold starts at around 3 MeV. Therefore, if we make the target thin enough such that the proton energy is about 3 MeV at the back of the target then the yield will not be affected. In such cases the charge will not be deposited in the target. This will solve the potential problem discussed in this paper. In addition, such a configuration causes less heat deposition into the target without changing the activation yield. For example, if a proton beam of 11 MeV is used for target bombardment, then the heat deposition into the target will be reduced by 30%. This in turn might prevent target boiling which has been a problem in many experiments.

Alternatively, with charges deposited in the water, we would be dealing with a charged liquid. It is then possible to influence the charged liquid by electric or magnetic field applied outside the target in favor of a more efficient heat transfer from the target to the target wall.

References:

1. See, for example, L. Pauling, *General Chemistry*, Dover, New York, 1988.
2. Note that, as will be seen shortly, the electric potential of the target due to charge accumulation is only of the order of kilo-volts.
3. T. J. Ruth, and A. P. Wolf, *Radiochim, Acta* 26, 21.

Questions paper 2, Formation of voids in a liquid target due to charge deposition,

Speaker: A. Behrouz, CTI

The questioner is identified where possible and the answers are provided by the speaker unless otherwise indicated.

Question:

I think it is very interesting, but a practical solution to the problem might be pressurizing the target or to reduce the depth of the target by 2-3 MeV. These calculations are interesting but not the solution to the practical problem

Answer:

I agree with you. The target might cave in.

If you send protons to back of the target the threshold is about 2 to 3 MeV so you don't want anything below the 2 to 3 MeV. This actually will be combined with the heat transfer because usually this target has poor heat transfer also. So the target will create more problems by combining this effect and poor heat transfer so they boil faster.

Question: John Clark, MRC Cyclotron, Hammersmith

I've struggled through your talk and I don't understand this space charge limitation at all. You have a target with a connection to it which is draining current away so you can measure target current. None of us run our targets open circuit. You are claiming that your charge is building up.

Answer:

You are talking about a millisecond, if it (charge) builds up the whole thing will blow up.

John Clark:

So who cares about a millisecond, in real time, in real chemistry, we are interested in an hour irradiation.

Answer:

You have to care, because if it gives you voids in milliseconds, it means your beam will hit the back of the target.

John Clark:

Added to which the water between the Bragg peak and the window is totally ionised. You have eliminated any consideration of chemical reactions.

Answer:

You cannot have a neutral plasma. The cell I showed for electrolysis is neutral. For each electron you also have a proton. But this does not have anything to do with ionisation. The fact that you put pure charge in it, that makes a difference. It does not have anything to do with

ionization.

John Clark:

You've avoided any observation of basic radiation chemistry and radical reactions in the particle track.

Answer:

This happens locally, if you see any reason, scientifically that you present, go ahead and I'll try to think of it, but I'll agree with you that you cannot build up charge there. It takes only a millisecond to give this charge. You always measure the same average current which you are putting on the target. This is not a sink for the charge, but charge builds up a little bit there.

Question: Rich Ferrieri, BNL

Just to throw another ring into the hopper from radiation chemistry text on aqueous media we are not talking about milliseconds, we are talking about 10^{-12} to 10^{-14} seconds, the time frame of a single vibration. You get positive ions, and these undergo secondary reactions producing a whole pool of secondary electrons, thermalized electrons, hydrated electrons. How do these play a role in your calculations? You have neglected the whole field of radiation chemistry.

Answer:

I don't think I did. The fact is the proton comes in, ionizes water, but again it is a little bit confusing, it is the ionization not the charge creation. In ionization the number of positive charges still equals the number of negative. If you ionize the whole thing, still the amount of positive equals the whole amount of negative. But in this case we are adding charge to a system in which the electron has very limited range of a couple of microns compared to metal when the electron can move very fast. Ionization and neutralization are two different things.

Question: Jeanne Link, University of Washington

I agree that you did bring up those subjects but I have to agree with Rich and John, you are having a lot of ionization in where you still have a neutral solution charge-wise, your first diagram showed a copper sulphate solution where you have good conductivity and your calculations may use numbers that are high, you are not taking diffusion into effect. You're thinking more of diffusion and you're not thinking enough of how fast you are carrying away charge because you have such ionisation. I'll have to look at your numbers, but I think your numbers and assumptions are low (with respect to charge transport).

Answer:

What is common within this one and what I talked about is not very much, you have the electric field here because you have the two electrodes. The net charge here is zero, nothing adds net charge to this. The issue was to point out the carriers of charge are ions, not the electrons. Electrons cannot jump and carry the charge. The ion has to diffuse, eventually to get from point A to point B. Even if your target is conducting it still does not help you, the molecule which gets the charge has to take it to the wall. If you follow this molecule you don't care if your water or your liquid is conducting or not.

Question: Jerry Nickles, University of Wisconsin

There's a lot of disagreement on that point. That charge carrier doesn't have to get to the wall, just a charge carrier has to get to the wall to maintain the neutrality. You are also treating this thing as a DC problem, when in fact you've got frequencies here that go up to gigahertz. Your beam flash is about 3 nanoseconds wide, it's an AC problem at least and I don't see any reference to permittivities and the AC characteristics of a circuit which has got about 100 puffs (picofarad) of capacitance, frequencies of gigahertz, that makes a 1Ω resistor. I think that a lot of people here are somewhat unhappy with this treatment.

Answer:

In terms of AC you are concerned about displacement current, we can bring up the issue, I agree.

Question: Ed Galiano, MD Anderson Cancer Centre.

I'm a slow learner, sir, so there's one thing you need to clarify for me. You mentioned that the transport of the ions to the walls of the target, and I don't want to get into the chemistry, that's not my field. I just want to look at the physics of this, because it's slow because of inner molecular collisions. Now, once contact is made with the walls of the target, it seems to me that strictly speaking from a Physics point of view, your problem is solved because you have continuity. It would be like moving a massive number of people through a slow vehicle like trains but just putting enough trains in there. Once the trains start to arrive you can move per unit time as many people as you wish.

Answer:

I agree. The moment you get to the wall it's like they tag the wall it's over, the issue is over. But they have to move from where the proton is deposited to the wall. The moment they get to the wall there is no issue. I quite agree with you. That's why I said they have to carry the charge to the wall. The moment they do it that's no issue. It takes certain times, because they constantly make collision with the neighbouring molecules. If an electron were ever to jump from one molecule to that, that says that effect does not occur. If we do not add copper sulphate to this pure water, we measure only a little bit of current because H_2O this will disassociate to H^+ and HO^- . The little bit of current we measure is because of that not that the electron carries the current. No matter what those are the ion should again tag the wall.

Question: David Schlyer, BNL

I have a problem with two of your assumptions. One is that the positive charged ions are the charge carriers. I see no difference between whether the fact if the ion stays in the middle of your solution and an electron makes its way over and neutralizes it in that way as if the ion moves to the wall. The other one is, that the electrons by your own equations, would have velocities mean free path on the order of 2 km per second rather than 1 cm per second. Second is that, by the $3/2 kT$ on the bottom of the equation there is no way that those electrons are thermal. Those are made at very enhanced energies, as a particle beam passes through the water and they are very highly excited. So that those two factors I think make this argument that you have to have positive charge carriers making their way to the wall under thermal conditions may not be the case in the water target.

Answer:

Your second reason actually coupled to the first reason. So, the first reason was that can electron carry the charge? The answer is a definite "no" because I can add pure water here and increase the electric heat. If the electron would carry like jumping from one molecule to the next, I would be measuring some current. In pure water I do not measure the current. If I increase the electric field I will break down the whole thing.

Question: Schlyer

Not if there's not a gradient. You are assuming that there is a gradient. I am assuming that if you have a positive charge buried in the center of your water that creates a gradient between the outside wall and the center of the water. That gradient is enough to drive the electron into the center of the water. If you have no gradient, if the water is sitting there ionised with either a positive or negative charge, there is no gradient between the outside of the water and the wall.

Answer:

I think by gradient you mean electric field.

Schlyer

Right, electric gradient between the inside of the target and the outside.

Answer:

The electric field I used was a self generated field. It's not very similar to this example, because there, the local charge has to make the electric field. See, I agree with you exactly, if there is no gradient or no electric field nothing will happen. So the local charge has to build up in order to push the ions out. So you need the gradient. The electrons won't push around because we see from this example.

Comment: Barbara Hughey, Science Research Labs

The cell doesn't have much in common with the target... (the rest of the question was inaudible)

Reply:

From the electric field point of view it is very common.

Here (cell) you have a positive and negative from the charge. In the case of the target, the charge has to be build up so the electric field drives the positive charge and we know in both cases the electron cannot move because when you have an electric field here you don't measure current.

The Yield of F-18 from Different Target Designs in the $^{18}\text{O}(p,n)^{18}\text{F}$ Reaction on Frozen $[^{18}\text{O}]\text{CO}_2$.

Mahmoud L. Firouzbakht, David J. Schlyer and Alfred P. Wolf,
Department of Chemistry,
Brookhaven National Laboratory,
Upton, NY 11973. USA.

The shortage of oxygen-18 enriched water has encouraged us to explore alternate methods of production of fluorine-18 where the recovery of the oxygen-18 enriched target material is extremely efficient. We have recently presented the results from a cryogenic target using carbon dioxide ice as the target (1). This is similar in design to a water ice target previously described (2,3). The amount of material required and the maximum beam current which can be put on the target are a function of the particular design. The effects of target cone length and number of cooling fins have been explored in order to optimize the target design.

Three different targets have been used to test these parameters. The three target are shown in Figures 1, 2 and 3. The first was the prototype target with a single heat sink at the rear of the target (Figure 1). The second is a target with several cooling fins and a short cone length which requires less target material (Figure 2). The third is a target with several cooling fins but a longer target length which allows for more efficient cooling of the material. The results from these studies are summarized in Table 1. The target with four cooling fins could be run at a beam current of 18 μA with no perceptible volatilization of the target material while the target with the single cooling block showed volatilization at about 8 μA . The long and short cone targets did not show a difference in the volatilization of the target material at the beam current limit of the 60" cyclotron (18 μA).

The short target did maintain production with a lower amount of gas frozen into the target. The amount of gas frozen into the target in all these runs is two to four times that calculated to be necessary to form an ice layer thick enough to stop the beam in these targets. This is probably due to an uneven carbon dioxide layer on the surface of the cone. Experiments are currently under way to explore both the uniformity of the layer and the optimum angle for the cone.

This cryogenic target gives extremely efficient enriched target material recovery (>99%) and simplicity of material transfer. The production yields are similar to those obtained with the oxygen-18 enriched water target at beam currents up to 18 μA (our cyclotron limit, not necessarily the limit of the target design).

This work was carried out at Brookhaven National Laboratory under contract DE-AC02-76CH00016 with the U.S. Department of Energy, supported by its Office of Health and Environmental Research and grant No. NINDS, NS 15380.

References:

1. Firouzbakht, M.L., Schlyer, D.J., Gatley, S.J., and Wolf, A.P. A Cryogenic Solid Target for the Production of [^{18}F]Fluoride from Enriched [^{18}O]Carbon Dioxide J. Nucl Med. 34 69P (1993).
2. Shefer, R. E. Klinkowstein, R. E., Hughey, B. J., Welch, M. J. Production of PET Radionuclides with a High Current Electrostatic Accelerator. J. Nucl. Med. 32 (1991) 1096.
3. Hughey, B. J., Shefer, R. E., Klinkowstein, R. E., Welch, M. J., Dence, C. S., and Livini, E., A Novel Cryogenic Oxygen-18 Target for the Production of Fluorine-18. J. Nucl. Med. 33:932 (1992).

Table 1.
Production for Various Target Designs

<u>Cone Length</u>	<u>Amount of CO₂ (liters)</u>	<u>Yield at EOB (mCi)</u>	<u>Percent of Theoretical (%)</u>
Long	2.0	56±4	80
Short	2.0	52±3	74
Long	1.2	53±4	76
Short	1.2	50±3	71
Long	1.15	43±2	61
Short	1.15	44±3	63
Long	0.63	12±2	17
Short	0.63	26±4	37

All runs were carried out at 6 μA for 10 minutes at an energy of 17.4 MeV incident on the carbon dioxide. Percent theoretical is based on the yield from 99% [^{18}O]CO₂. The dimensions of the long and short cones are given in the figures.

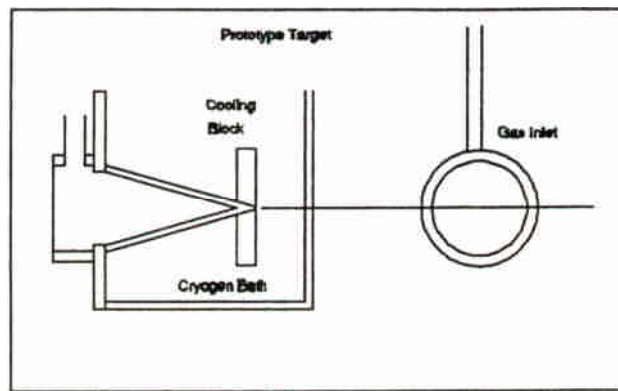


Figure 1. Prototype target design

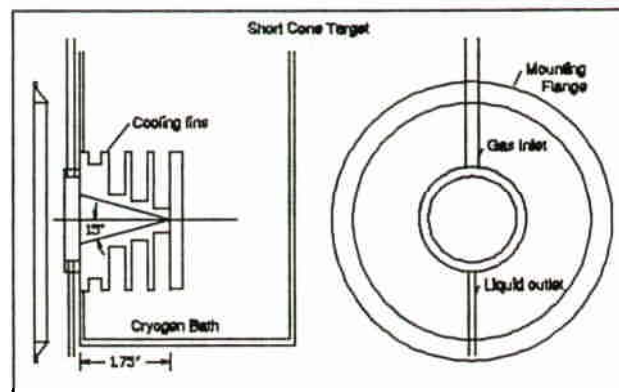


Figure 2. Short cone target

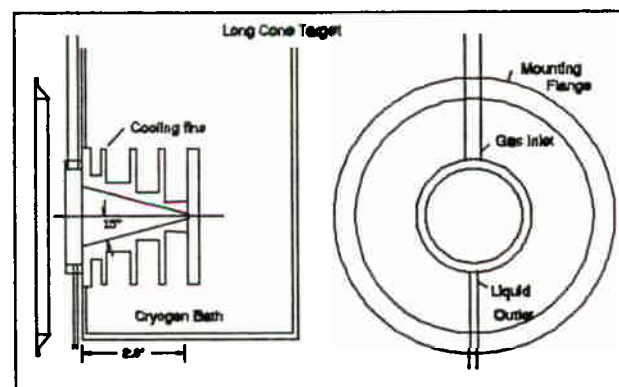


Figure 3. Long cone target

Questions for paper 3, The yield of F-18 from different target designs in the $^{18}\text{O}(p,n)^{18}\text{F}$ reaction of $[^{18}\text{O}]\text{CO}_2$,

Speaker: Mahmoud Firouzbakht, BNL

The questioner is identified where possible and the answers are provided by the speaker unless otherwise indicated.

Question: Barbara Hughey, SRL

First, I thought you said the system was warm when you filled it with the CO_2 , is that not true?

Answer:

Yes, we tried the system in many different ways.

Barbara Hughey:

If the system is warm then the gas should just uniformly fill the cone, why do you need to angle, you don't have a jet?

Answer:

The cone is very small, only 10 ml of gas is in the cone, the rest is in the bulb. When we fill it with the gas it gradually becomes cold and it has more chance for gas to be uniform.

Barbara Hughey:

You need the gas to condense and you need to add more gas?

Answer:

Yes. We did it another way. First we cooled the cone and let the gas go, ...(inaudible). But, it still is not uniform.

Barbara Hughey:

Have you calculated the theoretical current, that you should be able to get with that cone angle? If I remember right, the vapour pressure of CO_2 is very high, even with no beam on it at $77^\circ(\text{K})$.

Answer:

We did some calculation but we don't rely on calculations because they don't always work. We went up to 18 (MeV) as I said during the irradiation, we monitored the pressure. So if the pressure started going up we know the ice will start to melt.

Barbara:

It's not melting, it's subliming. You should be able to transfer that to a temperature, effective surface temperature and how does that agree. Have you been able to find thermal conductivity numbers for frozen CO_2 , I don't know if that data is available?

Answer:

Ok, the whole purpose again, is making F-18 efficiently, easily and in this system we can make F-18, we can recover 99% of the gas, that is the whole purpose.

Barbara Hughey:

I realize that, I am trying to understand what the limitations might be.

Answer:

We have not tried calculations.

Barbara Hughey:

The short cone vs. the long cone that's just a difference in surface area. You're not changing the angle, you're not improving.

Reply:

We are not changing the angle but the whole purpose for that to see if we can use less CO₂ and make enough and also for angle, we designed another target, which is a flat target but we can change the angle. Pretty soon we will have the result of which angle is the best for this target and also for all the solid targets that we irradiated.

Barbara Hughey:

One last comment on the target with no fins, how close were you to the burnout heat flux for liquid nitrogen? You can only cool 10 watts per cm². with liquid nitrogen, I don't know how close you are to that limit. That will get you before the ice does, possibly. I mean that you had very small surface area on that cone and very high beam power. What was the beam power deposition on that cone without fins, was it 10 watts per cm² or was it less? The ones without fins, the surface area of the outside of the cone.

Answer:

That one we couldn't go any more than 8 (μA).

Question: Tim Tewson, University of Texas Health Science Center

Have you tried washing out the cone with acetyl nitrile with K₂CO₃ and kryptofix rather than the water?

Answer:

No, only water and with very dilute NaOH.

Question: Jerry Bida, CTI

I wondered if you measured any local charge deposition in the ice?

Answer:

No we didn't.

Jerry Bida

That was suppose to have been humorous!

The focus of your target development research was to fulfil the radioisotope production needs of BNL. Why did you run in the solid phases as opposed to the gas phase?

Mahmoud Firouzbakht:

What type of gas?

Reply:

CO₂.

Answer:

First of all, it is very simple to work for the ice target in the area of a small target. Second, the beam goes on the surface of the cone, if you use gas it goes through. The washing of the target is more difficult than washing the target when we use ice. Because the whole target is about 10 mL when we use cone when we freeze all the CO₂ on the surface of target. If we use a gas target we need a long target again, we have a problem of beam so I think this is the best way to make it from the gas.

Jerry Bida

You don't need a long gas target.

Rich Ferrieri, BNL

I'd like to make a comment with regard to that. Once you get involved with larger volume and/or high pressure gas targets, you run the greater risk of affecting the purity of the CO₂. In addition, the extracted fluorine-18 might not be in a synthetically useful form.

Mahmoud Firouzbakht:

And also, if you make it from CO₂ gas if you use a gas it breaks into CO and O and what we can not get the ¹⁸O back again.

Jerry Bida

If I remember my literature correctly I thought CO₂ was quite radiation robust. CO₂ in the solid and liquid phase will undergo radiolysis more quickly than in the gas phase.

Answer:

If this is the case on the ice we cannot recover that, we cannot freeze oxygen.

Comment: Mike Welch, Washington University

Go back to your radiation chemistry books, there is much less radiolysis as you go colder in virtually everything from water to CO₂.

Question: Tom Ruth, TRIUMF

Jerry (Bida), what about the hot atom reaction between CO₂ and fluorine, would you expect to see some fluorinated forms of carbon in the gas phase?

Reply (Bida):

I don't think so, but I might stand corrected on that.

Comment: David Schlyer, BNL

As a point of interest, we see essentially no transfer of radioactivity from the gaseous phase from the cone. Down around 3-4% of the fluorine radioactivity that is transferred.

Tom Ruth

What I was wondering was if you were to do it in the gaseous state, versus CO₂ in the solid state.

Answer:

No.

Question: Ferenc Tárkányi, Hungarian Academy of Sciences

Have you observed some changes in the surface after repeated irradiations with the beam stop in these copper cones? You have to wash out with acid which can change the surface.

Answer:

You should not use any acid in that because if the target becomes acidified then the fluoride becomes HF and transfers as a gas. When you wash the target try to wash it with basic solution. As long as it is above 7 (pH) you are okay.

Question: Ferenc Tárkányi

Did the irradiations effect the yield in any way, because in normal gas target, washing out the target the surface usually changes many times and the resulting activity washed out isn't so high.

Answer: We didn't see any effect. We got all of the gas back.

Question: Ferenc Tárkányi

What is the partial pressure of gas in target CO₂ when you freeze because you are measuring if it is melting or not with the pressure.

Answer:

Do you mean what is the pressure inside the Cone?

Ferenc Tárkányi

What is the pressure inside the cone when it is freezing?

Answer:

The pressure is 1 torr, a few torr .

Ferenc Tárkányi

And you measure in such a way that you know whether it is melted or not? You use a pressure transducer - you are looking if the pressure is changing or not.

Answer:

Yes, we look at the pressure in case for the target without fins, during the irradiation when the current went above 8 μA , we saw the pressure is climbing so we know the ice started to melt because during the run the target is open to the line and storage bottle so if the pressure starts climbing we know the ice starts to melt.

Ferenc Tárkányi

Because if I understand, the target is not melted because the yield is linear with the beam current. If it is melted it can sit in other places, melted somewhere then it will not be linear, the yield, current fie. Which means, practically your target is not melted. After it is not linear it means it is melted because the target material is somewhere else.

Answer:

Yes.

Question: Jerry Nickles

Have you seen any evidence by decreasing yield for example, from run to run, that you are getting isotope exchange with water?

Answer:

No. We did lots of runs, we have not seen any change.

David Schlyer, BNL

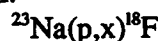
After the runs we thoroughly evacuated target, rinsed and dried it. There was no residual water left.

Production of ^{18}F from Sodium-metal-target

R. Schwarzbachs P. Bläuenstein, I. Huszár, J. Jegge and P.A. Schubiger
Radiopharmacy Division, Paul Scherrer Institute
CH-5232 Villigen PSI, Switzerland

Introduction

Fluorine-18 is produced in large scale for application in PET, mostly by the $^{18}\text{O}(p,n)^{18}\text{F}$ reaction. Looking for an alternative to this method, a reaction presented by Lagunas-Solar [1], which also yields ^{18}F has been examined:



We expected a much higher yield by producing ^{18}F from Na instead of ^{18}O -water due to the higher beam current. We wanted to know to which extent the more complicated process of separating ^{18}F from Na would reduce the yield due to the decay of ^{18}F .

The presence of the accelerator with $E_p = 72$ MeV together with our experience with the Rb metal target for the ^{82}Sr production, brought about a fast development and testing of the Na target.

Table 1 gives an overview of the target for ^{18}F production

target system	gas	liquid	soild
target material	Ne + 1% F_2	$\text{H}_2\text{O}, >95\% \text{ }^{18}\text{O}$	Na (metal)
chemical form	F_2	F^-	F^-
beam current	< 30 μA	10 - 25 μAh	90 - 100 μA
yield	0.37 Gbq/ μAh 10 mCi/ μAh	2.9 - 3.9 Gbq/ μAh 50 - 55 mCi/ μAh	2.9 - 3.9 Gbq/ μAh 80 - 100 mCi/ μAh

Fig. 1 shows the expected excitation function of $^{23}\text{Na}(p,x)^{18}\text{F}$ [1]. The shaded region corresponds to the energy range used in this work.

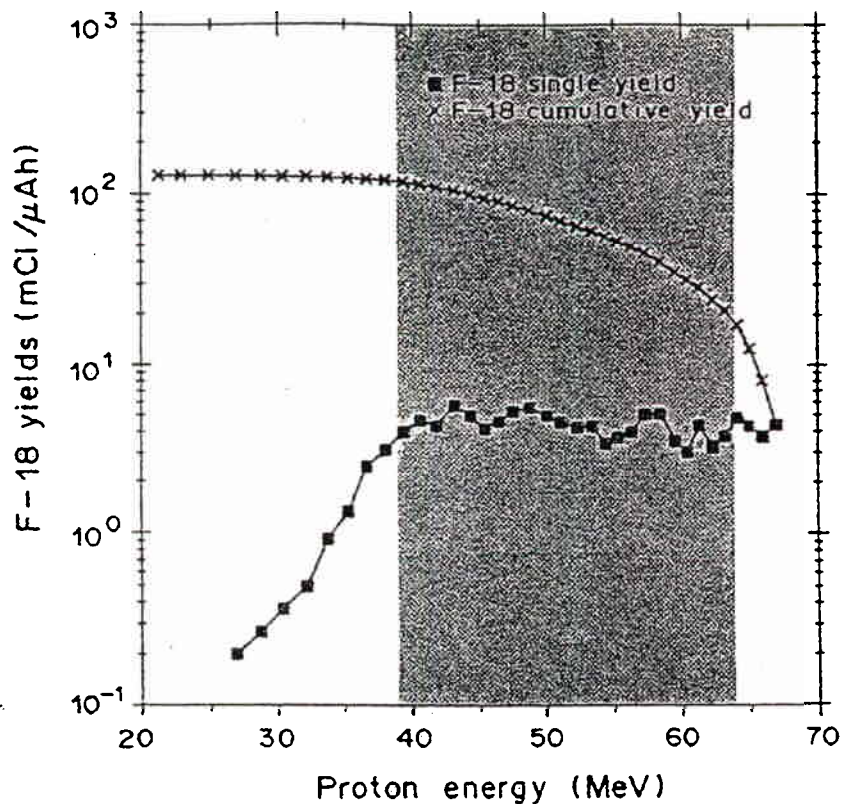


Fig. 1. Protons on ^{23}Na targets. Fluorine-18 single (thin-target) and cumulative yields (mCi/ μAh) as a function of proton energies (MeV). The ^{18}F cumulative yields reaches 82 ± 10 mCi/ μAh in the 63 - 39.5 MeV proton energy range

Target Construction

The sodium metal target consists of 6.5 g of Na (Merck p.A, $\rho = 0.970$ g/cm³) enclosed in a stainless steel cylinder of 20 mm diameter and 30 mm length (Figure 2). Due to the excellent heat conductivity of Na metal, the target can be irradiated with a proton beam of about 100 μA .

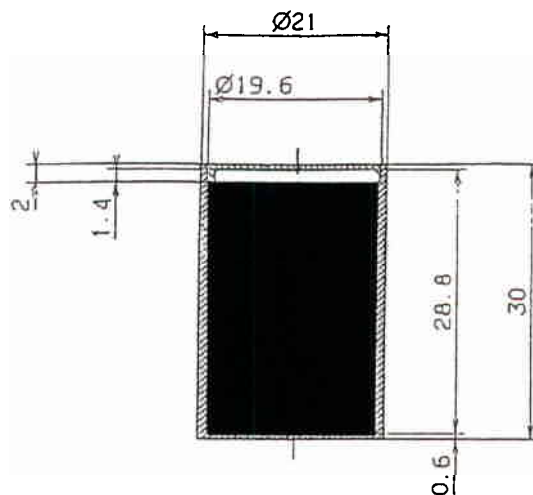


Figure 2.

The Rb target holder had to be adapted only slightly to use it with the Na target (Figure 3).

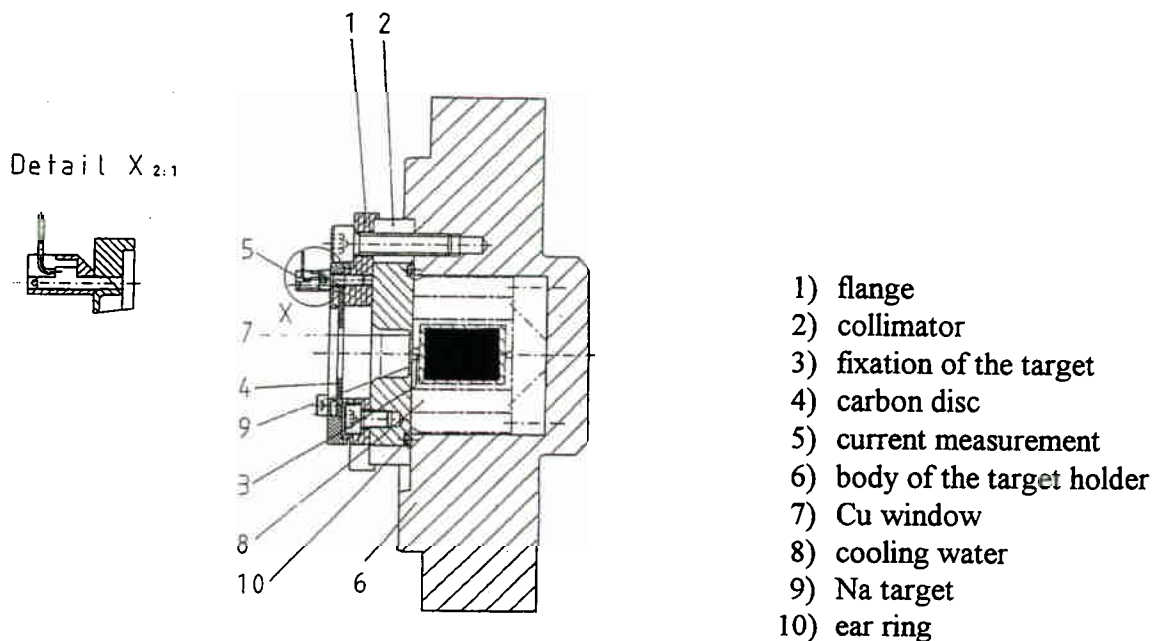


Figure 3.

Results

The irradiation of natural Na with protons ($E_p=63 \rightarrow 39.5$ MeV) yields ^{18}F as well as unwanted sodium isotopes ^{22}Na and ^{24}Na . Moreover, the stainless steel target capsule becomes activated with several radionuclides. However, these contaminants do not dissolve during the processing of the Na metal.

Table 2a.

Target Radionuclides

nuclide	$T_{1/2}$	activity [Mbq/ μAh]
^{18}F	110. min	3030.
^{22}Na	2.6 a	0.67
^{24}Na	15.0 h	2.0

Table 2b.
Container Radionuclides

nuclide	$T_{1/2}$	activity [Mbcq/ μ Ah]
^{48}V	16.1 d	0.59
^{51}Cr	27.7 d	2.7
^{52}Mn	5.7 d	11.2
^{54}Mn	312.2 d	0.15
^{55}Co	17.5 d	26.2
^{56}Co	77.3 d	0.37
^{57}Co	270. d	0.11
^{58}Co	70.8 d	0.26
^{56}Ni	6.1 d	0.3
^{57}Ni	1.5 d	7.0

Target Chemistry

1. Dissolving

- * the target is opened
- * 75 mL of methanol is added
wait until reaction stops
after 10-15 minutes mix 75 mL of water for hydrolysis

2. Separation of ^{22}Na and ^{24}Na

- * Na^+ is eliminated with a cation exchange resin (AG 50 W x 8) in H^+ form and neutralized with OH^-
- * ^{18}F is trapped on an anion exchange resin (AG1 x 8) carbonate form
- * both resins are rinsed with 150 mL of water

3. Elution of ^{18}F fluoride

- * the anion exchange resin is rinsed again with 5 mL of water
- * ^{18}F is eluted using 3 times 0.3 mL K_2CO_3 solution (20 mg/mL)

4. Synthesis for testing

- * the ^{18}F solution is evaporated to dryness
- * FDG labelling is started by adding the triflate precursor

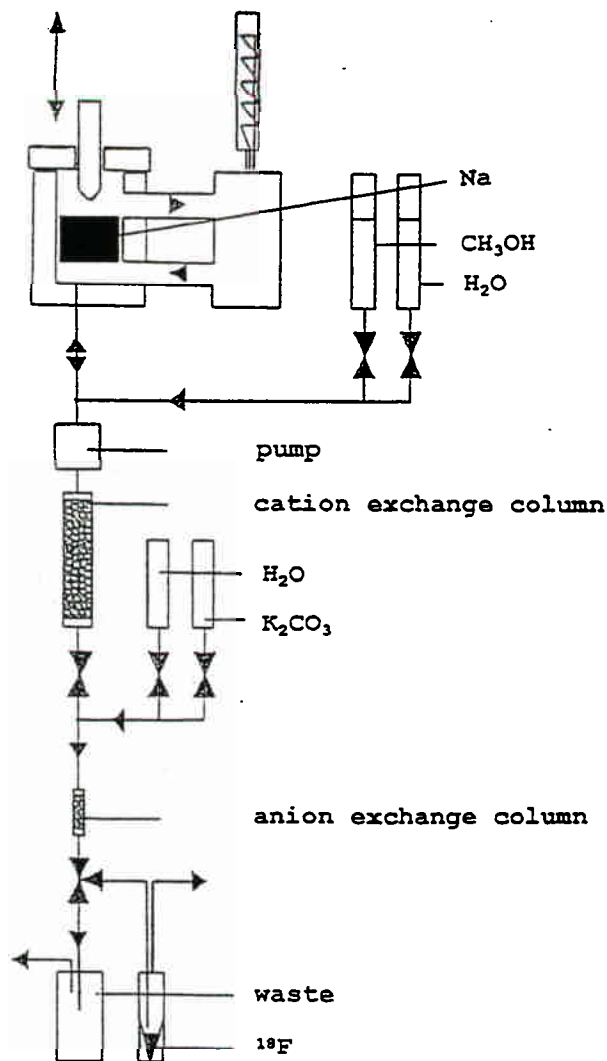


Figure 4. Schematic of the apparatus.

Conclusion

¹⁸F was successfully produced in the expected high yield by irradiation metallic Na with protons. The quality of ¹⁸F obtained after separation from the other radionuclides was assessed by radioanalytical methods (ie. measuring energy of the decay and radioactive half-life) and tested with a synthesis of ¹⁸F-FDG. This method provides a viable alternative for producing large amounts of ¹⁸F⁻ for radiotracer synthesis.

References

1. M.C. Lagunas-Solar, Int. J. Appl. Radiat. Isot., **43**, 1005 (1992).

Surface-Sensitive Analysis of Materials Used in the Production of PET Radioisotopes

Bill Alvord

CTI, Inc. 810 Innovation Drive, Knoxville, TN 37933-0999

Introduction

The use of computer operated cyclotrons for clinical production of radiotracers for PET has made data on target performance (observed by a variety of users and with large statistics) recently available. The issues of consistent fluoride ion yields and repeatable FDG synthesis yields are of singular importance to the ordinary clinical user. For widespread manufacturing of compounds like FDG, it will be essential to have any issues affecting yield well understood. Much work has been done on water targets looking at the effect on yield of impurities in target water (before and after irradiation)^{1,2,3}, dose rate³, synthesis setup¹, overpressure⁴, and cooling conditions.⁵ It is in this environment that we have begun to look at the surface chemistry of target body and window materials in order to better understand the mechanisms of target performance and lifetime. Ample anecdotal evidence exists for phenomena of "burn in," slow or rapid deterioration due to contaminants in target water, and the required target rebuild or cleaning procedure for best yields. However quantitative methods for understanding the same phenomena are few.

One of the most commonly used diagnostic tools for target failure analysis to date has been simple visual inspection of the windows and target body during target rebuilding. One can get a good idea of beam hot spots, contamination in helium recirculation systems, and accumulation of unwanted material in the beam strike. However, the color and finish of a deposit is subject to interpretation, and yields no chemical information or thickness of deposit. More quantitative methods exist.⁶ Table I illustrates several surface analysis methods and their characteristic exciting and emitted particles.

Table I. Summary of surface analytical methods.

excitation by	detection of		
	electrons	ions	X-rays
electrons	AES,SEM	ESID	EMPA/EDX
ions		SIMS	PIXE
X-rays	ESCA/XPS		XFA/XRD

Among these, some are more commonly used for a survey of the material in question. Scanning Electron microscopy with energy dispersive x-ray analysis (SEM/EDX) can look at the elemental composition of material 10 μm deep (called the information depth), while giving a picture of the surface at up to 10000x magnification. However, SEM/EDX can not give chemical bond information. Scanning Auger electron spectroscopy (AES) can give an image of the surface in question showing the distribution of a given element, but again yields no chemical information. Secondary ion mass spectroscopy (SIMS) has an information depth of 1nm, and can provide isotopic information; but is not generally

used for the first scan. Electron spectroscopy for chemical analysis (ESCA) or x-ray photoelectron spectroscopy (XPS) can give limited chemical state information, and has an information depth (in the case of this work) of 40 Å. Coupled with a sputtering ion gun to remove thin layers of material, this method allows depth profiling of the surface in question. All of the methods listed above are available at Martin Marietta Energy Systems in Oak Ridge, Tennessee. The work presented here focuses on the use of ESCA for target surface analysis.

Several types of data are available from ESCA. Usually, a *survey* scan is done which collects electron energies over a broad range to establish the presence of expected and unexpected elements. The data is plotted in counts versus energy, showing the characteristic peaks of each element present. Once the elemental composition of the sample is known, the same data can be reduced to an *atomic concentration table*. The peak size is corrected for sensitivity factors associated with each element. This information can be used to set up narrow energy region scans. Electrons are collected only at the narrow energy ranges associated with the strongest peaks of the known materials on the sample. Depth profiling can be accomplished by collecting photoemission data while sputtering with 4kV argon ions. After sufficient data is taken at each energy, the ion gun can sputter off approximately 100 Å when operated for 30 seconds (referenced to SiO₂ on Si), and the process is repeated. The resulting depth profile can be presented two ways. The atomic concentration of elements versus sputtering time can be plotted in an *atomic concentration profile*. Also a cascaded array of peaks or *montage* can be generated, showing the history of the peak shape and position through successive sputter cycles. This is helpful in identifying chemical changes to the material throughout its depth profile.

Discussion - Havar foils

The data is presented in the form of several case studies. In the first, we have looked at havar window samples that have been taken from the fluoride ion target at the University of Tennessee Medical Center. Three foils with different colored deposits were taken from a collection of discarded windows, and descriptive names were given to these samples; Green Sample, Brown Stripe, and Black Smudge. All the samples had a visually unblemished area available for a control scan as well as the area of the deposit. No historical data on the foils was available other than they had all been run with a nickel plated copper target. A survey scan and minimal depth profiling (one sputter cycle, 10 seconds) were done on each of the foils. A summary of the results is presented in Tables II and III. A typical survey scan is shown in Figure 1.

All of the expected (Fe, Co, Ni, Cr) and several unexpected elements were found in the surveys of these foils. Copper was found on the Black Smudge and the Brown Stripe, presumably from deterioration of the nickel coating in the copper target. Nickel was found on all of the samples, in some cases in higher amounts than specified for Havar. This could be due to migration of the nickel from the target body plating, proton sputtering of the plating, or diffusion of nickel from the bulk of the foil to the surface from galvanic or thermal mechanisms. The effect of this migration and the depletion of the nickel in the bulk of the foil (if any) on the mechanical and chemical characteristics of the foil has yet to be investigated.

Silicon was observed on almost all of the samples, before and after sputtering and in control and deposit areas. The source of the silicon is most likely o-ring lubricant. Control scans on unirradiated foils smeared with two different greases show higher levels of silicon, phosphorous and sulphur. The role of silicon in the performance of this target is

not known. The percentages are in some cases surprising. The Black Smudge and the Brown Stripe had more than 3.3 at.% silicon before and after sputtering and in control and deposit areas. Sulfur, zinc and phosphorus were also observed in significant quantities. The Green Sample had 4.3% phosphorus in both the pre and post sputtering scans. The source of this phosphorus is not yet known. The Brown Stripe had 3.1 at.% sulfur on the surface and 1.2 at.% after 10 seconds of sputtering. The Green Sample had zinc in the control area, more after sputtering, and to a lesser degree in the deposit area.

Table II. Summary of x-ray photoelectron (XPS) atomic concentration percentages survey results for three Havar samples of the **expected** elements. The smaller percentage elements (W, Mo¹, Mn, and Be) were not found to any appreciable degree in the survey data.

Sample / Sputter time	C 1s	O 1s	Co 2p ₃ <small>see note 2</small>	Fe 2p ₃ <small>see note 2</small>	Cr 2p ₃ <small>see note 2</small>	Ni 2p	Cu 2p
Brown Stripe - control / 0 sec	63.9	22.9	yes	yes	1.9	0.4	-
Brown Stripe - control / 10 sec	29.5	29.2	~11.5	~6.6	12.3	4.3	-
Brown Stripe - 0 sec	32.6	44.0	~1.1	~0.6	-	8.1	5.1
Brown Stripe - 10 sec ³	6.9	46.1	-	-	-	15.2	16.2
Black Smudge - control / 0 sec	54.7	30.3	-	-	2.6	2.5	-
Black Smudge - control / 10 sec	6.6	37.5	13.6	9.0	18.0	7.6	-
Black Smudge - 0 sec	45.5	41.4	0.4	-	1.4	3.6	11.0
Black Smudge - 10 sec	16.2	54.6	-	-	-	12.6	4.8
Green Sample - control / 0 sec	38.6	42.4	-	-	0.8	9.8	-
Green Sample - control / 10 sec	7.2	48.0	-	-	9.8	28.6	-
Green Sample - 0 sec	17.8	51.8	-	-	-	20.5	-
Green Sample - 10 sec	10.8	51.0	-	-	-	24.2	-

¹ N and Mo have photoelectron peaks in the same area (400 eV).

² Fe, Co and Cr have main photoelectron peaks in the same regions as the Ni Auger peaks. The atomic concentration percent values are rough estimates and may be high.

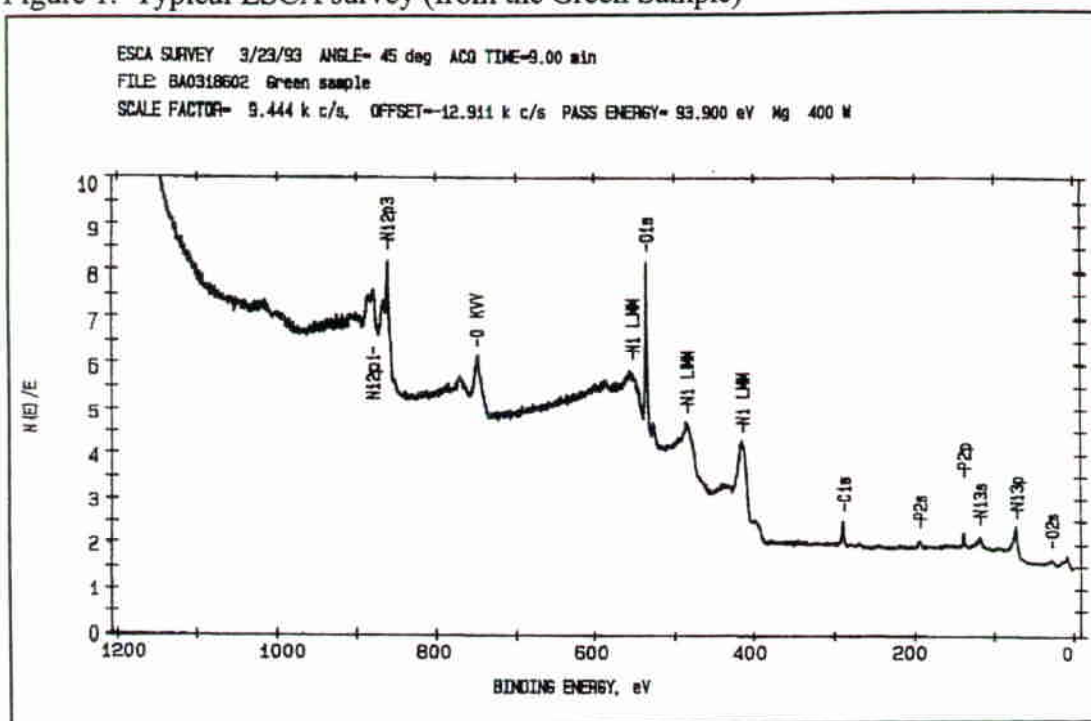
³ Used the Mg anode to shift the Ni Auger peaks and verify amounts of Fe, Co, and Cr. No Fe, Co, or Cr were noted.

⁴ Main constituents of Havar are Co (42%), Cr (20%), Fe (18%), Ni (13%), W (3%), Mo (2%), and Mn (2%).

Table III. Summary of x-ray photoelectron (XPS) atomic concentration percentages survey results for three Havar samples of the **unexpected** elements.

Sample / Sputter time	N 1s	Si 2p	S 2p	Pb 4f	P 2p	Zn 2p3	Mg 2s
Brown Stripe - control / 0 sec	0.8	6.8	0.8	-	-	-	-
Brown Stripe - control / 10 sec	0.7	4.3	0.7	-	0.9	-	-
Brown Stripe - 0 sec	1.8	3.3	3.1	-	-	-	-
Brown Stripe - 10 sec	2.1	3.6	1.2	-	-	-	4.5
Black Smudge - control / 0 sec	1.3	5.0	-	0.3	1.7	-	-
Black Smudge - control / 10 sec	-	~6.1	-	-	-	-	-
Black Smudge - 0 sec	0.7	3.3	1.8	-	-	-	-
Black Smudge - 10 sec	1.4	5.4	0.5	-	-	-	-
Green Sample - control / 0 sec	0.7	3.2	-	-	-	0.6	-
Green Sample - control / 10 sec	0.2	1.2	-	-	-	2.5	1.3
Green Sample - 0 sec	-	-	-	-	4.3	-	-
Green Sample - 10 sec	1.6	-	0.4	-	4.3	0.4	-

Figure 1. Typical ESCA survey (from the Green Sample)



The ESCA method is sensitive enough to pick up absorbed gases on surfaces so almost all the samples in this report show carbon and oxygen on the surface as delivered to the lab. Without sputtering, the carbon, nitrogen and oxygen contribute significantly to the observed photoemission signal. In most cases the first sputter cycle of 30 seconds removes this layer. The Green Sample did not show reduced oxygen with sputtering in the deposit although it did on the control surface. The other samples did exhibit much less oxygen after even the first sputter cycle. The conclusion is that only the green deposit was an oxide. All three coatings had been presumed to be oxides of some element, so this was a surprise. The higher level of nickel in the Green Sample and the green color point to this sample being nickel oxide. This is confirmed by the shape of the nickel peak observed (Fig. 2a). This can be compared to nickel metal and nickel oxide peaks (Fig. 2b).

Pittsburgh Silver target

In the fall of 1992 we received a target from our customer at the University of Pittsburgh. It was a stock fluoride ion target which is 10mm diameter by 2 mm deep and is made of 99.99% silver ingot (Fig. 3). It had exhibited a decline in ^{18}F - yields that was unrecoverable by standard target cleaning procedures. We studied this target and another stock target that had run and produced good ^{18}F - yields in our factory. Both targets were surveyed and profiled in two areas, one inside the beam strike and one outside of the beam strike on the target face.

The survey of the stock target revealed nothing surprising (Fig. 4.). Cobalt was found in the beam strike of the stock target but not on the control area. Silicon was detected on the control area (close to the o-ring groove) but not in the beam strike. Chlorine was found on the control area but not in the beam strike. The Pittsburgh target had several marked differences (Fig. 5, Table IV). Zinc was detected, at an atomic percentage of 1.5 at.%, in the beam strike but not elsewhere. A substantial amount of silicon was detected on the control area (15.1 at.%) and less but significant amount (1.5 at.%) in the beam strike. Large amounts of silicon and zinc in post irradiated water have been reported¹, but no

conclusion was drawn as to their effect on ^{18}F - production or FDG yield. Combined with the data presented here, it appears that these elements may be responsible for poor ^{18}F - yields.

Figure 2a. Expanded plot of nickel peak from Green Sample

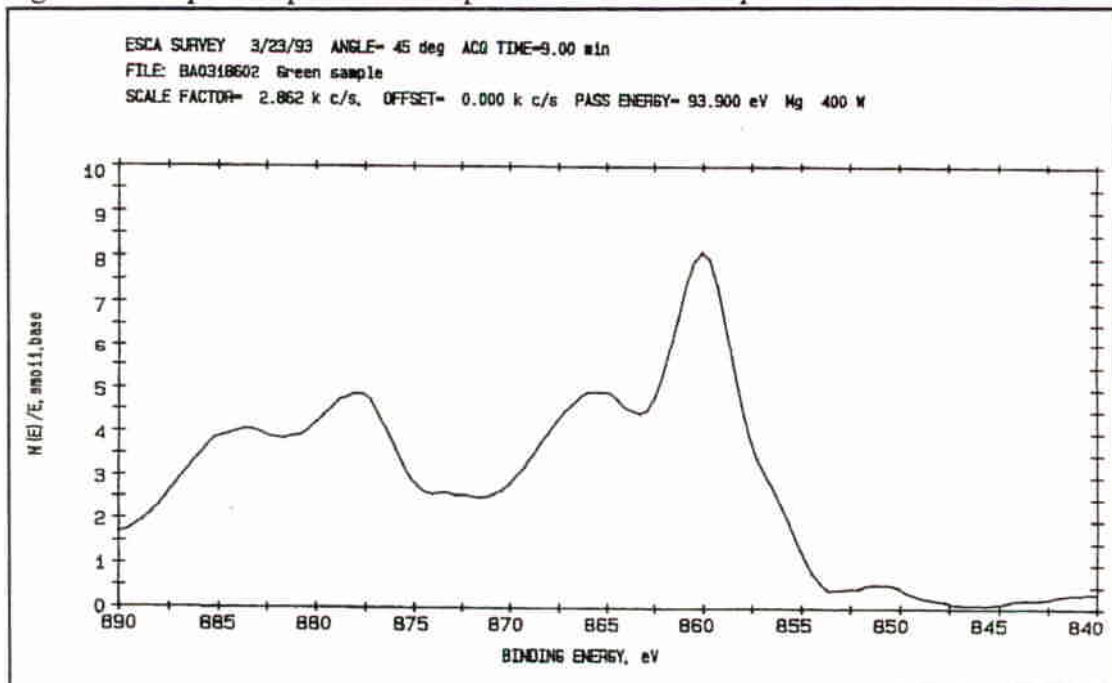


Figure 2b. Typical nickel peak and nickel oxide peak. Reprinted from Handbook of X-ray Photoelectron Spectroscopy. Moulder, J.F. et al. Perkin-Elmer Corporation, pub. (1992)

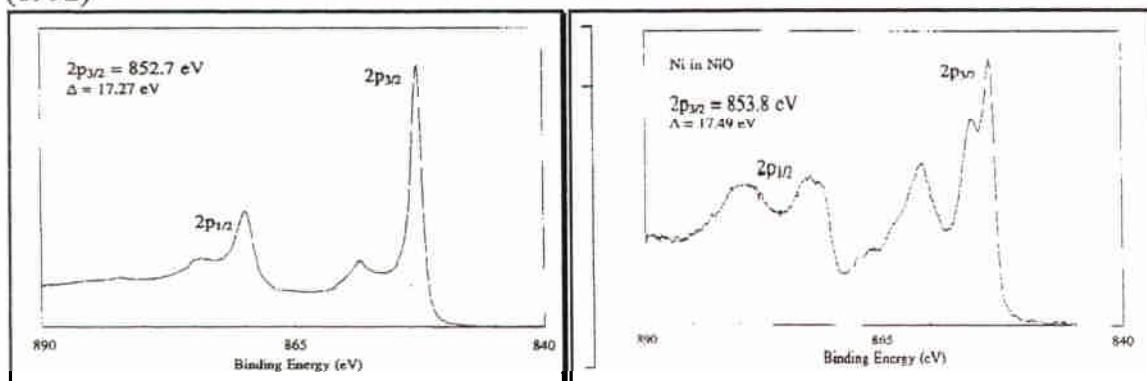


Figure 3. Silver reflux target cross section.

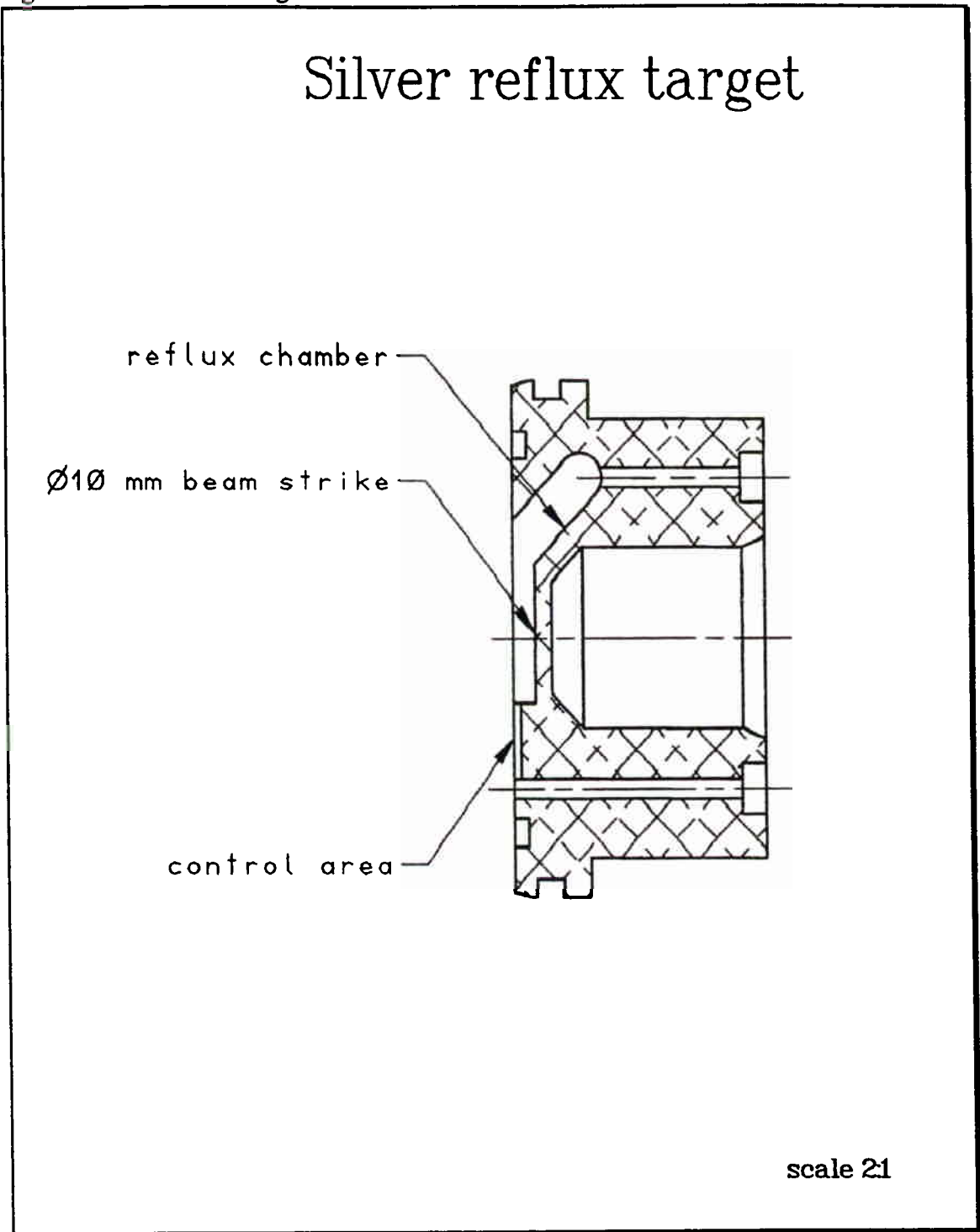


Figure 4. ESCA survey of the stock silver target.

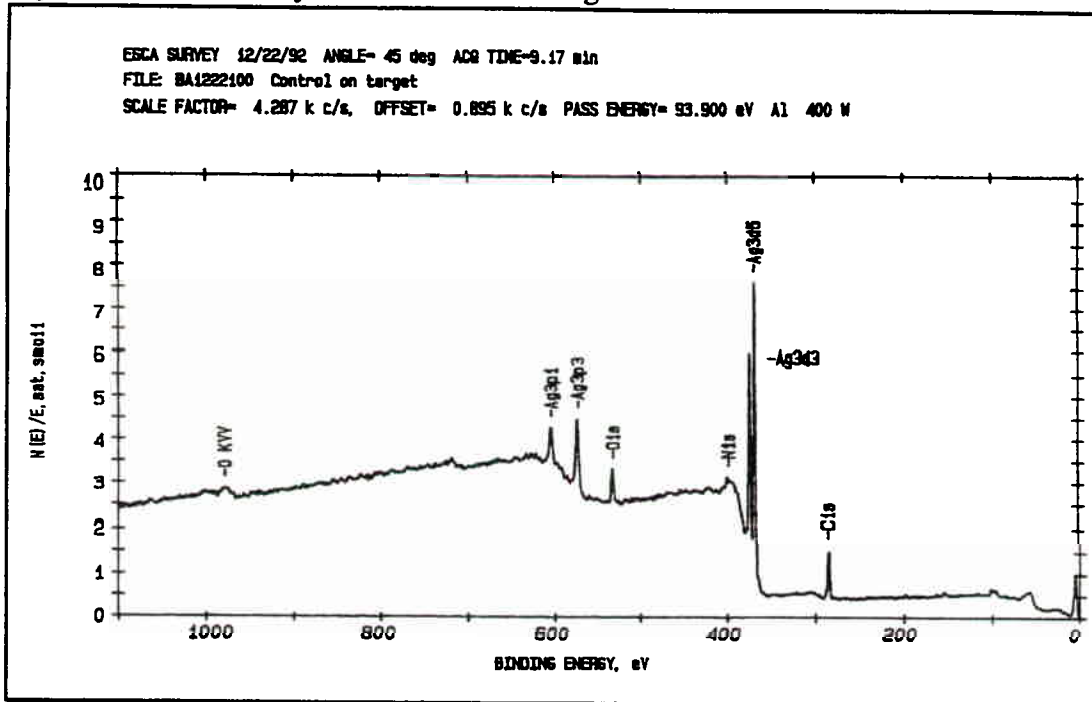


Figure 5. ESCA survey of the Pittsburgh silver target.

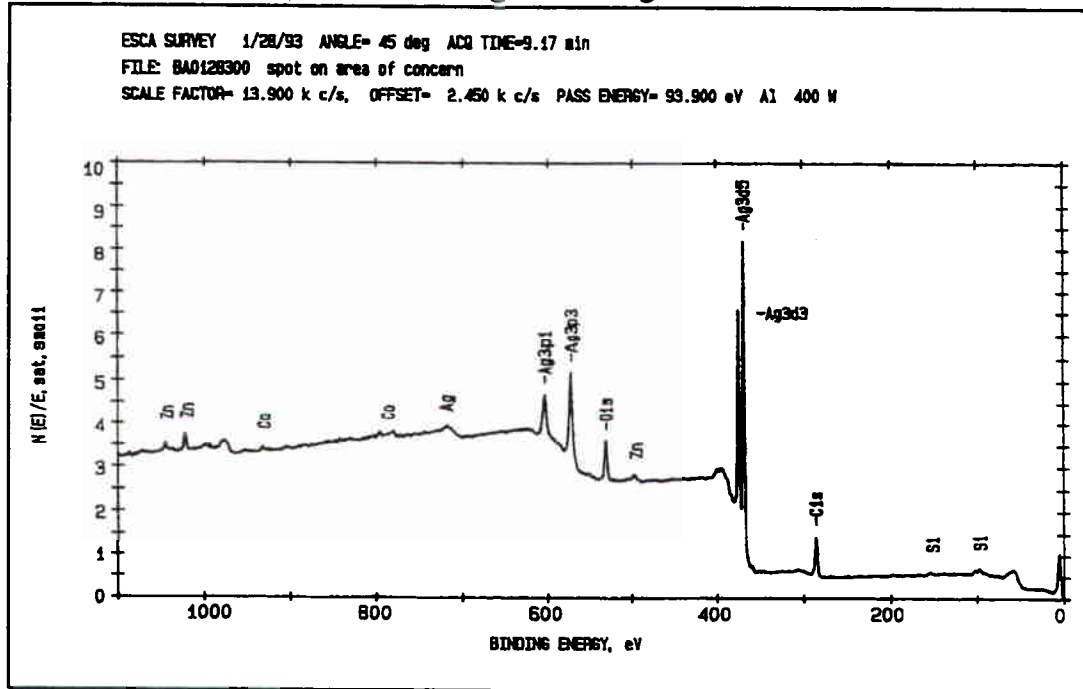


Table IV. Summary of x-ray photoelectron (XPS) atomic concentration percentages survey results for two silver targets.

Sample	C 1s	O 1s	Ag 3d	N 1s	Co 2p	Cl 2p	Si 2p	Zn 2p _{3/2}
Stock - control	55.0	15.7	22.7	3.4	-	0.8	2.3	-
Stock - beam strike	20.6	34.7	42.3	-	2.5	-	-	-
Pittsburgh control	61.0	22.3	1.5	-	-	-	15.1	-
Pittsburgh - beam strike	46.7	22.1	23.9	3.0	0.6	0.6	1.5	1.5

Another element that showed up in two of the scans was chlorine. It was found at .8% on the control area of the stock target, and .6% in the beam strike of the Pittsburgh target. It was only on the surface in the stock target, but took several sputter cycles to be removed from the Pittsburgh target (Fig. 6). It appeared to be in a form analogous to metal chlorides. Chlorine (in the form of dilute HCl) has been shown to enhance radiolysis of water in the presence of fast neutrons⁷, and the same process would be expected for a water target under proton irradiation. The chlorine in the beam strike of the Pittsburgh target could have contributed to excessive radiolysis in their production runs, causing the target to run dry by the end of a 1 hour run. High gas production rates can also lead to reduction of average target density, reducing the effective thickness of the target below yield thickness. There is an apparent correlation between the presence of chlorine on the target walls with low ¹⁸F- yield. What remains to be investigated is if there is a threshold or optimal condition for chlorine in the target water and on the surfaces of the target. Solin et al.³ have found that when the chloride ion in the post irradiated water is low (<40 μmole/L) so is the ¹⁸F- yield. This has led us to further investigations involving the role of trace chlorine in target performance.

Silver target - intentional contamination with chloride ion

Our own HPLC studies of unirradiated enriched water from a variety of sources show concentrations varying from 2 to 10 ppm (equivalent to 56 to 282 μmole/L) (Fig. 7). Dolin et al.⁷ have shown that (in the case of fast neutrons) radiolysis dramatically increases with chloride ion concentrations over 1 mmole/L. With this in mind we hypothesized that chlorine could remain in the target from run to run (as silver chloride or some other species) and enter the target water under irradiation. Changes from lot to lot of enriched water would be clouded by long term surface conditioning effects. In addition, chloride could accumulate on the target walls leading to deterioration of performance and eventually target failure. Silver chloride is soluble in 100 degrees C water at 591 μmole/L⁸. This drops to 25.1 μmole/L at 10 degrees C. We have intentionally run a target with very high (48 mmole/L, equivalent to 1700 ppm) concentrations of HCl in natural water to correlate radiolysis and chlorine.

A silver target body similar to the one above was taken directly from stock and analyzed with ESCA. This target had never been irradiated. Surface chlorine at levels equivalent or higher than the Pittsburgh target were found in all areas (Table V, Fig. 8).

Zinc was also found in very small percentages. The target was then cleaned with the standard cleaning procedure used at CTI (5 minutes sonicate in acetone, 5 more in methanol, rinse and sonicate in HPLC grade water). The subsequent scan still showed surface chlorine at a variety of places on the target (Table VI, Fig. 9). We then began a series of runs bombarding natural water for the $^{16}\text{O}(p,)^{13}\text{N}$ reaction, and monitoring radiolysis with the apparatus below (Fig. 10). The evolved gas was measured in a 100 cc cylinder inverted in a beaker of water. The runs are summarized in Table VII.

Figure 6. Montage of the chlorine peak from the Pittsburgh silver target beam strike. Curves are sequenced back to front.

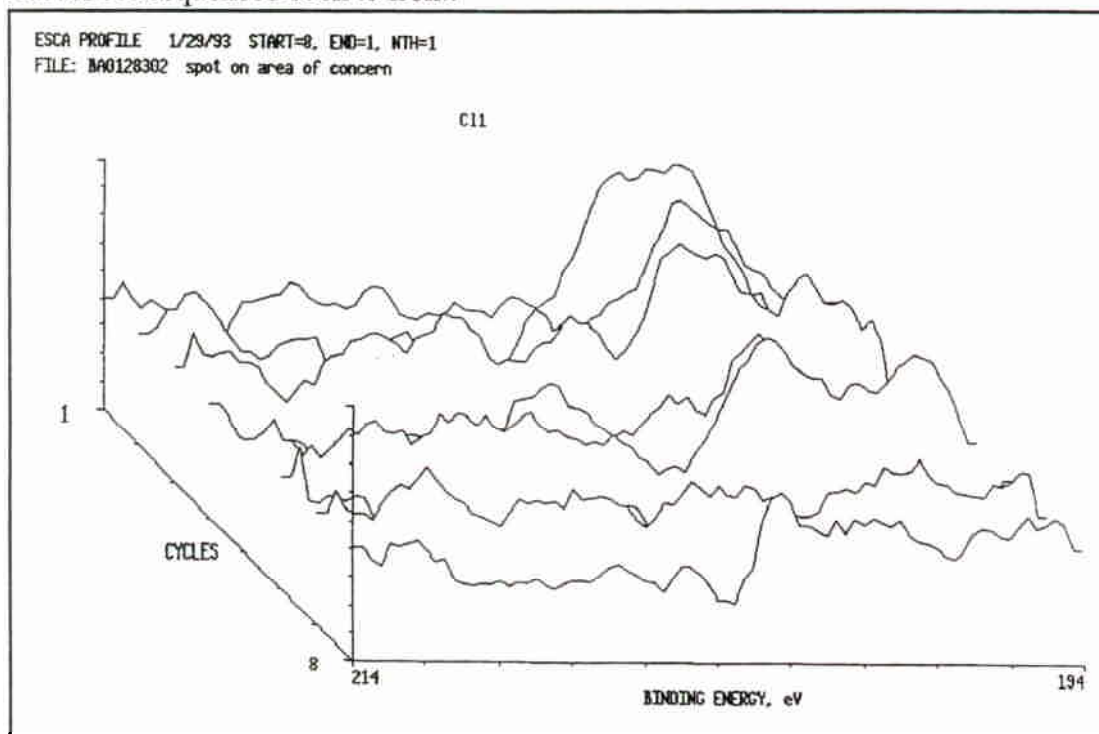


Figure 7. HPLC analysis done on unirradiated ^{18}O enriched water.

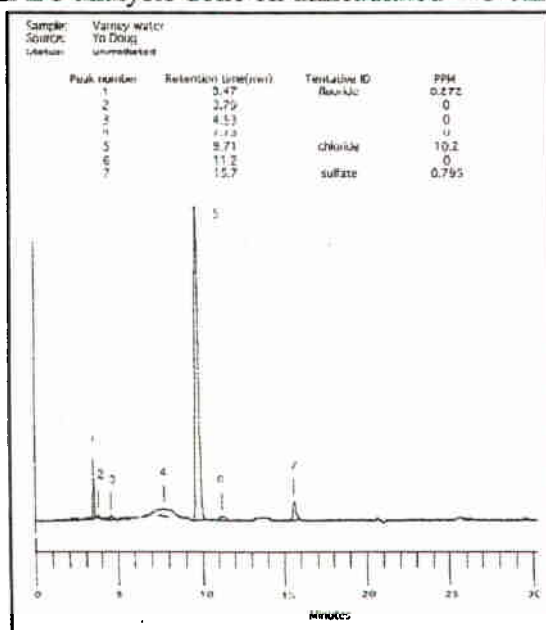


Figure 8. Montage of the Chlorine peak on the silver target before cleaning. Curves are sequenced back to front.

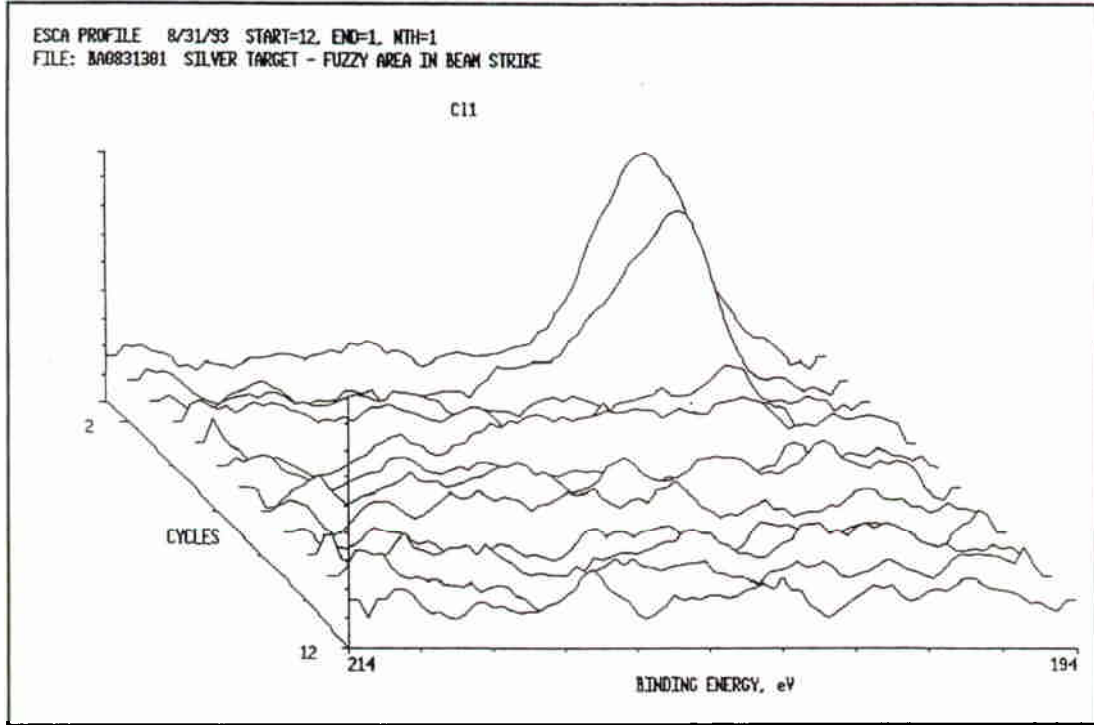


Figure 9. Montage of the Chlorine peak on the silver target after cleaning.

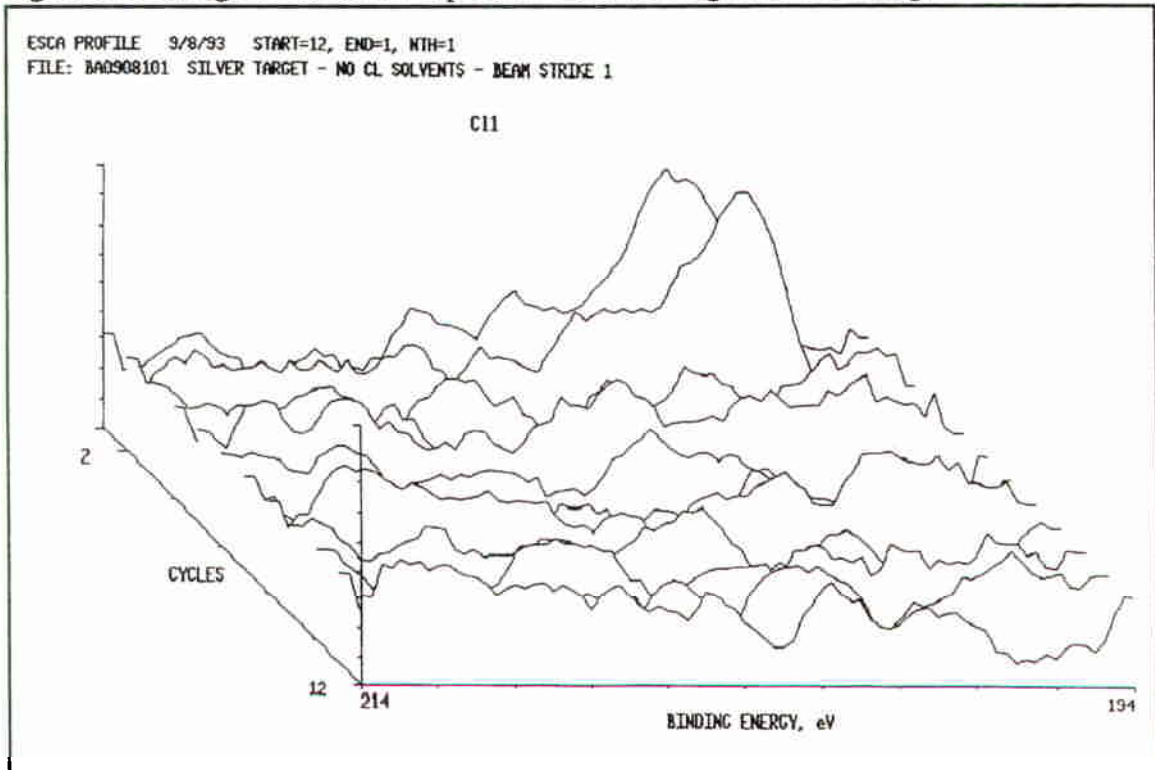


Figure 10. Schematic of the apparatus.

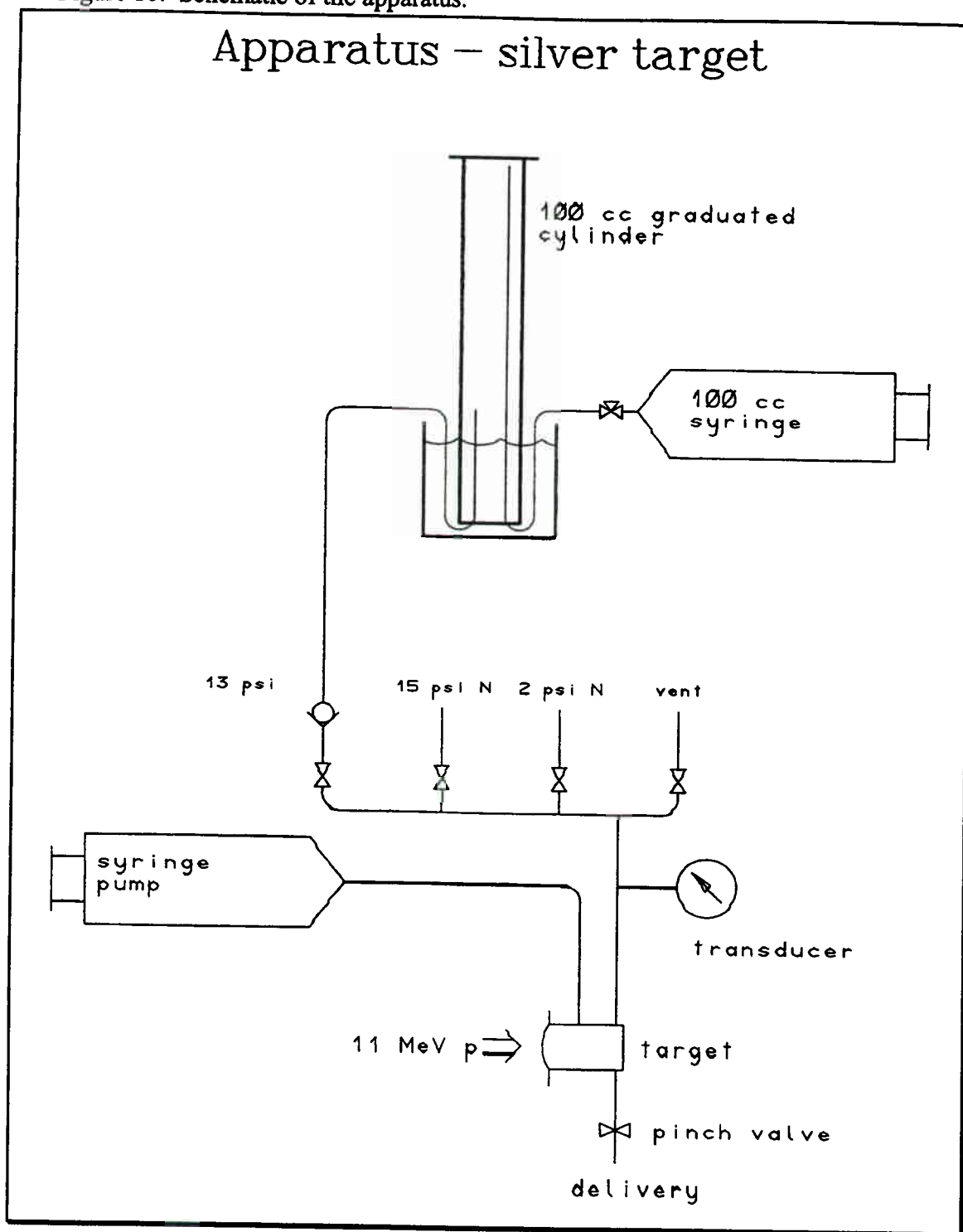


Table V. Summary of x-ray photoelectron (XPS) atomic concentration percentages survey results for the silver target as received from vendor. Beam strike 1 & 2 refer to two places in the same beam strike.

Sample	C 1s	O 1s	Ag 3d	Cl 2p	Zn 2p3
Beam strike 1	71.1	16.3	9.4	0.8	0.4
Beam strike 2	66.0	11.9	20.6	0.8	-
control	72.9	18.2	6.5	1.0	0.2

Table VI. Summary of x-ray photoelectron (XPS) atomic concentration percentages survey results for the silver target after cleaning.

Sample	C 1s	O 1s	Ag 3d	Cl 2p	N 1s
Beam strike 1	44.4	16.6	33.7	0.6	4.7
Beam strike 2	46.3	13.8	30.2	1.8	7.8
control	68.2	20.1	9.0	0.5	2.1

Table VII. Summary of beam runs on a stock CTI target using HPLC grade natural water. All runs were done at 20 μ A

Run #	1	2	3	4	5	6	7	8	9	10	11	12	13	14
Time of bombardment (min)	20	20	20	5	5	5	20	20	20	20	20	20	20	20
gas production rate (cc/min.)	10.0	6.8	6.9	10.4	9.8	10.0	7.1	4.8	4.7	1.1	0.45	0.45	0.55	0.90
Cl ion?	N	N	N	N	N	N	N	N	N	170	170	170	170	N
										0	0	0	0	
										ppm	ppm	ppm	ppm	

Before chloride ion treatment the target showed a steady decrease in evolved gas over 9 runs, all at 20 μ A and from 5 to 20 minutes of bombard time. The gas rate did not change appreciably during any one run, and seemed to be dependent on the number of runs, not the amount of beam time. The target produced 10.0 cc/min. of gas during the first run and 4.7 cc/min during the 9th run.

The target was loaded with .048M HCl in water, made from the same bottle of HPLC grade water used in the previous runs. The radiolysis rate immediately dropped to 1.1 cc/min. and over four 20 minute runs dropped to .45 cc/min. This result was not expected. When the target was reloaded with only HPLC water, the evolved gas rate went back up to 0.9 cc/min., but not close to the former lowest rate of 4.5 cc/min. More data is required to establish if this is a permanent alteration of the radiolysis rate from this target.

The target was dismantled and the silver body visually inspected. The back of the beam strike had a dull gray appearance, but the reflux area remained fairly bright silver. An ESCA survey and profile were done on two locations in the gray area in the beam strike and on a control area on the face of the target. The pre-sputtering surveys in all three locations turned up silver and chlorine and the usual carbon, nitrogen and oxygen, but no other unexpected elements (i.e. metals) (Fig. 11). A profile of the deposit showed chlorine in the gray surface of the target at least 300 Å deep (Fig. 12). After 5 minutes of sputtering, oxygen, carbon and nitrogen were not present in significant quantities. No chlorine below the surface was seen on the control area (Table VIII, Fig. 13).

Table VIII. Summary of x-ray photoelectron (XPS) atomic concentration percentages survey results for the silver target after chloride ion treatment with beam and 5 minutes of sputtering.

Sample	C 1s	O 1s	Ag 3d	Cl 2p
Beam strike 1	5.9	4.0	78.4	11.7
Beam strike 2 ¹	-	-	91.0	8.9
control	5.5	2.0	92.5	-

¹ Absence of carbon and oxygen due to overlap of sputtered areas. Beam strike
² started having been sputtered approximately 300 seconds.

It is clear that high radiolysis rates are undesirable from the standpoint of consumption of target water and thinning of the target. From this data one can conclude that chloride ion in large amounts (>10 µmol/L) does not increase radiolysis of water under proton irradiation. To the contrary, under our experimental conditions we see a dramatic decrease in the rate of gas evolution. No other elements that might have skewed the reaction towards recombination remained in detectable levels on the target surface. However, this level of chlorine in the target would almost certainly poison subsequent syntheses of FDG, making copious amounts of chlorodeoxyglucose. It is clear from the cleaning of the target pre-irradiation and the few runs done post-irradiation that the target readily absorbs chlorine and the two are then not so easily parted. It is also clear that a few runs with water high in chloride ion will affect the next several runs in evolved gas rate and potentially fluoride ion and FDG yield. This is a work in progress. Further work will be done to establish the optimum amount of chloride ion (if any) desired in the target water and on the target walls. It would also be of interest to study any surface specific differences from running a silver window with this silver target. The appropriate cleaning method to remove any species deemed detrimental to yield could be investigated by ESCA as well.

Figure 12a. Atomic concentration depth profile of spot 1 in the beam strike.

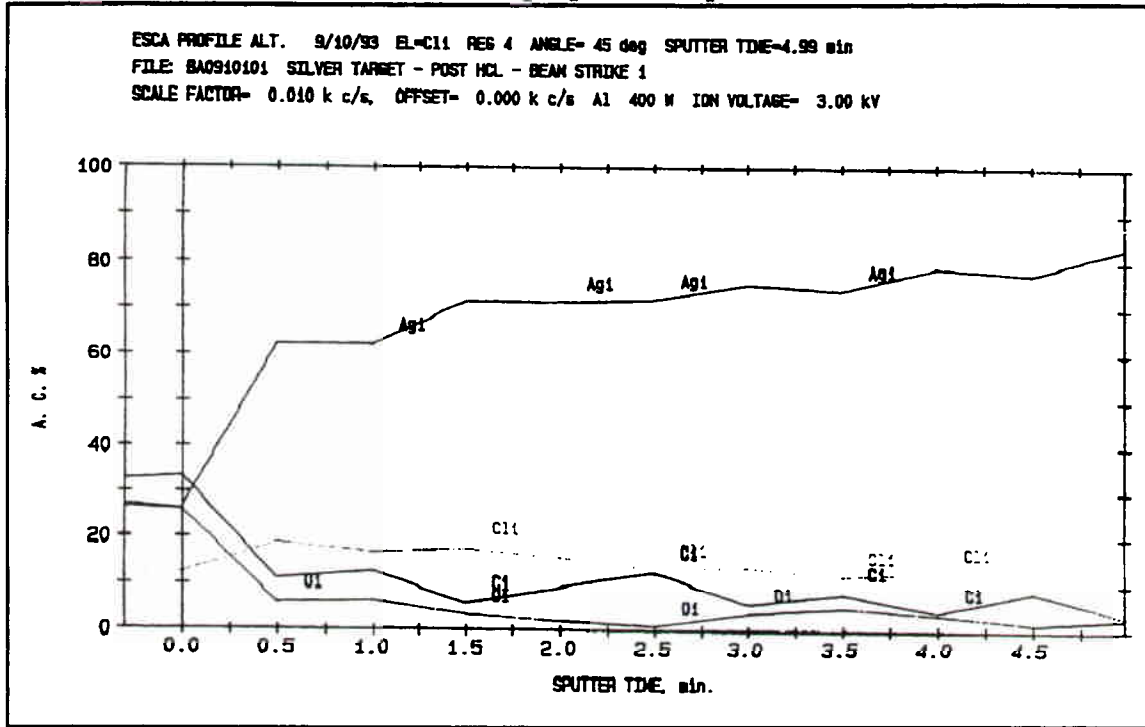


Figure 12b. Atomic concentration depth profile of spot 2 in the beam strike.

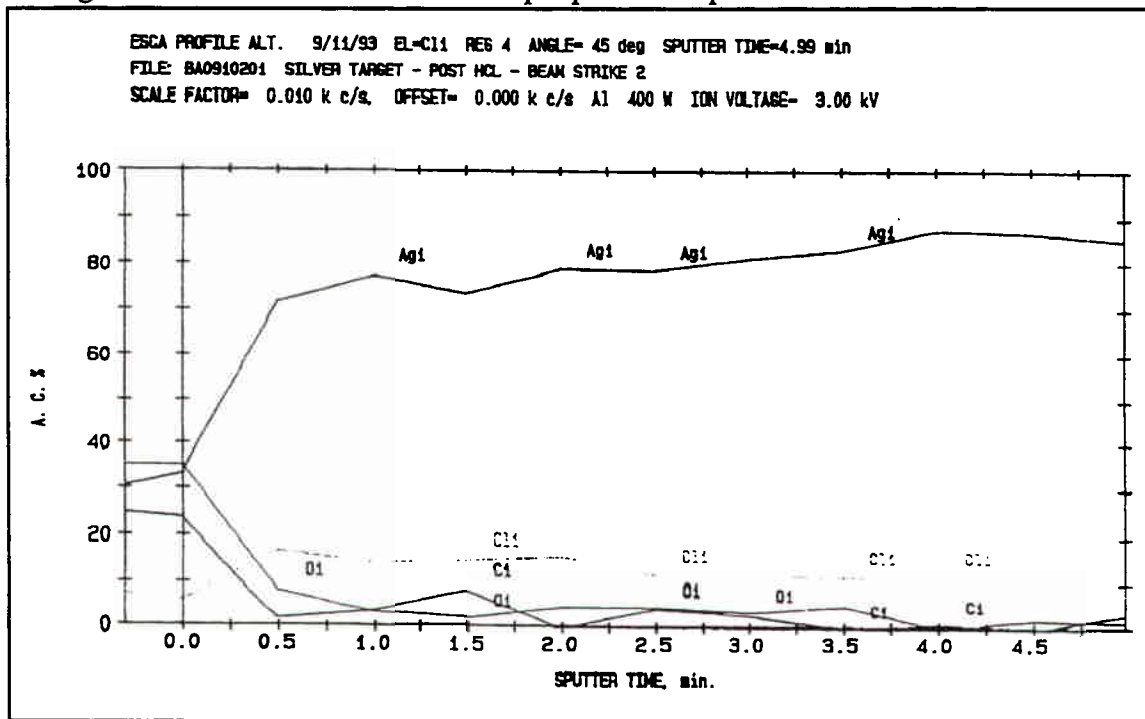


Figure 13a. Montage of the chlorine peak from spot 1 in the beam strike.
Curves are sequenced from front to back.

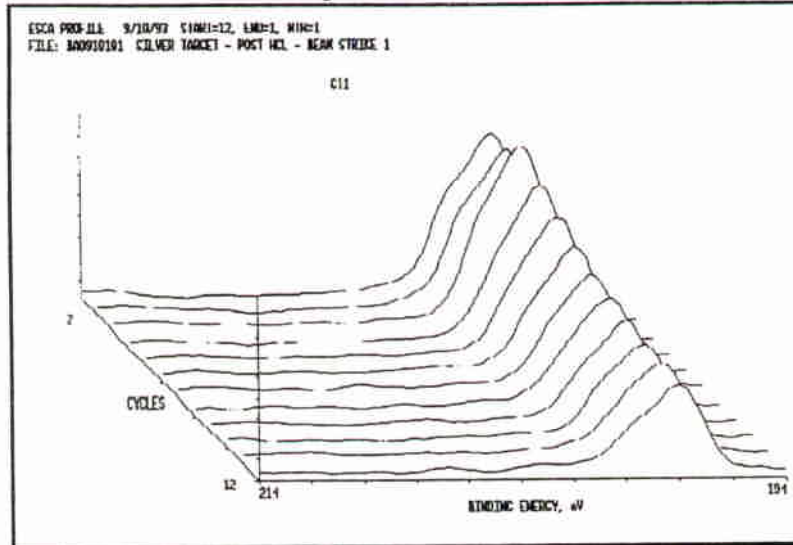


Figure 13b. Montage of the chlorine peak from spot 2 in the beam strike.

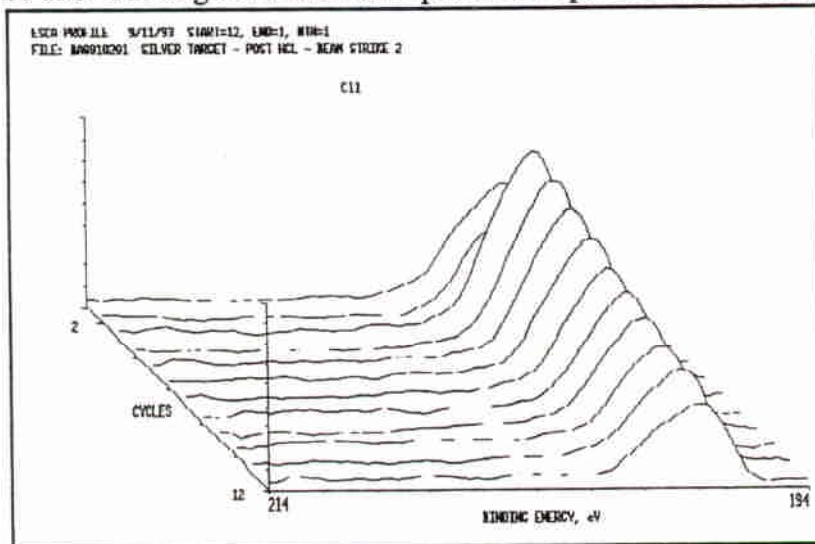
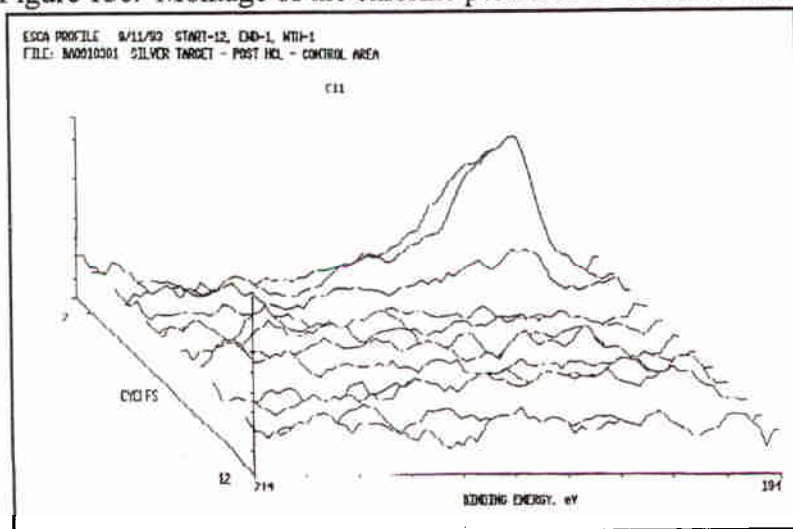


Figure 13c. Montage of the chlorine peak from the control area.



Conclusion

ESCA has been shown to be an invaluable tool in detecting contaminants and conditions on target and window surfaces. It can be used for post-mortem failure analysis of targets as well as in structured experimentation on target surface chemistry. Its use will make a positive impact on the issues of reliability and repeatability facing clinical users of accelerators for PET isotope production.

This document was prepared by Bill Alvord et al. as a result of the use of facilities of the U.S. Department of Energy (DOE) which are managed by Martin Marietta Energy Systems, Inc. (Energy Systems). Neither Energy Systems, DOE, the U.S. Government, nor any person acting on their behalf: (a) makes any warranty or representation, express or implied, with respect to the information contained in this document; or (b) assumes any liabilities with respect to the use of, or damages resulting from the use of any information contained in this document.

Reference

1. Harris, C.C., Need, J.L., Ram, S., Coleman, R.E.: Production of F-18 Fluorodeoxyglucose with a Computer-Controlled Synthesis Unit. *Proceedings of the Third Workshop on Targetry and Target Chemistry*, June 19-23 1989, Vancouver, British Columbia, Canada. T.J. Ruth, Ed. pp 123-128
2. Jegge, J., Zimmermann, R., Schwarzbach, R., Reddy, G., Nickles, R.J., Schubiger, P.A., Christian, B., Baker, E.: Enriched Oxygen-18: Testing the Waters. *Proceedings of the Fourth Workshop on Targetry and Target Chemistry*, September 9-12, 1991, Villigen, Switzerland. R. Weinreich, Ed. pp 125-126
3. Solin, O., Bergman, J., Haaparanta, M., Reissell, A.: Production of ^{18}F from Water Targets. Specific Activity and Anionic Contaminants. *Appl. Radiat. Isot.* 39, 1065-1071 (1988)
4. Heselius, S.J., Schlyer, D.J., Wolf, A.P.: A Diagnostic Study of Proton Beam Irradiated Water Targets. *Appl. Radiat. Isot.* 40, 663-669 (1989)
5. Steinbach, J., Guenther, K., Loesel, E., Gunwald, G., Mikecz, P., Ando, L., Szelecsenyi, F., Beyer, G.J.: Temperature Course in Small Volume ^{18}O Water Targets for ^{18}F F-Production. *Appl. Radiat. Isot.* 41, 753-756 (1990)
6. Hantsche, H: Comparison of Basic Principles of the Surface Specific Analytical Methods: AES/SAM, ESCA (XPS), SIMS, and ISS with X-ray Microanalysis, and Some Applications in Research and Industry. *Scanning* 11, 257-280 (1989)
7. Dolin, P.I., Ershler, B.V.: Radiolysis of Water in the Presence of H_2 and O_2 due to Reactor Radiation, Fission Fragments, and X-Radiation. *Proceedings of the International Conference on the Peaceful Uses of Atomic Energy*, August 8-20, 1955, Geneva, Switzerland. pp 565-575
8. Kohl, W.H.: Handbook of Materials and Techniques for Vacuum Devices. Reinhold Publishing Corporation, 1967. pp 433-435

Questions for Surface Sensitive Analysis of Materials Used in the Production of PET Isotopes

Speaker: Bill Alvord of CTI

The questioner is identified where possible and the answers are provided by the speaker unless otherwise indicated.

Question: Rich Ferrieri, BNL

Bill, the persistent chlorine peak you referred to appears to be the result of a very thick layer..(inaudible). Is there any evidence in the literature for say, a diffusible chlorine species in silver that may be diffusing to the surface as its being depleted through the sputtering action?

Reply:

My answer to that is, I don't know.

Rich Ferrieri

There has been some evidence of other carbonaceous materials doing that in metals and I wonder whether you seeing the same sort of thing happen here. It may be just a diffusion phenomena that you are experiencing.

Answer:

Right, in the case where I aggressively chlorinated it, I think it's fairly clear that it's the presence of chlorine that did it because outside of the beam strike that's not there. Now on the other hand, the stuff I showed that doesn't really seem to clean off, that may very well be what's going on rather than a chlorinated solvent remaining behind but I just have to look into that further.

Question: Bruce Wieland, Duke University

We routinely measure radiolysis rate on all of our fluoride ion production runs which we do about 3 or 4 times a week. 20 μA for 60 minutes about make on the average 550 mCi and this is a little intuitive because I haven't put all the data together but we generally run between 40 and 100 ml total of gas collected for that one hour run.

Bruce Wieland

For a one hour run?

Answer:

For a one hour run. And, what I think I've noticed is that if you go above the 100 ml mark that you generally have a fluoride ion production problem. You generally have a lower yield of fluoride ion and if you go to very, very low radiolysis rates like below 40, maybe 15 or 20, we sometimes then have reactivity, we make F^- activity but we have trouble with the FDG synthesis. So, I have to collect some more data and see if what I can make out of it. But one of the things that might indicate a problem with the high radiolysis rates is if you calculate the amount in a beam strike in that target I believe is 80 μL per millimeter and it's two millimeters thick so you got 160 μL in a beam strike and you are making an awful lot of gas so if your radiolysis gas is high enough that you have reduced the density of the target material by having vapor voiding by

gas bubbles, then that would make physical sense that your yield of F would go down.

Why you would have poor FDG yields at very low radiolysis rates, I will leave that to the chemist.

I agree with you. I think its interesting that I anticipated showing that chloride was going to enhance radiolysis seeing that it doesn't. In fact it may have the opposite effect and your observations and Solin's (Turku) observations tell me that maybe when you get very low chloride ion content, the FDG yields might, I don't know why they would go south (decrease), but the low chloride ion content might cause you to actually have high radiolysis again.

Question: John Clark, MRC Hammersmith

Bill, I'm trying to focus in on one or two things that intrigue me here. When you put the chloride into the target, do you still have chloride in solution at the end of radiation or is it all on the silver?

Answer:

With the amount that I put in, I am certain that I still had some in solution. Now, I did an intermediate wash every time I ran, and I washed the target again in the hopes of not having remaining chloride contribute to more or less radiolysis in the next run. In other words, trying to have it start from the same condition after having been rinsed with a water free of any chloride ion but I did not look at my water coming out and do any HPLC on it, so I can't tell you conclusively. I know that the chlorinating solution, the .048 molar solution is I'm sure I didn't exhaust all the chlorine in that at the end of the run. I did brief runs of 20 minutes.

John Clark

I'm trying to dissect in my mind whether the silver chloride surface has any recombination capabilities. I mean platinum obviously has, but I know no reference that silver chloride is good at recombining radiolytic gas. But presumably if you aren't making radiolytic gas then the target pressure doesn't go up so the boiling point of the water stays low. And that has a very simple explanation why yield would be low, because you've got a boiling target.

Answer:

Right, I mean I can tell you that all I had was an observation that in fact I didn't have a lot of gas produced but I was still producing some throughout the whole thing it wasn't as if there was no radiolysis or no evolved gas but I was producing some even during the chlorinated runs.

Question: Marc Berridge, University Hospital of Cleveland

One of the things I clued on there was the silicon, or the silicon levels. In the earlier data you showed quite a bit back, it looked as if your control area had more of it than the beamstrike area. And having seen something that was counter-intuitive your chlorides apparently suppressing the radiolysis it makes one wonder because silicon is a known problem and did you chase that any further?

Answer:

No I haven't chased that any further I mean the reason I think it's higher on the controller is it's

close to the O-ring and it's a simple act of, I think it's from O-ring lubricant and that it's migrating to the beam strike from the O-ring.

Marc Berridge

Where exactly is the control area?

Answer:

I could show you.

Comment: (Jerry Bida, CTI)

Point is well taken, Marc, we have not done a good job of looking at a, quote, controlled surface.

Answer:

Because it seems that where silicon or radiolysis either go up or go down, you have a potential explanation for one of these problems anyway.

Yes, just to answer your question, the control area is this flat outside of the beam strike, anywhere between the O-ring and the edge of the beam strike and for all I know, in some cases, I measured very close to where the O-ring was. In the case of a control area on a foil there were just to keep the dose low as I was moving it to and from Oak Ridge, there was a little teeny snip of foil and it really could have been anywhere, probably close to the beam strike in that case. But those are the sort of things we need to look into. We have found out more questions than answers as I said, so it's one of the things that I want to look at is how much it is contaminating our product.

Question: Tim Tewson, University of Texas Medical School

I would like to make a comment about what is actually meant when people talk about the low yield from the target because there are in fact two possible causes, things that could be going on here. One is simply that you're not making the Fluorine-18, but if you are not making the Fluorine-18 that means there is not enough O-18 in the way of the protons and you've got voids. But, the other possibility is that the stuff is sticking to the target. You are making it, but it is sticking to the target and a low yield in the case of, I admit that your situation is very mysterious but it could be that when you have chloride on the target surface, the fluoride sticks to the target surface better and it doesn't wash out so that you are making it and you're just not getting it out of the target.

Answer:

Right. Now in Bruce's case, things were sort of indicative of chloride poisoning or a chlorine poisoning, he was still getting great F out but not making FDG with it.

Tim Tewson

If it comes out and you don't make FDG with it, it's not F.

Answer:

Or something else came out.

Tim Tewson

Something else. It's got Fluorine-18 in it, but it's not F.

Answer:

Or chlorine came out.

Yes, it could be making chlorodeoxyglucose.

Tim Tewson

Well, is it the amount of triflate that most people put in? I meant certainly the amount of triflate that we put in, I think the amount that most other people put in, it swamps out the amount of chlorine that you are talking about by a factor of, running a quick number in my head, a 100,000?

Answer:

We would have to know what amount of chlorine is coming out of the target. That's just the thing, there is obviously some mechanism for chlorine wanting to stay in the target and not come unless there is very aggressive circumstances for it and I just don't know how much chlorine is coming out of this target.

Tim Tewson

I mean, certainly, it's really difficult to measure. You have a target that's been bombarded and you want to know how fluoride is stuck to the target, it's not an easy job to do. I mean, I don't know how to do it but I think Jerry is going to talk about his neutron detection in just a minute.

Comment: Jerry Nickles, University of Wisconsin

Yes, your question gets answered if you count neutrons.

Tim Tewson

Yes, if you count the neutrons as they come out, the neutrons tell you if you're making the fluorine or not.

Question:

On the silicate, I believe that as you pour the water in you use get more silicate off this. So you always get silicon.

Answer:

Both silicon and chlorine are pretty ubiquitous, they're pretty hard to get rid of but the mechanisms for why they stick or how you can get them off the surface if they are poisoning something are not well understood.

Question: Bob Dahl, North Shore Hospital

We keep seeing the chlorine, the thing that bothers me is that we still really don't know where it's coming from. John Need, didn't you have some analysis done on O-18 water? What was the chlorine content in that, do you remember?

Answer: by John Need, Duke University

I don't know that. I do know that the metal numbers were very high and that the water we used was very interesting, it went into the target clear and came out milky.

Answer: Bill Alvord.

I would draw your attention to this. This is un-irradiated water. This is from the vendor although it may be several vendors mixed together, I can't blame any one vendor. I especially don't want to, having some of them in the audience. But, there were 10 parts per million of chloride ion in that stuff just the way we got it, so that's one place where the chloride ion is coming from.

Bob Dahl

Well if you repetitively bombard water in a target using a new batch each time, and you absorb a little bit of the chlorine each time, that's probably one of the most likely sources isn't it.

Answer:

Uh huh. I think its exactly my point.

Comment: Richard Ehrenkauf, Wake Forest University

I don't know exactly how much chloride we have in the starting water though we have done a lot of analysis of metal ions in some of those samples using atomic absorption but we have analyzed probably close to 100 samples determining how much chlorodeoxyglucose was in those samples. And, it's of the order of about 5 μg of chlorodeoxyglucose per mL and our samples are about 10 mL so we can go back and calculate how much actual chlorine that was incorporated into FDG.

Question: Carlos Gonzalez-Lepera, University of Pennsylvania

If the actual chemistry at the surface level, it actually takes place at a few atomic layers, a few, probably 20 to 40 \AA , isn't it a little bit self defeating, the fact that then you have to sputter those layers to analyze your material. What the chemistry, I think I should be looking for is the one you actually take out of the target and don't even do any sputtering, otherwise you are sort of looking at your base material but that is not even the material that is actually working in your target chemistry system.

Answer:

Yes, I don't neglect when I show chlorine peaks that only come off with sputtering, I don't neglect those as significant, I think those are significant and that the sputtering is just to give us more information. I don't know how much of that surface may be eroded or things may diffuse through it, but I can tell you that there's chlorine right there on the surface and I do think, as you say, that just even the first 20 or 40 \AA is very important to the target chemistry.

An Investigation of Aluminum Alloy 6061 Heat Treatment and its Effect on Iodine Absorption in Nordion Gas Targets

D. R. WILLIAMS, S. HEILEMANN, B. WEBSTER, J. ORZECOWSKI

**NORDION INTERNATIONAL INC. , VANCOUVER OPERATIONS
Vancouver, British Columbia, Canada**

Abstract

The yield of I-123 from gas targets used by Nordion has been noted to vary from target to target given identical irradiation conditions and target geometries. It is suggested that changes in the microstructure occurring during welding of the aluminum 6061-T6 alloy used to make the target, may have an effect on the yield. Various samples of aluminum 6061 were heat treated to the T0, T4 and T6 conditions. The surface microstructure of representative samples were compared, including the machined surface finish as well as the grain structure of the sample. These samples were immersed in a sodium iodide solution labelled with I-123 under similar conditions as that found in the gas target during a production run. The samples were then rinsed and counted for activity remaining on their surface.

Introduction

There has been a number of discussions in the literature on the various factors at work affecting gas target yields (ref. 1, 2, 3). In the case of gas targets used by Nordion, many of these parameters such as target thickness, target material, beam quality, target geometry and for the most part, material of target construction have remained the same for over five years. Yet variations in yield from apparently identical target assemblies have been noted. Average yields from recent Nordion production runs on four separate gas target assemblies indicate that the average yield can vary up to 13% between targets.

It has been speculated that the difference between these targets may be introduced during their manufacturing stage. The manufacturing process of gas targets used and supplied by Nordion has been controlled to the point of final dimensional and initial material specifications only. The final metallurgical state of the 6061-T6 aluminium alloy used in target construction is not controlled. The temper, and therefore the microstructure of an alloy is known to affect its corrosion characteristics (ref 4 and 5). For example, one of the effects on corrosion characteristics that different microstructures have on 6061

aluminium alloy is that the solution potentials between the T6 and T4 tempers are -0.83 V and -0.80 V respectively versus a standard calomel electrode (ref 6). It then seems reasonable to expect that the microstructure may have an effect on the target chemistry and the ability to remove product (in Nordion's case I^{123}) from the target's internal surface.

The construction of all Nordion's gas target starts with aluminum alloy 6061-T6 bar stock. This alloy is heat treatable with the "T6" referring to a specific heat treatment and there by a particular microstructure. The T6 heat treatment is specified to maximize the strength and hardness of the base material for manufacturing purposes. After initially machining the bar stock down to form the inner core of the target a water cooling jacket is welded on to the assembly. Significant temperatures are experienced by the aluminum at this time and depending on the welder's skill a large heat affected zone about the weld can be produced. This heat affected zone can quite easily extend into the inner target chamber walls and significantly alter the base material's temper and microstructure. To put the temperatures involved with welding in perspective with the temperatures required to alter 6061's temper it is useful to compare a typical heat treatment and the welding procedure. Nordion specifications call for target parts being welded to be preheated to 205°C before welding. Starting with this base temperature it is not difficult to imagine the base material's temperature to be increased another 200°C or so during welding (aluminum melts around 660°C). In order to anneal 6061 aluminum (ie change its temper to the T0 condition), its temperature is raised to 415°C, held for one hour to insure even heating and then allowed to air cool (ref 7). To further complicate this thermal history of the target, it is not uncommon to have a target rewelded a number of times because of weld porosity.

All the above is to say that once the target has been welded and final machining is complete, we do not know what the exact metallurgical state of the target is. There are, however some clues as to the general state of the material. Since it is more difficult for machinists to get good surface finishes on soft 6061-T0 aluminum, examining the quality of machined surface finishes performed after welding gives some indication as to the extent of the heat affected zone. From such examinations it would appear that at either end of many targets the heat affected zones are quite large and have resulted in significantly softening the aluminium within the target chamber.

EXPERIMENTAL

To investigate the effect of 6061 aluminium microstructure on target yield it was decided to take coupons (samples) of 6061-T6 aluminium, heat treat selected coupons to the T0 and T4 condition, immerse the coupons under various conditions in a solution of I^{123} labelled sodium iodide, dry the coupon, rinse the coupon with deionized water and compare the activity in the wash water with the activity left on the coupon. This same procedure was applied to coupons of T6 material of varying machined surface finishes.

A piece of 0.25"x 4" 6061-T6 aluminum flat bar with letter of compliance was purchased from A&M Non Ferrous Metals of Richmond B.C. This was cut into 42 identical one inch strips with a 0.25" hole at one end to facilitate holding the coupons. Each coupon was stamped with a number to identify it throughout the tests. The first twelve coupons were sent to Commercial/Stack Heat Treaters, Inc. of Seattle Washington where coupons 1 to 6 were annealed to the T0 condition and coupons 7 to 12 were annealed and then solution heat treated and naturally aged to the T4 condition. Coupons 13 to 30 remained in the T6 condition and were given various machine finishes. Coupons 13 to 18 were lapped with 120 grit emery cloth, coupons 19 to 24 were given approximately a 63 micro inch (μ ") machined surface finish. Coupons 25 to 30 were given approximately a 125 μ " machined surface finish. Both machine finishes were made using an end mill. The remaining coupons were kept in their T6 condition with a "mill" surface finish (ie. the surface finish as supplied from the mill).

Coupons were then organized into six groups of seven coupons each. Each group contained one coupon of each temper (T0, T4, T6) with a mill surface finish and one coupon of each surface finish (mill, lapped, 63 micro inch and 125 micro inch) with a T6 temper. The first of these groups was reserved as metallurgical samples and were sent to Baker Materials Engineering of Vancouver B.C. for confirmation of heat treatment, hardness testing and micrography. The remaining groups were used for the immersion tests.

The second group of coupons was strapped together using a plastic cable tie wrap through the 1/4" hole at the top of the coupon. A plastic spacer was placed between each coupon to avoid any galvanic affects between the coupons. The entire second group of coupons was then placed in 100 ml solution of .022 mg/l NaI labelled with 50 μ Ci (0.5 μ Ci/ml) of I^{123} for one hour at room temperature. After one hour the coupons were removed from the solution, allowed to drip dry, separated, blotted on tissue paper and placed in individual bottles containing 100 ml of deionized water for several minutes to rinse. The wash solution and coupon were then measured separately using an Eberline RM 14 with a model 44-3 low energy gamma scintillation probe.

The third group of coupons were assembled in the same way as the second. The NaI concentration was increased to 1.1 mg/l and activity increased to 15 μ Ci/ml. This time the coupons were left in the NaI solution for 18 hours and after blotting on tissue were heated to 60°C on a hot plate for four to five hours before rinsing with 100 ml of deionized water. As before both the rinse water and coupon were counted using the RM 14 with LEG probe.

The fourth, fifth and sixth groups were all treated identically. As far as the immersion times, drying and rinsing the coupons, the basic treatment was similar to the second group. The NaI concentration was decreased to 0.1 mg/l ,the activity increased to 13 μ Ci/ml and the solution temperature raised to 60°C. However, unlike any of the previous groups these coupons were purposefully arranged in a galvanic cell. The reason for this arrangement was to simulate the actual situation that occurs in the target. Coupons of the Havar foil used on Nordion targets were placed between each aluminum coupon.

Electrical contact was made by bolting the entire assembly together using a treated stainless steel rod and using stainless steel washers for spacers. The assembly is shown in figure 1.

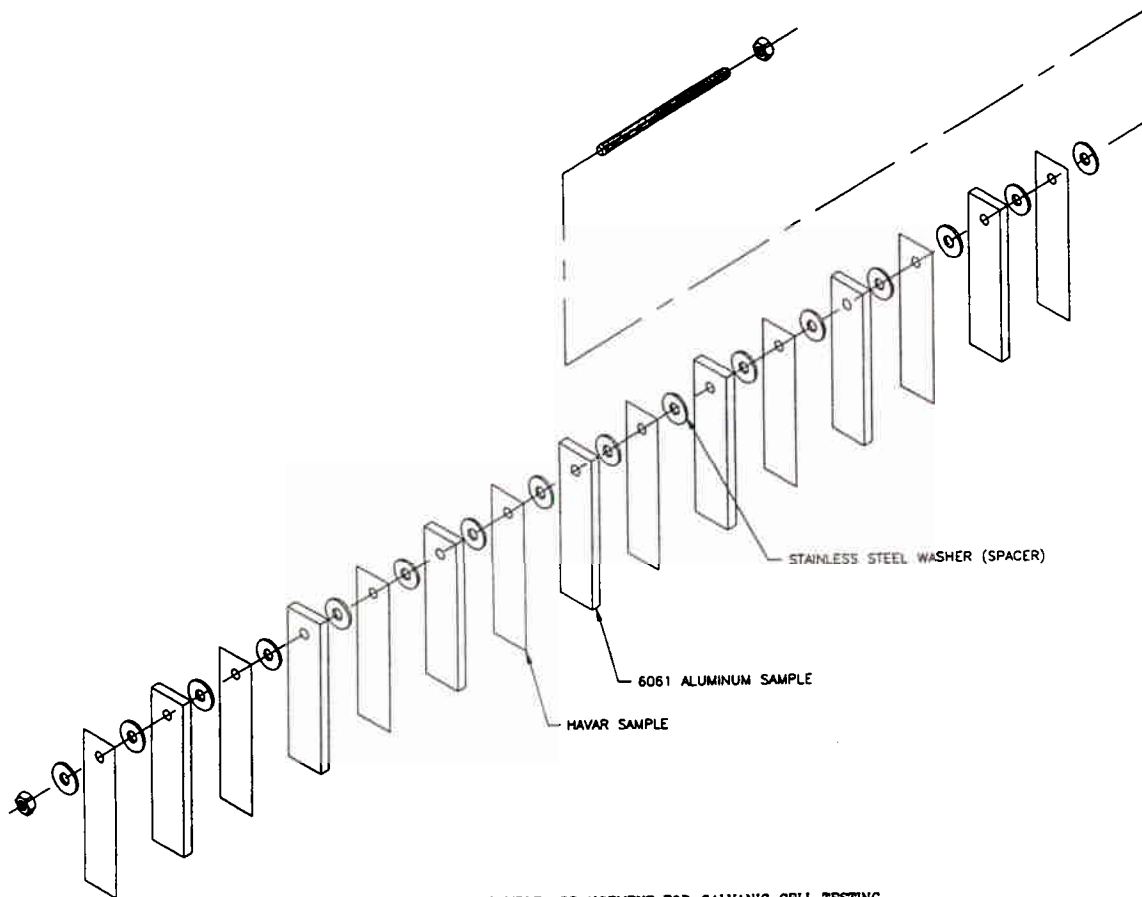


FIG. 1. SAMPLE ARRANGEMENT FOR GALVANIC CELL TESTING

RESULTS AND DISCUSSION

The coupons sent out to Baker Material Engineering Ltd. for micrographing confirmed that the coupons were within the specifications for T-0, T-4 and T-6 tempers. Baker Material Engineering also measured the relative grain size of each coupon's microstructure. The grain size was determined by comparison with ASTM E112 charts (ref 6) on a transverse section. Micrographs supplied by Baker Materials Engineering are shown in the appendix, figures 1 through 4. The result of this comparison is shown in table 1. The higher number on ASTM grain size the smaller the individual grains are and subsequently the finer the microstructure of the metal. The information to be drawn from this is that there is very little difference between the grain size present in the T-4 and T-6 coupons and that the T-0 coupons have significantly finer structure.

TABLE 1**Coupon Temper and ASTM Grain Size**

Temper	Grain Size (ASTM)
T-0	6
T-4	3
T-6	2 to 3

From the activity measurements of the rinsed coupons and the rinse solution the activity remaining on the coupon was calculated as a percent of the total. This "percent of activity remaining on the coupon" can not be said to be an accurate reflection of the actual retention of iodine on the aluminum coupons or with in the target because the self shielding effect of the coupons and rinse water was not taken into account. It should be noted that, no attempt was made to identify the species of iodine present, or measures taken to prevent oxidation of the iodine during the experiment. The value of these measurements come from being made in an identical fashion for comparison purposes.

Three different comparisons were made using these measurements. The first comparison made was between methods of coupon treatment and iodine retention . This comparison was made with coupons having a mill surface finish and T-6 temper only. The mean percent retention and standard error was calculated and are listed against the coupons group number in table 2. The next comparison made was between coupon surface finish and iodine retention. Measurements on coupons of T-6 temper, regardless of coupon treatment were chosen. Again the mean percent retention and standard error was calculated and are listed against the coupons surface finish in table 3. The third comparison was between the coupon relative grain size and percent iodine retention. This comparison was made using coupon measurements of a mill surface finish and all treatments. Table 4 shows the mean percent retention and standard error listed against the relative grain sizes from table 1.

In Table 2 it can be seen that for all, except the second group the method of treating the coupons did not have a great affect on the amount of iodine retained. The low value for the second group may be due to a stronger influence on retention because of the lower iodine concentration. From the other groups the affect of time of exposure, solution temperature or whether the coupons were arranged in a galvanic cell or not does not seem to make much of a difference on the retention of iodine. It should be noted however that rapid corrosion of the coupons was observed in groups 4, 5 and 6 where the galvanic arrangement and elevated temperature was used. Also the activity in the rinse water and samples for groups 4 and 5 were an order of magnitude higher than any other group.

TABLE 2**Comparison of Coupon Treatment and Iodine Retention**

Coupon Surface Finish:	Mill
Temper:	T-6

Group	Percent Retention	Standard Error
2	31%	1%
3	73%	3%
4	63%	7%
5	79%	4%
6	69%	7%

In table 3 it can be seen that the various surface finishes used in these tests did not have a significant affect on iodine retention. The spread in the retention column is surprisingly small considering that all the different treatments were included calculating these averages. On the other hand the main factor affecting the standard error with in each group is most likely due to the different treatments.

TABLE 3**Comparison of Coupon Surface Finish and Iodine Retention**

Coupon Treatment:	All
Temper:	T-6

Finish	Percent Retention	Standard Error
Lapped	62%	12%
63 μ " Machined	57%	12%
125 μ " Machined	60%	11%
Mill	63%	18%

The comparison of the grain size with retention in table 4 gives some indication that the microstructure does have an affect on retention of iodine. It would seem that as the microstructure becomes coarser (smaller ASTM grain size) the retention increases. It should not be concluded that the retention is due to grain size. Other features are changing along with grain size and may eventually be found to affect the retention. As

can be seen in the micrographs the Mg_2Si precipitates are more numerous and larger in the T-0 than either T-4 or T-6. As well, as the grain size decreases the number or total length of grain boundary increases, which may play a role. As in the surface finish comparisons the major contributor to error is thought to be the different treatments given the various coupons

TABLE 4

Comparison of Coupon Grain Size and Iodine Retention

	Coupon Treatment:	All		
	Coupon Surface Finish:	All		
	ASTM Grain Size	Temper Retention	Percent Error	Standard
	6	T-0	49%	21%
	3	T-4	65%	13%
	2 to 3	T-6	63%	18%

CONCLUSIONS

The intent of this work was to explore the possibility that the thermal history of Nordion's gas targets may account for some of the observed variations in I-123 yield that occurs from target to target. It appears from the results that there may be an effect and that a target made of 6061-T0 may result in a higher iodine recovery. However, these results should be considered as preliminary and this paper as a report on work in progress. The exploratory nature of this work characterized by the various treatments given the coupons in an effort to simulate the way in which iodine may be found in the target, resulted in the wide spread of the final results. Likewise a more thorough method of measuring the activity on the coupons and in the rinse water is necessary for more accurate results.

In addition to the above, the affect of using dissimilar metals in target construction should be considered by designers. The observed increase in chemical activity when the aluminium and Havar were arranged in a galvanic cell is of some concern. Pitting corrosion, which is typically associated with galvanic corrosion has been observed in a gas target recently taken out of service at Nordion.

Acknowledgements

I would like to thank Mr. Harvey West, P.Eng. of Baker Materials Engineering Ltd., Vancouver, B.C. for his advise and metallurgical evaluation of the aluminum coupons.

APPENDIX

Micrographs of 6061 Aluminum Samples

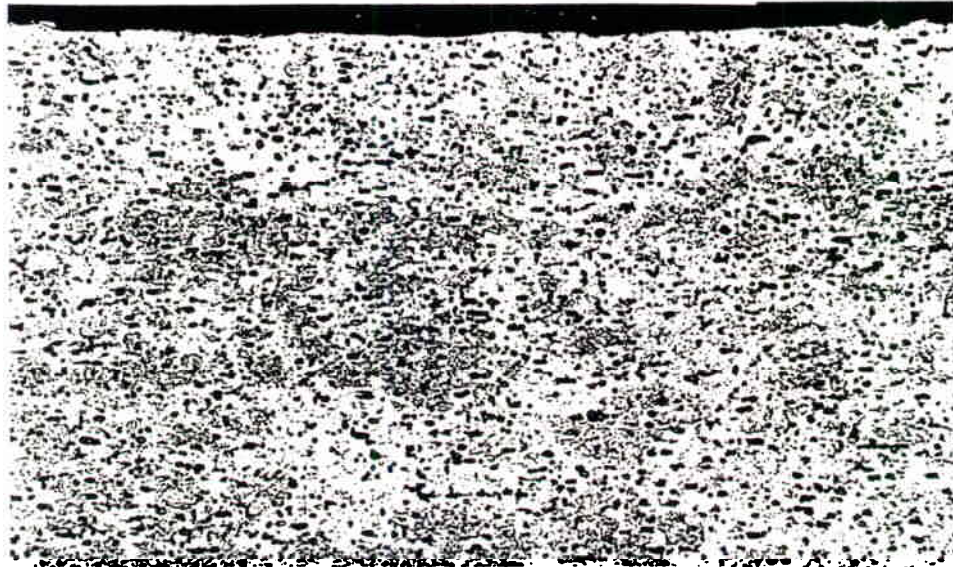


Figure 1: x160

Kellers Reagent

The surface structure of the annealed sample.

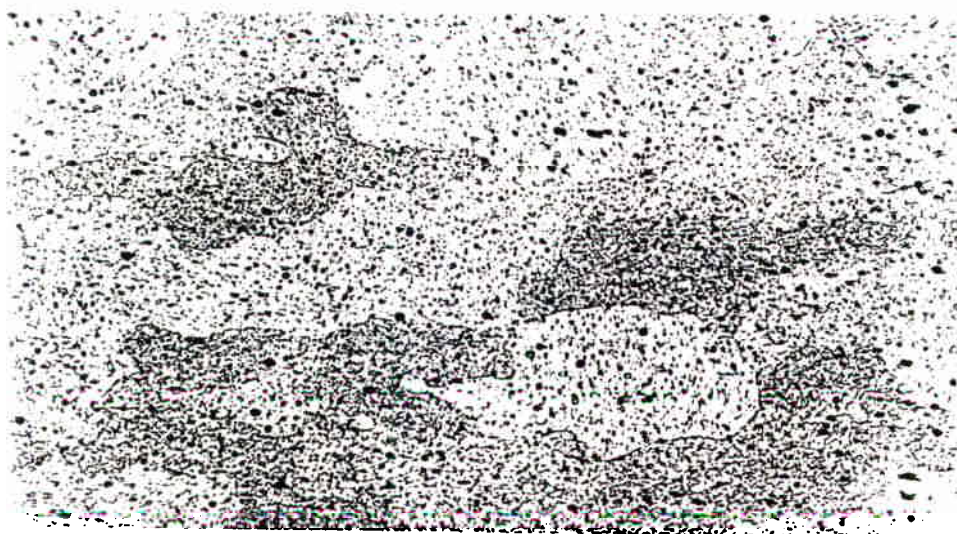


Figure 2: x160

Kellers Reagent

The surface structure of the T4 sample.

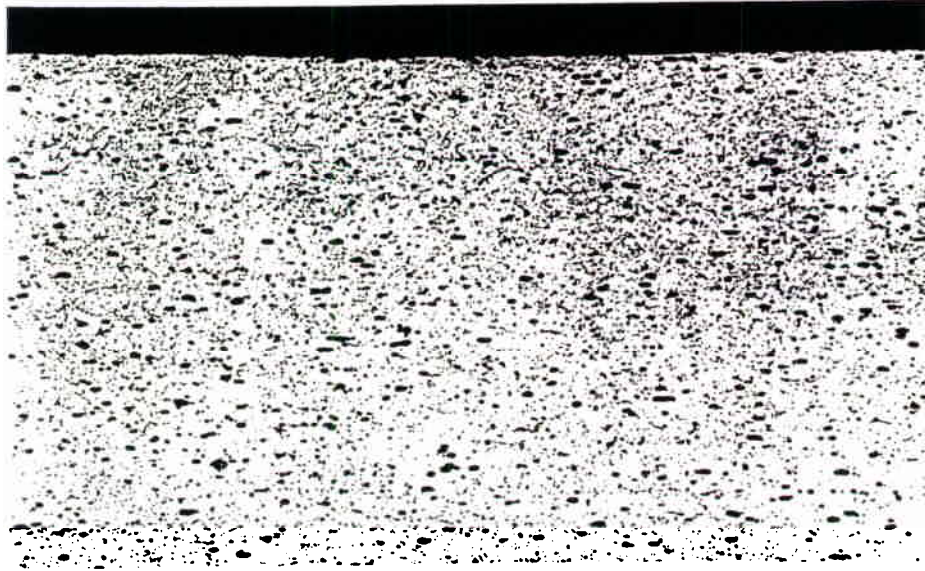


Figure 3: x160

Kellers Reagent

The surface structure of T6 temper sample No. 19.

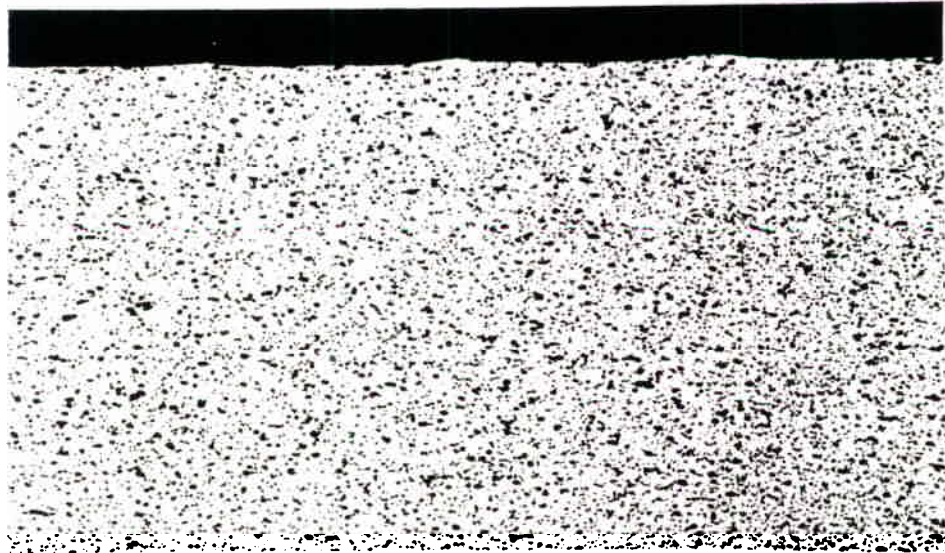


Figure 4: x160

Kellers Reagent

Comparison structure of T6 temper illustrating the variance of the distribution of the Mg_2Si precipitates.

References

- 1 Mulders J. and Steenhuysen. (1985) Quantitative autoradiographic measurement of the scattering of protons in a krypton gas target. *Int. J. Appl. Radiat. Isot.* Vol.36, No.11, pp833-841.
- 2 Firouzbkht M., Schyler D. and Wolf A. (1992) Effect of foil material on the apparent yield of the $^{124}\text{Xe}(p,x)^{123}\text{I}$ reaction. *Appl. Radiat. Isot.* Vol. 43, No.6, pp.741-745.
- 3 Ruth T., Adam M., Jivan S. and Lofvendahl J.(1991) The effect on yields due to beam focusing on an [Fluorine-18] F_2 target. *Proceedings of the IVth International Workshop on Targetry and Target Chemistry* (R. Weinreich, ed.) September 9-12, 1991. PSI Villigen, Switzerland. pp 113-114.
- 4 Metals Handbook, Vol 13, Corrosion, 9thed. ASM International pp. 587 "Corrosion Ratings of Alloys and Tempers" and pp. 593, table 6.
- 5 Corrosion Control in the Chemical Process Industries, Dillon C. P., M^cGraw-Hill 1986, Sec. 3.5.2, pp25.
- 6 Metals Handbook, Vol 13, Corrosion, 9thed. ASM International pp. 584, table 1b.
- 7 AMS Standard 2770C-1980, "Heat Treatment of Aluminum Alloy Parts"
- 8 ASTM Standard E112, "Determining Average Grain Size".

Questions for 61 Heat Treatment and Its Effect on Iodine Absorption on the Nordion Gas Targets.

Speaker: Dan Williams of Nordion

The questioner is identified where possible and the answers are provided by the speaker unless otherwise indicated.

Comment: Jerry Nickles, University of Wisconsin

I think your work is directly relevant to people who are using aluminum targets for the 2 shot elution of $^{18}\text{F-F}_2$ also.

Reply:

I found it very interesting in the last presentation, that somebody mentioned that silicon is bad for F-18 targets. If aluminum is being used in F-18 targets, it would be interesting to see what affect the different alloys, because not all aluminum alloys have silicon as an alloy addition. I think it's basically the 600 series that is a and manganese, silicon and copper are also in the 6061 as well.

Question: David Schlyer, BNL

Have you tried treating, annealing the aluminum and then bringing it back to T6 afterwards. Does that behave any differently than T6 that had never been annealed at all?

Answer:

We attempted to heat treat targets after welding and due to mechanical problems, we can't do it because part of the heat treatment is that the heat treaters have a furnace with a trap door in it and to change it into a T6 material, they will heat it up to about 560°C for an hour or two and then the trap doors open just like a bomb-bay and they drop it into a glycol bath. We talked to them and said, "do you think there is going to be any problems with this because we have a jacketed device here." And they said, "no, no I think we can do it." "Yeah sure, okay, go ahead try it." Well, we did this and as I said there are final machining procedures after this would all be done. And the machinists chucked this thing up in the lathe to rebores the target and of course, it's quite trivial, when you cool the outside of the target, the inside is still piping hot and they bent the inner bore of the target and it was about one quarter of an inch out and so we just sort of wrote off the idea of trying to heat treat this particular design of target. I am hoping to talk certain people into allowing me to design a target that actually doesn't have a welded jacket on it but a mechanically fixed jacket so that we can take the center of it out and heat treat it to our hearts content.

Question: John Clark, MRC Hammersmith

I realize you are not a chemist and I really enjoyed your presentation metallurgically and as a machinist. But, why do you throw these samples into sodium iodide solution with sodium iodide bulk material because boy, what your target sees, in real life, is no added carrier of iodine.

Answer:

That's right. As I said, it's very much a comparative method ...

John Clark

Yes, but you are obliterating the signal, I think.

Answer:

Yes. What we have accomplished with doing these tests is there appears to be an effect here so now we have a bit of ammunition to go back and say we want to do more tests and carrier free would be one of those tests. One thing I should mention too is something that didn't really show up in my presentation, is the amount of chemical activity that we found once we put our samples into a galvanic couple. The first two samples we purposely isolated them from one another so that there would be no galvanic affects or at least as far as we know, there would be no galvanic affects. When we purposely coupled these things together and put them into the solution, and quite predictably we saw quite a bit of chemical action as well. The amount of activity remaining on the sample and in the wash water increased by an order of magnitude as well.

Question: Carlos Gonzalez-Lepera, University of Pennsylvania

I want to emphasis again, that what I think we're talking about a bulk effect into the material and I think it's pretty well known that any aluminum material has a very thick layer of aluminum oxide on the surface and that is where most of the chemistry takes place. So, I think it's important to try to go and look deeper into the first few layers of your sample instead of just trying to analyze the grain structure although it could affect your surface structure but most of the chemistry, I mean 100% of the chemistry takes place within a few atomic layers on the surface and then it could be a little bit irrelevant to see what sort of treatment you have done to the material, except that you have changed the surface structure.

Answer:

Yes, one of the things that you mentioned to the other gentleman, the thing that came to my mind was that it may not actually be, although we measured against the actual grain size, that may not be the feature that is causing this observed change. It might be something else that is changing along with the grain size, for example, the magnesium-silicon alloy. Some of those particulates are going to be intersected by the machine's surface of the bore in the T0, there may be a higher percentage of magnesium-silicon exposed on the inside of the bore. What kind of affects does that have on the oxide layer? I don't know, but that might be what is happening.

Question: John Clark

When you get around to doing the no carrier added iodine. Two things, have a quick look at the autoradiographs at a microscopic level because your auger electrons should get pretty good resolution and the second thing is the weld wrought material, is that exactly the same alloy, or do you have welds inside the target?

Answer:

No there are no welds inside the target, it is only on the outside.

John Clark

On the jacket?

Answer:

Yes, it is different.

Question: John Need, Duke University

One thing, I know that on welded aluminum that is then re-machined and if its left on the inside of targets, left sitting around, you can see in the vicinity of where you have welds, very definite color differences?

Answer:

Yes.

John Need

That may be due to machining problems or it may be due to chemistry problems. One thing that might be suggested is perhaps trying to use a plasma arch cleaning of the interior of these at some point in the manufacture.

Answer:

Yes, part of the reason for doing the comparison with the various machine finishes was to get an idea of just how the machine finish was going to affect that. I was actually kind of surprised that we didn't get more of an affect to tell you the truth.

Question: Rich Ferrieri, BNL

Back at PSI (4th Workshop) we talked about a 6061 aluminum target for ¹¹C-CO₂ production and some the problems related to trying to enhance specific activity and we agonized over surface area affects and oxide layers and we developed some very crude spectroscopic methods to show us that in fact these oxides when struck with beam would produce CO₂ and put this back into the gas. What we found though is a method of cleaning the 6061 aluminum. After polishing and putting the target on line, we introduced what we called burnout gas mixture which you can buy from Matheson. It's neon with 5% oxygen and we just filled the target to say, 100-200 pounds per square inch pressure and subjected it to about 30 minutes of beam time. You do this repetitively, flushing the target and it seems to burn out any of the surface material that might be left from the cleaning or machining.

Answer:

That's rather interesting because in our installations we have found that if we don't do a helium irradiation (the target doesn't work as well). Usually we do it just to check and see if everything is all aligned before putting expensive Xenon gas into the target. We fill the target with helium and do irradiation. We don't have any hard data on it, but it's generally felt that is needed to do something.

Comment: Rich Ferrieri

This is now written into our operating protocol when we open the target up to air for say, a window change, or whatever, the first run on the target involves at least 15 minutes of this burnout process.

Answer:

Burnout gas and it's neon and ...

Question:

Neon and 5% oxygen.

Answer:

5% oxygen, that's interesting.

Comment: Tom Ruth, TRIUMF

Dan, since people are making suggestions, I think you should be very careful about how you measure your activity. Using a gross counter like that (ionization counter) you can really make very large errors and since this is important work, I think it would be worth doing carefully.

Reply:

Yes, one of the things we wanted to get a feel of was whether or not we had enough to go do more sensitive experiments.

Heat Transport in Targets and What it Means to ME.

Dr. R.J. Nickles
University of Wisconsin in Madison.

A Contribution from the floor with anecdotal observations

I would just like to point out, that we used to start out where we simply look at still water with beam on with an effort to try to understand some of these things that broke this session up this morning. This is in fact just a low beam of radiation, of neutral water as we approach the point of which time the excitement happens with possibly, accelerated radiolysis or what not.

The talk that should have been going on at this time, dealt with reclamation of enriched materials. A case of which, in our case, is reclaiming ^{94}Mo as we are trying to make $^{94\text{M}}\text{Mo}$ in situ with vacuum sublimation. What I wanted to just bring back to you in terms of simple tricks that we used that might help us in matters of understanding heat transport in targets, is to mock up a pseudo beam, and this is just it, it's a pseudo beam, an oxygen-hydrogen torch running on a metered oxygen-hydrogen source, such as to simulate about a 100 watt beam on target, 10 μA at 10 MeV. By doing optical pyrometry and calorimetry and the usual thermal measurements on these types of things, you can do a fair job of at least trying to get the feel of what your target's feeling like when it's being hit by the beam.

In particular, the papers of today that we're talking about beam profile in space and the possibility of new and unstudied mechanisms of radiolysis and heat transport, I will just share with you the results of a recent experiment we did at Wisconsin at the request of CTI to look at the actual temporal profile of the beam during irradiation. And by that, I mean the actual time structure of the beam pulse which in our case is a 27 MHz fundamental. We looked at its temporal profile by a fairly common technique known as the gamma flash. What you do is simply start a time to amplitude converter (TAC) on the RF, stop it on some signal which is prompt with the arrival of the beam on target.

If you're shooting on O-16, it's simply the 6 MeV gamma coming from inelastic scattering and by using a fast scintillator, in this case pilot U, we can actually get the time resolution which is far greater than the few nano second gamma flash width. What we are looking at here is the output of the TAC and the output of the gamma spectrometer, pilot U, in a two-dimensional image, if you like, gamma energy against time difference with each beam pulse coming in. Now, the width of the big gamma flash proves to be between 3.5 and 7 nanoseconds out of the 36 nanoseconds that separates the beam pulses giving us an idea of the temporal frequencies that are happening here. They are, as I say, of the order of GHz, quite a lot higher than we ever expected. I bring up this possibility.

There may be another variable, if somebody has to bunk the field before it gets debunked, let me try to bring out the possibility. There may be a hidden variable here, which in our case would be the anode power supply voltage which determines the width of this gamma flash, the

width of the beam pulse on the target. And, if there were any kind of radiochemical specie acting as a contaminant or poison, it had a lifetime, for example some free radical, that had a lifetime of the order of 10^{-10} to 10^{-9} seconds, the beam pulse whether it's broad or narrow, relative to those chemical species lifetimes could in fact determine the local concentrations during that time in which water decides to radiolyse or fluoride ions decide to get trapped, this type of thing. So, I just leave you with this possibility that we are certainly dealing with something here both with water targets and gas targets that is there are many phenomena that seem to be eluding us still. I bring up the possibility of temporal profile.

RECOVERY OF ENRICHED STABLE ISOTOPES IN RADIONUCLIDE PRODUCTION

A.A. Razbash, Yu. G. Sevastyanov, O. N. Polyakov, N. N. Krasnov
N. A. Konyakhin, Yu. V. Tolstouhov, A. G. Maklachkov.
Cyclotron Company Ltd. Obninsk, Russia

Introduction

The wide application of radionuclides in different fields of science and industry demanded an increase of their production. One of the ways to increase the radionuclide production on present cyclotrons is the use of the targets from enriched stable isotopes. This allows one to raise the productivity in some cases by two or more times and to increase radionuclidic purity. It should be noted, however, that enriched stable isotopes are very expensive. Therefore it is advisable to use such raw materials more than once.

In the last ten years, we have used stable isotopes extensively for making of the targets. Zinc-67 and zinc-68, cadmium-111 and cadmium-112, nickel-58, silver-109, thallium-203 have been employed for the production of gallium-67, indium-111, cobalt-57, cadmium-109 and thallium-201 respectively. It is evident that we have given consideration for repeated use of stable isotopes. The technique for the recovery of enriched stable isotopes has been developed. In this report the schemes of the recovering processes are presented.

Nickel-58

The solution of nickel-58 liable to purification contains significant quantities of copper, cobalt-57 and zinc-65 radionuclides and some quantities of iron as a universal impurity. The most undesirable impurity is iron because cobalt-56 obtains during the irradiation from it. The recovery technique is based on the differences in anion-exchange behavior of elements in hydrochloric acid solutions [1]. The scheme of this process is presented on Fig. 1

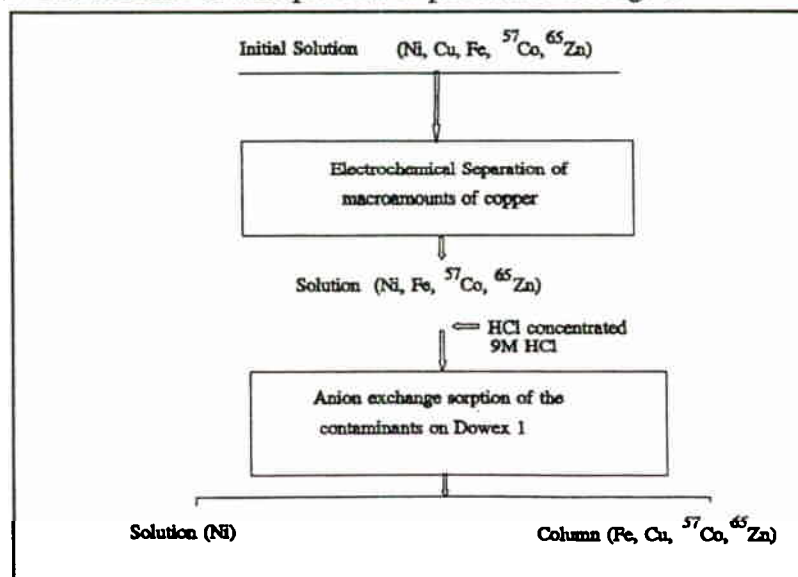


Fig. 1. Scheme of nickel-58 recovery

It should be noted that the final product contains ultra quantities of sodium-22 and manganese-54 since the suggested technique did not provide the purification from them. But during the making of the target by electrolytic Al deposition of nickel these contaminants remain in the electrolyte. This technique ensures the recovery of practically all nickel from initial solutions.

Zinc-67, 68

Depending on gallium-67 production method (deuteron or proton bombardment) the targets from zinc-67 or zinc-68 are used. The target represents a copper block with a thin nickel layer covered with stable zinc by electrodeposition. Its treatment includes the dissolution of irradiated zinc in hydrochloric acid and following organic solvent extraction of gallium-67. Therefore the remained solution contains besides zinc and also some quantities of copper, nickel and cobalt-57. It should be provide for the purification from iron too. The technique accepted in our enterprise (Fig. 2) is based on the well-known data about anion-exchange behavior of elements in hydrochloric acid /1/ and so it is like the other one published in literature /2/. During the zinc target irradiation zinc-65 ($T_{1/2} = 244d$) is obtained. These procedures do not provide for the zinc isotopes separation and so to decrease a radiation danger during the recovery, making and following working with the target before the irradiation the zinc-67, 68 solution should be kept up to 2 years. The suggested process allows to recovery about 95% of stable zincs.

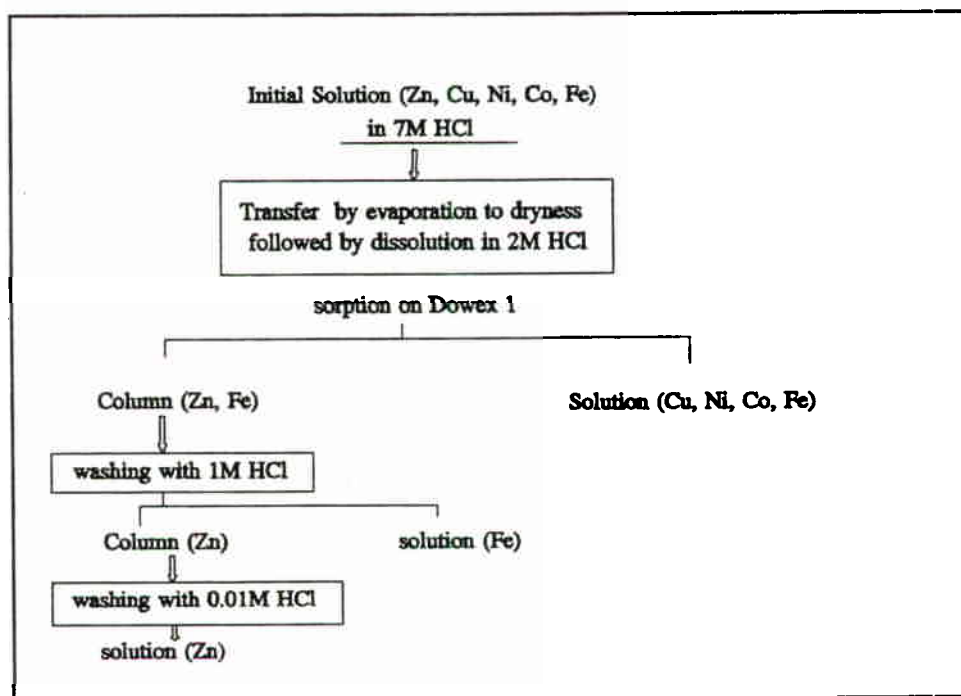


Fig. 2. Scheme of zinc-67, 68 recovery

Silver-109

After the separation of cadmium-109 from the irradiated target the residue represents a pulver of metallic silver and copper mixture contaminated with cadmium-109 and zinc-65. The recovery technique is based on precipitation operations (Figs 3).

Silver-109 is contaminated with radionuclides silver-110m ($T_{1/2} = 249,8d$) and silver-106m ($T_{1/2} = 8,46d$) after target irradiation and so it has to keep up some time before the regeneration procedures for a decrease of total activity of the sample like in a case of zinc-67, 68. Used procedures ensure the recovery not less than 90% of the starting quantity of silver-109.

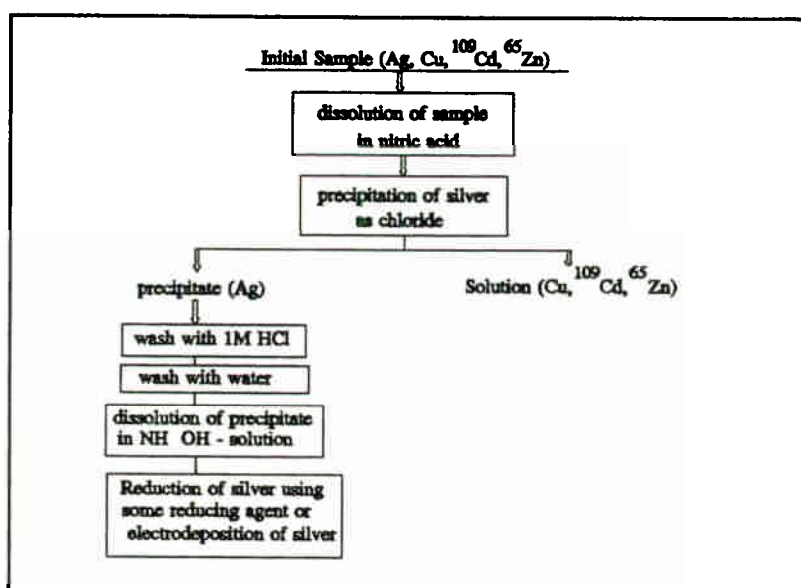


Fig. 3. Scheme of silver-109 recovery.

Cadmium-111, 112

The target for indium-111 production represents a copper block with a thin layer of nickel which is electroplated by cadmium-111 or cadmium-112. The chemical treatment consists in dissolution of the irradiated cadmium layer in nitric acid and following indium-111 isolation using cation exchange chromatography. So the solution of stable cadmium after the treatment contains copper, nickel and zinc-65 and cobalt-57 radionuclides. From such mixture cadmium isotopes have to separate. The scheme of the separation technique is presents, on Fig. 4.

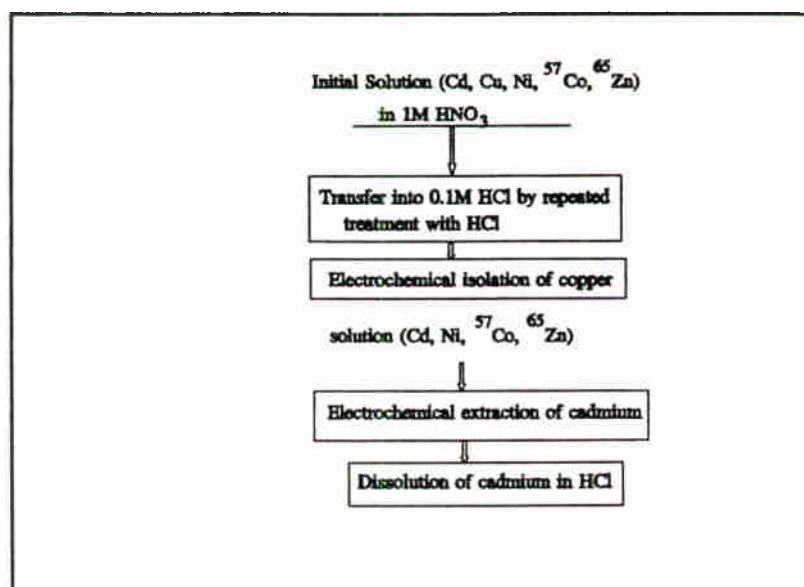


Fig. 4 Scheme of cadmium-111, 112 recovery

It should be noted that at the electrochemical extraction of cadmium the deposition of some quantities of zinc-65 takes place and if you want to decrease the zinc-65 impurity some more it has to repeat the stage of the electrochemical extraction of cadmium. This technique allows to recovery about 95% of starting cadmium isotopes.

Thallium-203

The solution of thallium-203 to be for a purification represents the solution of thallium bromide in butyl acetates. The probable contaminations are copper and zinc-65. The recovery process is based on the low volatility of the thallium /I/ halogenide (Fig. 5) and ensures the recovery more than 90%.

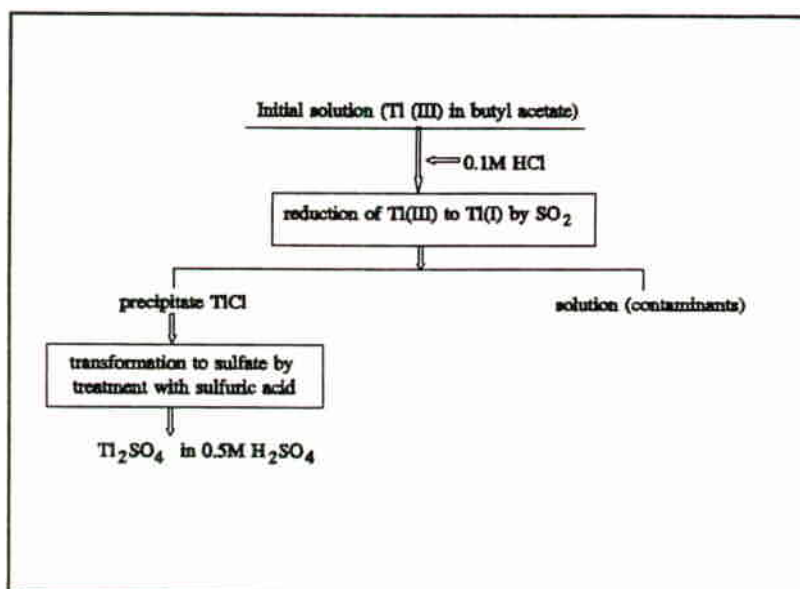


Fig. 5. Scheme of thallium-203 recovery

Conclusion

The developed technique consist of the simple operation. They ensure the recovery of about 90 - 95% of enriched stable isotopes and allow a high extent of purification from undesirable impurities. The content of chemical impurities in the regenerate as a rule do not exceed the one in the starting material. At the realization of the recovery processes the pure reagents are used and so the isotope dilution do not take place practically. This is confirmed that the radioisotopic purity do not change after the irradiation of the targets from the recovered materials. The comparatively high extent of the recovery allows to add only small quantities of the "fresh" stable isotope to the process of the radionuclide production.

References

1. A.Kraus, F.Nelson, Anion Exchange Studies of Metal Complexes, in: *The Structure of Electrolytic Solutions*. National Bureau of Standards, Washington, 1959.
2. T. E. Boothe, R. D. Finn, J. S. Sinnreich, E. Tavano, Factors influencing the routine use of isotopically enriched zinc-68 for the preparation of gallium-67. *J. Labelled Compounds and Radiophar.* 23, 1337 (1986).

PRODUCTION OF LONG-LIVED RADIOISOTOPES AND ITS APPLICATION TO CALIBRATION SOURCES FOR PET CAMERAS

Carlos Gonzalez-Lepera

Cyclotron Facility
Center for Functional and Metabolic Imaging
University of Pennsylvania
Philadelphia, PA 19104 USA

ABSTRACT

An internal solid target station was developed for the JSW3015 Cyclotron. Manual loading and retrieval of irradiated targets is executed with minimal operator intervention, thus reducing exposure. Preliminary results concerning the production of small amounts of the radioisotope ^{22}Na (2.6 yr. half-life) via the reaction $^{24}\text{Mg}(d,\alpha)^{22}\text{Na}$ are presented. Chemical extraction of the product from the target matrix and construction of linear sources for PET cameras is also discussed.

INTRODUCTION

In house production of long lived radioisotopes (several months to a few years half-life range) with a medium size cyclotron presents a viable alternative not fully developed except for commercial purposes. Available sources suitable for calibration of PET cameras, dose calibrators or other instrumentation do not always conform to a desired shape or intensity. Cost of these sources is also a factor to be considered. A typical 0.5 mCi ^{22}Na source averages \$1500. Unfortunately, handling of irradiated solid targets usually presents the dilemma of either large initial investments in remotely operated systems or relatively high personnel exposures during target removal process. To investigate alternatives to these problems we developed a new solid target station for the JSW3015 that --at least for small and medium scale production levels-- simultaneously minimizes both problems.

Internal targets benefit from using full beam energy if required while avoiding the requirements of foil cooling hardware. On the other hand the target material should possess certain physical properties. Vapor pressure of the material during irradiation must be within acceptable operational limits (typically $<10^{-5}$ Torr). Radioisotope migration to the surface and escape from the target needs also to be considered to avoid possible contamination of beam line and accelerator components. Installation of a cold trap near the target could alleviate this problem.

SOLID TARGET STATION

One of the three beam lines of the University of Pennsylvania JSW3015 Cyclotron was adapted as an internal solid target station. It consists of a small vacuum chamber and removable target holder. Fig. 1 shows a schematic of the setup. The vacuum chamber was assembled using standard vacuum components (ISO NW 40) including auxiliary pumping port and electrical feedthroughs.

The target holder consists of a 35 cm long by 25 mm outside diameter stainless steel tube. Water cooling to the target is supplied by a smaller diameter coaxial tube. A *quick-disconnect* feedthrough allows rapid insertion or removal of the target holder. Personnel exposure is minimized by the length of the tube and process swiftness. Targets are held in place by a nut cap providing good thermal contact between target and holder. A ceramic (*Maycor*) ring centers the target holder inside the vacuum chamber. An electrically isolated graphite collimator --5 mm thick, 14 mm aperture-- shields the target holder from direct exposure to the beam while providing beam current monitoring to optimize beam incidence on target.

Machining of the targets to a funnel-like shape with a 53° included angle increases the amount of target surface exposed to the beam, improves target cooling and also facilitates radioisotope extraction.

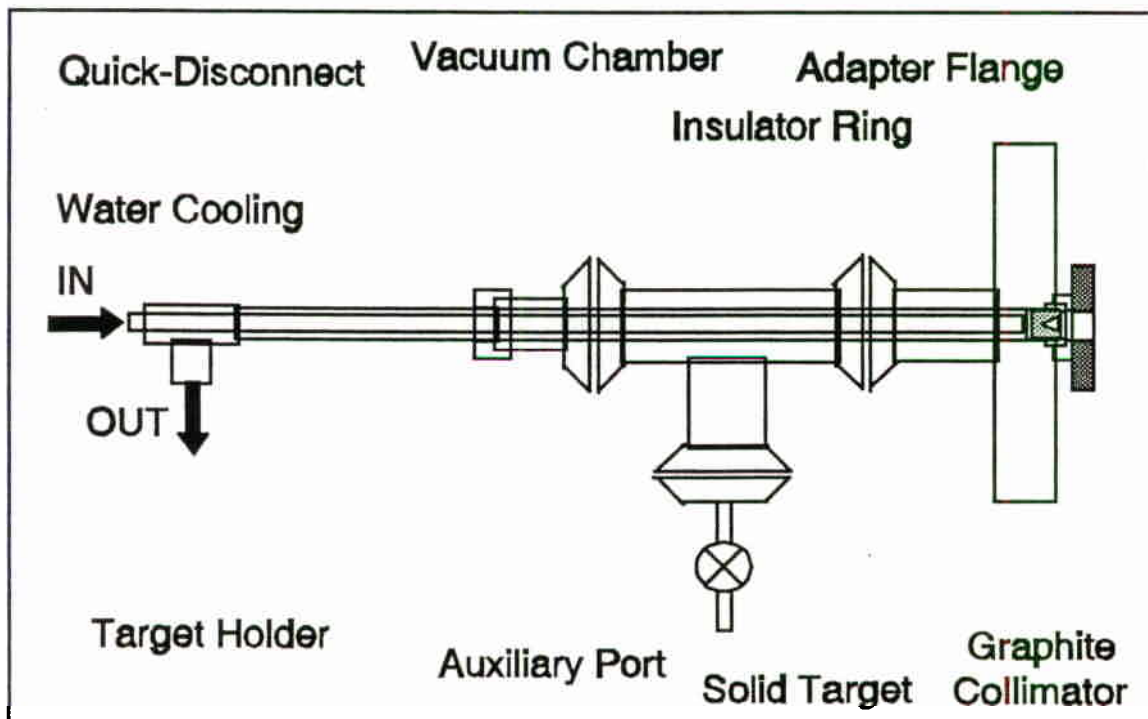


Figure 1

PRODUCTION OF SODIUM-22

Sodium-22 was selected as our first radioisotope to test the solid target station. β^+ end point energy and branching ratio very similar to ^{18}F together with 2.6 yr. half-life makes this radioisotope very practical for calibration of PET cameras.

A medium energy cyclotron (30MeV protons or 15 MeV deuterons) can produce ^{22}Na through several reaction channels. The reaction $^{24}\text{Mg}(d,\alpha)^{22}\text{Na}$ presents the largest cross section for the projectiles and energies under consideration. Measured thick target yields for 16 MeV deuterons on ^{24}Mg are $2.93 \mu\text{Ci}/\mu\text{A}\cdot\text{hr}^{-1}$. Irradiations were performed with our 15 MeV deuterons beam.

The target was machined from 99.8% purity Mg rod. According to the supplier², natural isotopic abundance is expected for this material. A short test run was conducted and the irradiated product --without chemical extraction-- was analyzed by gamma-ray spectroscopy (HPGe detector). Traces ($< 10^{-5}$ per ^{22}Na) of ^{56}Co and ^{58}Co were found together with the main product. Impurities like ^{58}Ni , ^{59}Co and ^{56}Fe present in the target material are responsible for these radioisotopes. An increase in target purity was considered not necessary for our purposes given the low level and relatively shorter half-life of the observed byproducts.

The same target was finally irradiated three times over a two days period for nearly 7.5 hr. Typical irradiation current values were around 12 μA . Except for a slight pressure increase during the first half hour of irradiation due presumably to target outgassing, pressures inside the vacuum chamber remained below 2×10^{-6} Torr during irradiation. Visual inspection of the target before chemical extraction of the radioisotope did not show any signs of beam-induced surface damage.

An integrated current of 70.2 $\mu\text{A}\cdot\text{hr}$ produced $183 \pm 25 \mu\text{Ci}$ of activity. This result is in reasonable agreement with our calculated thick target yield of $2.8 \mu\text{Ci}/\mu\text{A}\cdot\text{hr}$ for 15 MeV deuterons.

RADIOISOTOPE EXTRACTION

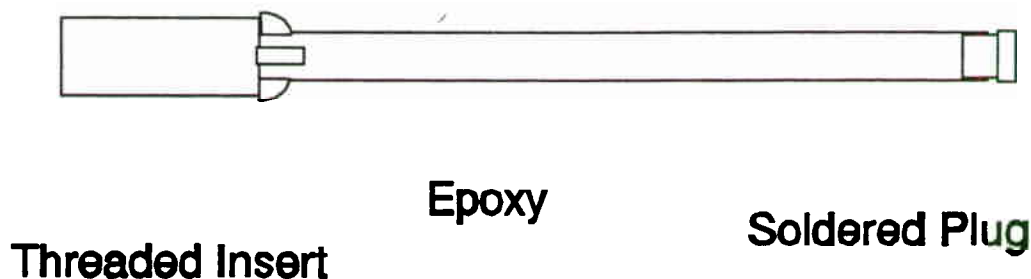
The target holder was placed inside a hot cell and the irradiated Mg target containing ^{22}Na was removed and mounted into a Teflon cup. HCl acid was used to dissolve the target obtaining $^{22}\text{NaCl}$ in solution. The Teflon cup holder facilitates target handling while only exposing the irradiated surface to the dissolving agent. The target was then rinsed with distilled water and the solution filtered with a Whatman #1 paper filter. Most of the MgCl was retained at the filter while the hot $^{22}\text{NaCl}$ solution was collected in a pear shaped flask. Evaporation of the product concentrated the $^{22}\text{NaCl}$. This sequence was repeated many times until practically all of the activity was registered in the collection flask.

SOURCE FABRICATION

A prototype (low activity) linear source was developed to study source deposition methods and final uniformity. A 1.6 mm (1/16") OD by 0.4 mm wall thickness by 15 cm long stainless steel tubing was sealed --silver soldered plug-- at one end. A smaller diameter polyethylene tubing was inserted into the first one. The $^{22}\text{NaCl}$ --3 μCi --

dissolved in water was transferred into the stainless steel tubing. Slow withdrawal of the plastic insert assured that no bubbles were being trapped inside the tubing. The tubing was left open until dry and a threaded insert was epoxyed to the open end. Fig. 2 shows details of the source. Except for a small spot near the center that deviates near 20%, uniformity of this rod source is within 10%.

Rod Source



Construction of a second source is under way. In this case a 3.2 mm diameter tubing will be used to deposit near 100 μCi of radioisotope following the same procedure as previously described.

CONCLUSIONS

We have developed an internal solid target station with minimal investment. A ^{22}Na sealed source was fabricated. Work on a stronger source is being completed. A new Mg target is ready for irradiation and we expect to scale activity up to 1 mCi. Other parameters including maximum beam current supported by the target and alternative target geometries will be studied.

References

- ¹ BNL National Nuclear Data Center.
- ² AESAR/Johnson Matthey.

OVERCOMING CYCLOTRON ENERGY CONSTRAINTS THROUGH TARGETRY

R. Finn, Y. Sheh, J. Vecchione, D. Schlyer*, M. Firouzbakht*

Radiochemistry/Cyclotron Core Facility, Memorial Sloan-Kettering Cancer Center, New York, N.Y. and *Chemistry Department, Brookhaven National Lab, Upton, NY.

ABSTRACT

The past decade has witnessed a rapid growth in the number of PET-Cyclotron Facilities, each with specific clinical or research programs. This diversity of research interests has been partially responsible for the evaluation of the potential clinical utility of several radionuclides which had been previously dismissed from further consideration due to the lack of pure positron emitter decay characteristics.

The particular nuclear reaction utilized to produce such radionuclides is not always amenable to the classical gas or liquid target. Such is the case in our research effort which requires a solid target irradiation station compatible with a retrofitted Japan Steel Works target changer to The Cyclotron Corporation CS-15 cyclotron. We have fabricated such a target from readily available components. The operational characteristics and unique features of the target system are outlined.

INTRODUCTION

The Memorial Sloan-Kettering Cancer Center (MSKCC) cyclotron is a model CS-15 accelerator, originally manufactured by The Cyclotron Corporation and is one of the earlier accelerators dedicated to serve a biomedical research program¹. During the past few years, the cyclotron has undergone an extensive reconditioning and refurbishment effort while continuing to operate in support of the established clinical investigative projects. Enhanced performance through improved reliability and refinements to radiochemical production, has been achieved through the repairs and the modifications on the cyclotron subassemblies.

The cyclotron is presently capable of accelerating protons and alpha particles to an energy of 15 MeV, deuterons to 8 MeV and helium-3 particles to 23 MeV. As a component of the refurbishment effort, the target system², a forerunner of the present day automatic target changers, was replaced with a commercially available unit from Japan Steel Works in 1989.

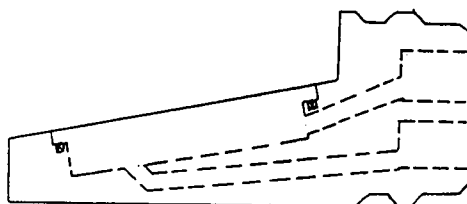
The versatility of a multiple particle cyclotron coupled with an active research program requiring unique short-lived radionuclides and/or radiolabeled reagents prompted our efforts to develop a novel solid target system compatible with the Japan Steel Works target changer.

EXPERIMENTAL

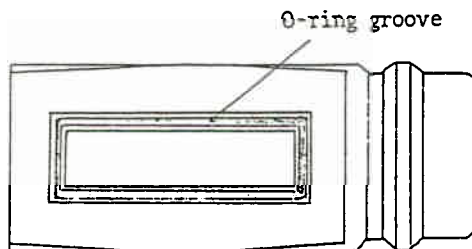
The refurbishment of the cyclotron at MSKCC included the installation of a state-of-the-art target changer and chilled helium foil cooling recirculation system. At the time of installation, the manufacturer had not designed a cyclotron target for the irradiation of solid or powder targets. Our efforts were directed toward the fabrication of an external target whose dimensions are dictated by the constraints of the auto target changer. Moreover, the target system envisioned was to address several potential scenarios, i.e. to handle powder as well as electroplated targets, to allow the reuse of target backing plates, to provide target alignment with the beam at a grazing incidence, and to operate either under chilled helium foil cooling or in vacuum.

Considering the target system as distinct two units, i.e. the target head and the target support housing, the first generation of the solid target head incorporates a modification of the inclined-angle external target which was utilized for the development of the tellurium-124/iodine-124 production³ at Brookhaven National Laboratory. As seen in figure 1, the detachable irradiation head is inclined at an angle of ten degrees to the beam plane. This results in an effective target thickness of nearly six times the actual thickness. Careful monitoring of the beam profile is required to insure that target material is irradiated and not the isolation flange.

TARGET HEAD



Side View

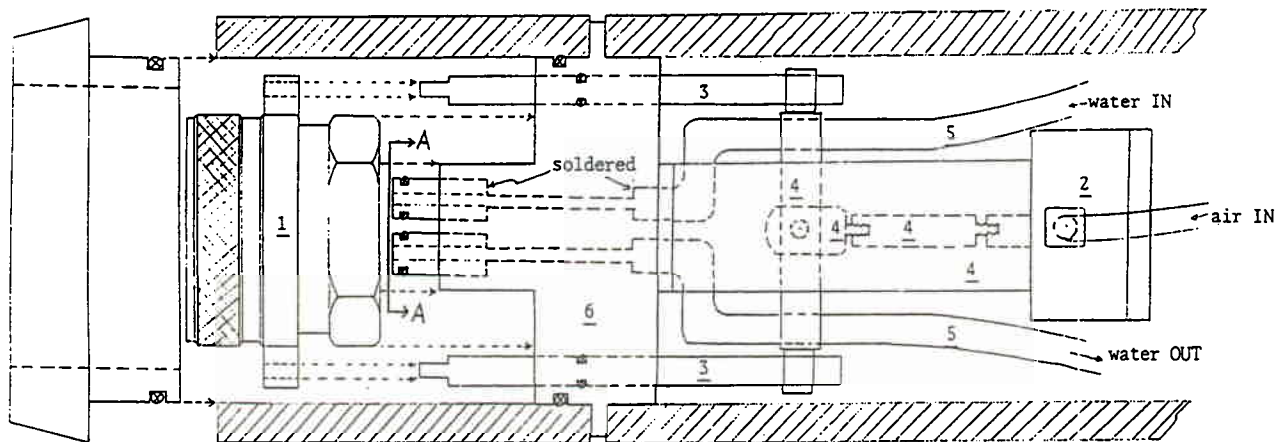


Top View

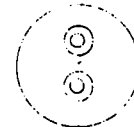
The schematic of the target housing component is shown in figure 2. Commercially available components were utilized in its fabrication. A Swagelok quick-connector (#B-QF16-B-1610) is the basis of connection of the target head with the housing. A pneumatic piston (Fabco Air Inc., Gainesville, FL.) is used to facilitate the remote release of the target head from the housing. All system operations are controlled from the target console via light pen. As with the chilled helium foil cooling recirculation unit, vacuum conditions are achieved through the o-ring compression by the target chamber housing with the automatic target chamber and the beam line vacuum pumping station. The vacuum isolation foil is completely removed.

TARGET HOUSING

SCALE: 1 : 1



- NOTE: 1. modified SWAGELOK #B-QF16-B-1610 quick-connect
 2. FABCO AIR #C70P pancaked pneumatic cylinder
 3. 1/4 " stainless steel rod
 4. cylinder linkage and support
 5. 1/4 " copper tubing
 6. machined brass piece



A-A view

RESULTS AND DISCUSSION

Until recently, the rate of production of cyclotron produced radionuclides has been generally limited by either beam current or thermal performance of the target materials. A third constraint is present at our laboratory. The desire to prepare specific radionuclides which are theoretically possible based upon the energy characteristics of the cyclotron. When allowance for energy losses of the irradiation particle is considered for both the foil cooling atmosphere and vacuum isolation foil windows, the desired nuclear reaction may no longer be possible. An example of this problem is our desire to prepare research

quantities of iodine-124 at MSKCC. The scarcity of enriched materials combined with their high costs as well as the required deuteron incident particle energy for the $^{124}\text{Te}(^2\text{H},2\text{n})^{124}\text{I}$ necessitated the evaluation of alternative nuclear reactions to prepare this radionuclide. A reevaluation of the $^{121}\text{Sb}(^4\text{He},\text{n})^{124}\text{I}$ nuclear reaction⁴ is being attempted. The threshold value for this nuclear reaction is 8.15 MeV, however the data indicates that irradiation of antimony with 15 MeV alpha particles could result in minimal but useful yields of this radionuclide.

Our preliminary studies with the solid target unit in the vacuum mode of operation with an electroplated natural copper target to prepare gallium-66 from the $^{63}\text{Cu}(^4\text{He},\text{n})^{66}\text{Ga}$ have shown that the incident energy upon the target is nominally 15 MeV and a target yield of nearly 200 uCi/uAhr for 1-2 hour irradiations. The results are in good agreement with published thick target yields⁵.

In summary, the fabricated solid/powder target unit was designed to fit the JSW automatic target changer and to allow irradiation of materials both with and without foil cooling. Its design allows for remote removal of the reusable target head and application of minimal target material to achieve thick target yields applicable to low energy cyclotrons. Consideration of intrinsic radionuclide activation was an important component in the target material choices.

ACKNOWLEDGEMENT

This work was supported in part by U.S. Department of Energy research grant #DE-FG02-86ER60407.

REFERENCES

1. Tilbury, R.S., Gelbard, A.S., McDonald, J.M., Benua, R.S. and Laughlin, J.S. A compact in-house multiparticle cyclotron for production of radionuclides and radiolabeled compounds for medical use. *IEEE Trans. Nucl. Sci.* NS-26:1729 (1979).
2. Lee, R., Dahl, J.R., Bigler, R.E. and Laughlin, J.S. A multiple target system for a medical cyclotron. *Med. Phys.* 8:703 (1981).
3. Firouzbakht, M.L., Schlyer, D.J., Finn, R.D., Laguzzi, G. and Wolf, A.P. Iodine-124 production: excitation function for the $^{124}\text{Te}(d,2\text{n})^{124}\text{I}$ and $^{124}\text{Te}(d,3\text{n})^{123}\text{I}$ reactions from 7 to 24 MeV. *Nucl. Instrum. and Methods*, B79:909 (1993).
4. Watson, I.A., Waters, S.L. and Silvester, D.J. Excitation functions for the reactions producing Iodine-121, Iodine-123 and Iodine-124 from irradiation of natural antimony with helium-3 and alpha particles with energy up to 30 MeV. *J. Inorg. Nucl. Chem.* 35:3047 (1973).
5. Dmitriev, P.P. Radionuclide yield in reactions with protons, deuterons, alpha particles and helium-3. *INDC(CCP)-263G+CN+SZ*, (1986).

Modeling of Target Thermal Properties for the BLIP Upgrade

L.F. Mausner, J.C. Hock^{*}, K.L. Kolsky, J.E. Tuozzolo^{*}
 Medical and AGS Departments^{*},
 Brookhaven National Laboratory
 Upton, New York 11973

INTRODUCTION

We anticipate imminent approval to upgrade the Brookhaven Linac Isotope Producer (BLIP). This is an interim measure to improve availability of some accelerator produced radionuclides during the period while LAMPF operations phase out until the construction of the ambitious National Biomedical Tracer Facility (NBTF). The goals of this two year effort are to (1) increase the average proton beam current by a factor of 2.3 to a maximum of 145 μA at 200 MeV, (2) increase operations to 46 weeks per year with 90% beam availability (1.5d/month maintenance $\sim 5\% + 5\%$ downtime), and (3) undertake production of several radionuclides presently only available from LAMPF (ie. ^{88}Y , ^{109}Cd , ^{22}Na). The higher beam current will improve production yields, specific activity, throughput and cost efficiency.

To reliably achieve this level of operation, modifications to the Linac are needed. The present limitations of the various Linac subsystems have been reviewed, and it is concluded that the best way to increase the average current is to make small improvements in several of the operating parameters, rather than trying to make a large increase in a single parameter. All changes are within the original machine design parameters.

The proposed parameter changes are shown in the following table:

TABLE I

	<u>Present</u>	<u>Modification</u>
Beam Current	25 mA	30 mA
Repetition Rate	5 Hz	7.5 Hz
Beam Width	450 μs	650 μs
RF Width	650 μs	850 μs
Average Current	56 μA	146 μA
Operating Weeks	20 wks.	46 wks.

These values can be achieved with improvements to the ion source, low energy beam transport system, RF coaxial transmission line, RF power supplies and BLIP beam transport section.

To handle the increased radioactivity levels and processing frequency, a portion of the Hot Laboratory will be renovated. This is to include 2 new hot cells, upgraded ventilation and liquid waste disposal systems, and renovations to several radiochemistry laboratories.

Similarly, at BLIP extra neutron and photon shielding is required to eliminate known weak spots. Because the deposited beam power will increase up to 29 kW, new target and cooling system design at BLIP will also be necessary. To begin this effort we have attempted to theoretically model the heat transfer properties of three typical BLIP targets, Zn powder for ^{67}Cu production, RbCl pellets for ^{82}Sr and molten Ga for ^{68}Ge .

THERMAL ANALYSIS

The heat deposited in the targets by the proton beam is removed by conduction and radiation of the target material to the cladding on the surfaces. From the cladding heat is then transferred by forced convection of the flowing coolant (water). Steady state heat transfer analyses of the BLIP targets are done with a finite element program called ANSYS¹. For this analysis ANSYS uses a two dimensional matrix for heat transfer in x and y directions. ANSYS applies conventional heat transfer theory: the first law of thermodynamics, Fourier' Law, and Newtons law of cooling. The first law of thermodynamics states that energy is conserved. Fourier's law states that the heat transfer rate by conduction is proportional to the temperature gradient times the area through which heat is transferred:

$$q = -k A dt/dx \quad (1)$$

where: q = heat rate transferred by conduction
 dt/dx = temperature gradient
 k = thermal conductivity
 A = area normal to heat flow

This equation is used to calculate the transfer of heat from the target center to its surface. Newton's law of cooling governs the rate of convective heat transfer between a fluid at one temperature in contact with a solid surface at a different temperature:

$$q = h A (T_s - T_f) \quad (2)$$

where: q = heat transfer rate
 h = heat transfer coefficient
 A = surface area in contact with fluid
 T_s = surface temperature
 T_f = the mean temperature of the fluid

The ANSYS user creates a solid model or geometry of the design with material properties, such as thermal conductivity, needed to perform the steady state heat transfer analysis subject to boundary conditions. The first boundary condition is heat generation per unit volume (Q) to simulate the heat generated by the proton beam. The second boundary condition is the forced convection heat transfer coefficient and the cooling fluid mean temperature, to simulate the cooling water flowing across the target surface.

ANSYS combines equations (1) and (2) to calculate the temperature difference between the target center T_o and the mean fluid temperature T_f . The output of ANSYS is a graph which shows the temperature gradient through the target. To simplify the model, only one quadrant of the target cross section was modeled as shown in Figure 1. The origin is located at the centroid of the target in which the y coordinate represents the thickness of the target and the x coordinate is the radial distance from the center.

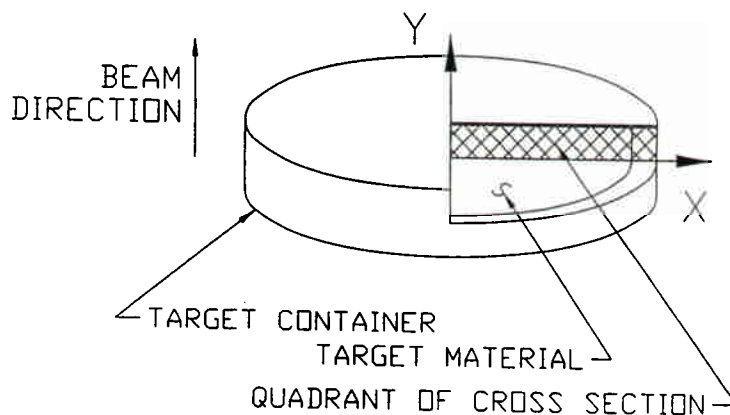


Figure 1. Schematic showing a single quadrant of the target cross section used in the thermal model.

The geometry of the cooling apparatus is shown in Figure 2. The following assumptions were made to calculate the forced convection heat transfer coefficient (h). Fully developed flow was assumed at the center of the cooling apparatus with the cross section of the cooling duct being rectangular. An empirically derived equation for h in a rectangular duct² is

$$hb/k = 0.98(59 + wC_p b/kxy)^{1/3}$$

where:

- h = forced convection heat transfer coefficient
- y = width of the duct
- b = height of the duct
- k = thermal conductivity of the fluid
- C_p = specific heat of the fluid
- w = flow rate

The methodology used to calculate the thermal conductivity (k) for the various targets differed due to the physical form of the target material. This data is input to ANSYS as a function of temperature. Experimental thermal conductivity data for liquid gallium can be found in reference 3. The conductivity for the rubidium

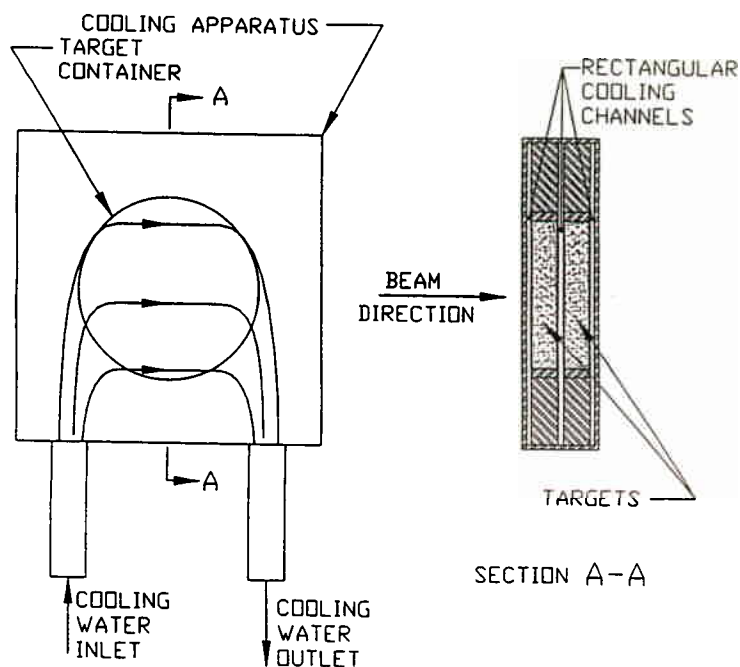


Figure 2. Geometry of the cooling apparatus.

chloride and zinc targets are theoretical values calculated with the method of Klemens⁴. This approach combines conduction through point contact of the particles making up the powder and heat transfer from radiation between the surfaces of the particles. A graph of thermal conductivity as a function of temperature for Ga, Zn, and RbCl is shown in Figure 3.

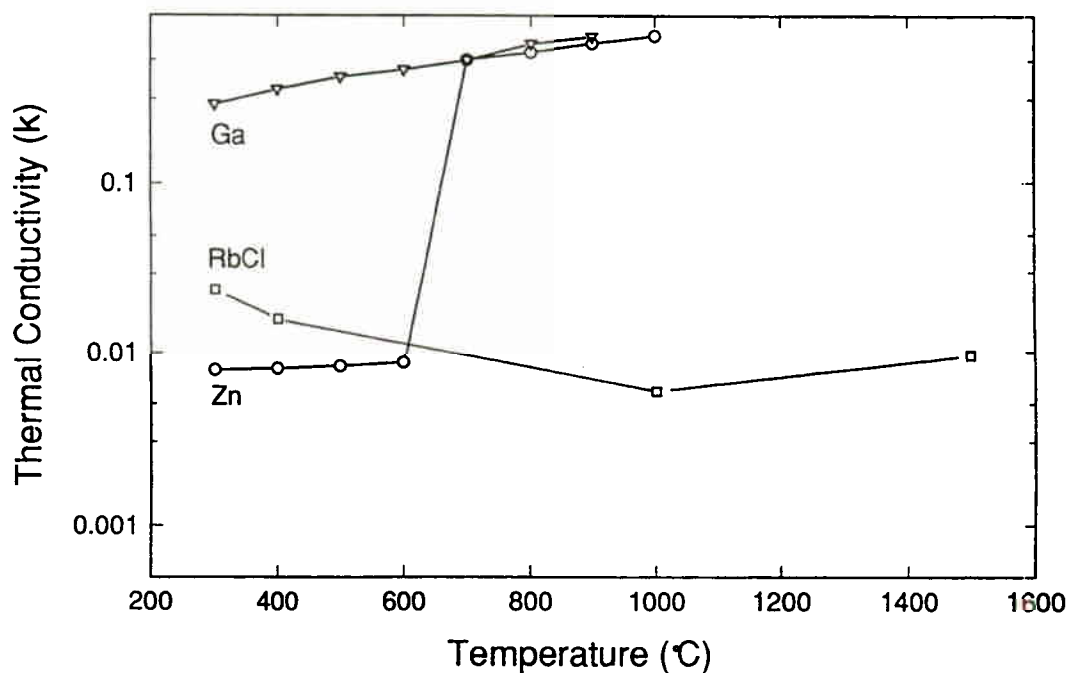
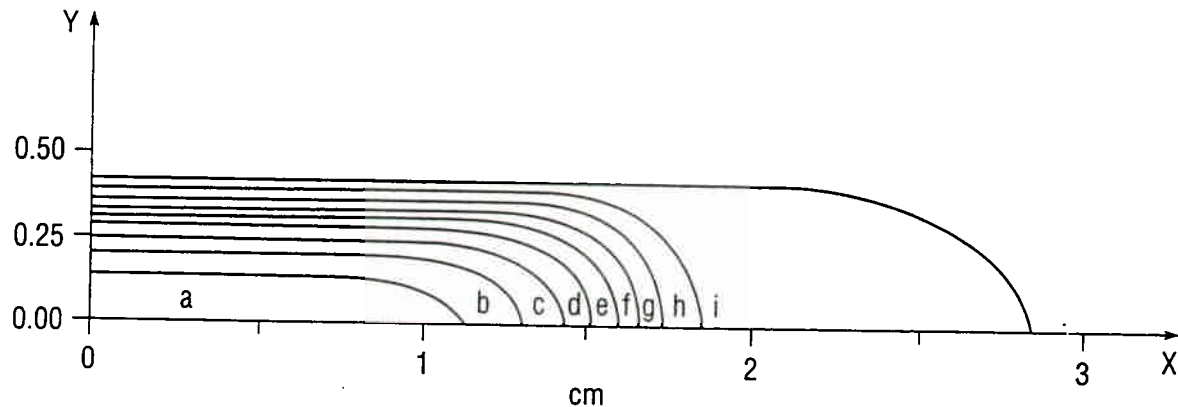


Figure 3. Plot of the thermal conductivity as a function of temperature for Ga, Zn and RbCl.

RESULTS AND CONCLUSIONS

A sample of the thermal distributions that ANSYS calculates is shown in Figure 4 for RbCl at the beam current anticipated for the BLIP upgrade. A quadrant of the target (see Figure 1) is divided into nine temperature zones. As expected, the highest temperature is reached at the target center. There is a large difference between the surface and central temperature in this case. This is a reflection of

RbCl Target, beam current 115 μ amp, beam spot 3.0 cm (FWHM)



Temperature Zones ($^{\circ}$ C)

(i) 27 - 388	(f) 1112 - 1474	(c) 2198 - 2560
(h) 388 - 751	(e) 1474 - 1836	(b) 2560 - 2921
(g) 751 - 1112	(d) 1836 - 2198	(a) 2921 - 3283

Fig. 4

the relatively poor thermal conductivity of RbCl. Table II summarizes the target data, including dimensions for Ga, Zn and RbCl targets, along with the beam spot size, melting and boiling points. Central target temperatures are given for the present conditions, as well as the anticipated intensities of the BLIP upgrade.

TABLE II: TARGET DATA

TARGET	Ga		Zn		RbCl	
FORM	MOLTEN		LOOSE POWDER		PRESSED POWDER	
DIMENSIONS (cm)	5 DIA X 0.84 THICK		5.7 DIA X 0.79 THICK		4.4 DIA X 0.81 THICK	
THERMAL CONDUCTIVITY	Experimental ¹		CALCULATED ^{1,2}		CALCULATED ^{2,4}	
MELTING POINT ($^{\circ}$ C)	30		420		715	
BOILING POINT ($^{\circ}$ C)	2403		907		1390	
BEAM SPOT FWHM	3.5cm		1.9cm		3.0cm	
BEAM CURRENT (μ AMP)	30	100	45	145	35	115
MAX TEMPERATURE ($^{\circ}$ C)	90	230	553	990	700	32

This thermal modeling approach gives qualitative agreement with empirical observation for existing conditions. It can be seen that the central temperature for the Ga target is quite modest due to its good thermal conductivity. However, ANSYS predicts that melting will take place in the center of the Zn target, as observed. At the anticipated beam intensities of the BLIP upgrade, ANSYS calculates very high central temperatures for the Zn and RbCl targets. As listed in Table 1, the maximum temperatures in these cases are higher than the boiling points. A redesign of the targets and cooling system is thus necessary.

Some of the proposed changes are to use a scanned beam spot to reduce power density. Also, higher melting ZnO (mp = 1975°C) will replace Zn metal powder. For RbCl we will attempt to use internal conductive fins to improve heat transfer from the target center. If necessary, we will switch to a molten Rb metal target. ANSYS simulations will be used to test target design ideas. To improve accuracy of the calculations, experimental thermal conductivity data may be obtained. We may also attempt to actually measure beam intensity profiles (and thus the power density) as a function of location in the target array.

REFERENCES

1. ANSYS is a registered trademark of Swanson Analysis Systems Inc.
2. Society of Automotive Engineers, SAE Aerospace Applied Thermodynamics, p.85 equation #:1c-105.
3. Powel RW, Ho CY, Liley PE, Thermal Conductivity of Selected Materials, National Bureau Of Standards.
4. Klemens PG. (1983) Theory of Heat Conduction in Evacuated Metal Powders, Conference: Thermal Conductivity 17, Gaithersburg, Md., June 1983.
5. Kodintseva AO. (1990) Thermal Conductivity of Alkali Metals, Izvestiya Sibirskogo Otdeleniya Akademii Nauk Seriya Tekhnicheskikh Nauk, no. 5, p.7-10.
6. Pettersson S., (1988) Thermal Conductivity of Alkali Salts, Journal of Physics C21 #9.

Target Design Considerations for High Specific Activity [^{11}C]O₂

Richard A. Ferrieri*, David L. Alexoff, David J. Schlyer,
Keith McDonald and Alfred P. Wolf

Brookhaven National Laboratory, Department of Chemistry
Upton, New York, U.S.A. 11973

INTRODUCTION

The importance of receptor imaging has stressed the need for pharmacologically active compounds that are labeled with high specific activity carbon-11. [^{11}C]H₃I is the most versatile, and by far the most widely used precursor for labelling such compounds with carbon-11 through [^{11}C]-methylation (Langstrom, *et al.*, 1976; Burns, *et al.*, 1984; Suzuki, *et al.*, 1985; Farde, *et al.*, 1986; Watkins, *et al.*, 1988; Hatano, *et al.*, 1989; Pascali, *et al.*, 1990; Dewey, *et al.*, 1990; Iwata, *et al.*, 1991). With careful handling of reagents for the reduction of [^{11}C]O₂ to [^{11}C]H₃OH, and for the subsequent iodination of [^{11}C]H₃OH to [^{11}C]H₃I, we have found as little as 3 nmol of carrier carbon introduced at this stage of synthesis with the exclusion of the [^{11}C]O₂ target system contributions. However, in the routine preparation of compounds through N-[^{11}C]-methylation using [^{11}C]H₃I, total masses are always higher than the synthesis mass contribution. This suggests that the [^{11}C]O₂ target system contributes carrier carbon to the final product mass. This conclusion prompted our recent evaluation of target materials and target design for [^{11}C]O₂ production.

STUDIES IN TARGET MEASUREMENT OF CO₂ MASS

DESCRIPTION OF ANALYTICAL SYSTEM: As shown in Figure 1, the flame ionization detector (FID) from a Hewlett Packard 5890A Gas Chromatograph was modified for carbon oxide analysis by incorporating a miniature nickel catalyst methanizer into its jet and operating the detector at 400°C (Goekeler, 1989). The catalyst reduces CO and CO₂ to CH₄ (a detectable species by FID) prior to their entering the flame region of the detector. The catalyst operates efficiently using the same H₂ supply as that needed to sustain the flame, and exhibits remarkable stability in its day-to-day usage when maintained under a continuous helium stream at about 200°C. The detector also exhibits a linear response to CO₂ with over three orders of magnitude change in concentration thus simplifying instrument calibration, and is capable of handling large sample throughput which is convenient for operation with a packed chromatography column.

The modified FID can detect 10 ppb of CO₂ within a 4 mL volume sample of target gas at STP. This level of sensitivity is about 10³ times higher than that seen with thermal conductivity detectors (TCD). Therefore, no preconcentration of samples is required, and a single 500 mL volume bulb of collected gas offers adequate sample for numerous measurements to be made. Typical methods of analysis using TCD required cryotrapping of CO₂ from large volumes of gas.

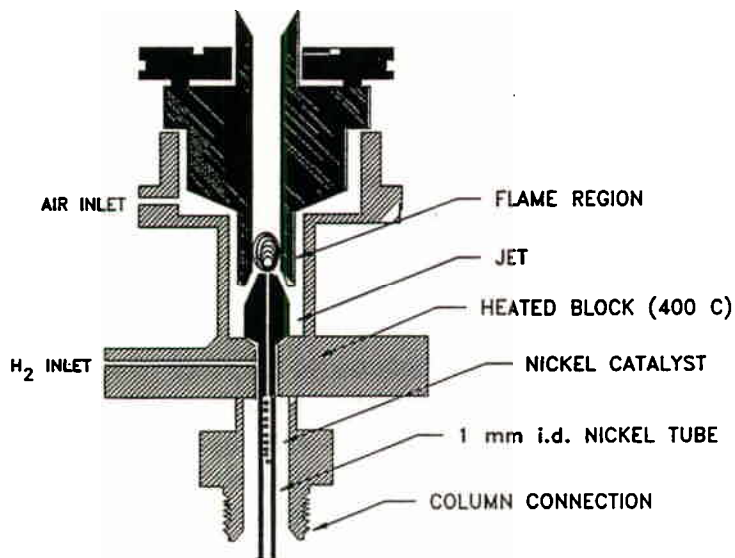


Figure 1 Modified flame ionization detector from a Hewlett Packard 5890A gas chromatograph used for carbon oxide analysis.

In the system shown in Figure 2, we used a 12 ft x 1/8 in. Porapak Q column with a 3:1 splitter at the column outlet to allow for on-line radioactivity measurements using a NaI scintillation detector. The system also has a small vacuum manifold which allows us to remove air once the sampling bulb is connected to the instrument. A 2-way switching valve allows us to sequentially fill and inject gas samples of known volume and pressure.

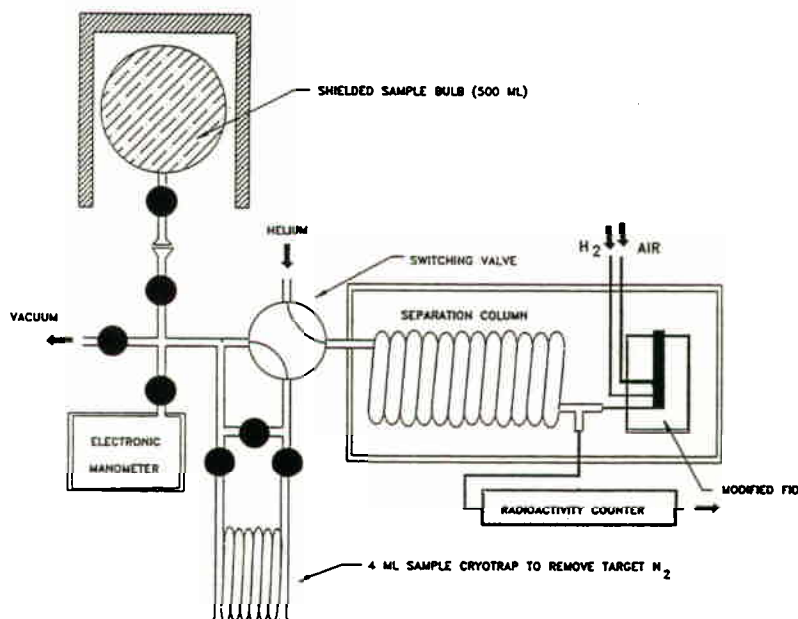


Figure 2 Gas sampling port and gas chromatograph for carbon oxide analysis.

RESULTS AND DISCUSSION: The analytical system previously described was used to measure CO_2 and total carbon concentrations within the UHP N_2 (99.999% purity, Matheson Gas Co.) used for producing $^{11}\text{C}\text{O}_2$. CO_2 concentrations as low as 2 pmol/cm^3 or 0.05 ppm were found. Total carbon concentrations were determined as CO_2 after combustion over CuO at 850°C , and were found to be 24 pmol/cm^3 or about 0.6 ppm. Our standard $^{11}\text{C}\text{O}_2$ production target is constructed of an aluminum alloy (approximately 97% purity), and has a volume of 212 cm^3 (3 cm i.d. x 30 cm length). The 16.5 mil thick front target window is also made from the same alloy. When pressurized to 10 atmospheres, the gas contribution amounts to 50 nmol of carrier carbon, assuming all carbon is combusted to CO_2 under irradiation conditions. However, levels of CO_2 arising from this target were much higher than this subsequent to irradiation from 17 MeV H^+ (13.4 MeV on gas) of varied intensity. In addition, the amount of CO_2 released was dose-rate dependent suggesting a material source of carrier carbon. Replacement of all organic seals (ie. front window o-ring and gas fittings) with indium gaskets failed to show an improvement in target performance suggesting that the aluminum itself was the source.

SURFACE ANALYSIS STUDIES USING ELECTRON INDUCED DESORPTION (EID) SPECTROSCOPY

DESCRIPTION OF ANALYTICAL SYSTEM: Electron probes are a commonly used analytical tool in material and surface analysis (Czanderna, 1975) because of their ease of generation at controlled energy and density. Electron probing of a surface can result in the emission of four types of particles (electrons, photons, ions and neutrals). Information derived from the nature and states of one or more of these species can then be related back to the composition and morphology of the surface.

Electrons can undergo inelastic collisions with atoms or molecules on a surface raising them to various excited and/or ionized states thus causing desorption. Since the mass ratio of electrons to atoms is very small, kinetic energy exchanges are minimal. Electronic transitions, however, have a fairly high cross-section at modest electron energies (less than 100 eV), and therefore can be utilized to desorb the outermost monolayer of material adsorbed on a surface. Of course, kinetic energy exchange can become important with the impact of higher energy electrons thus allowing one to probe fairly deep into the bulk of the material.

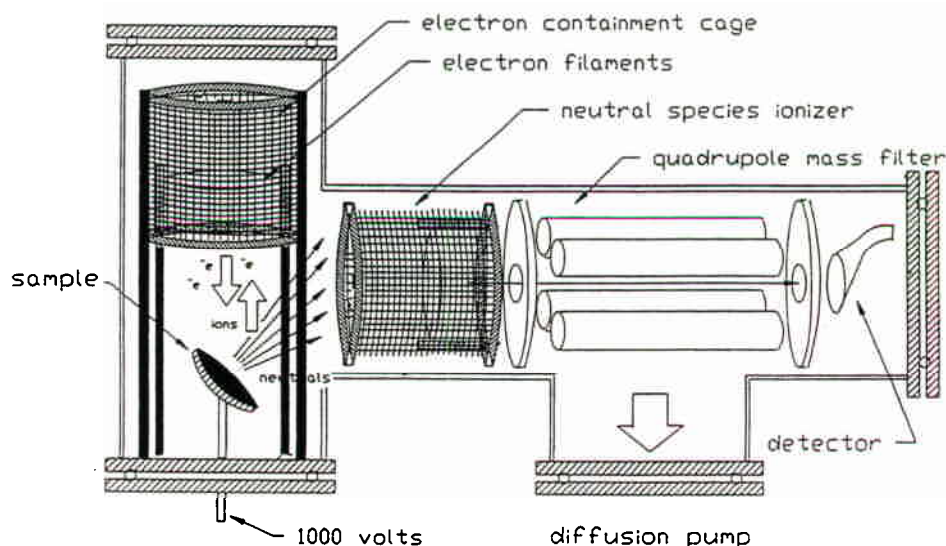


Figure 3 Electron induced desorption instrument used for surface analysis.

The EID instrument, shown in Figure 3, is designed for high-energy electron impact to probe both surface morphology, and bulk material composition in target aluminum alloys. The system is comprised of a high vacuum chamber possessing an easy access port for sample introduction, a high energy electron source and electron containment cage, and a quadrupole mass spectrometer with electron induced ionization and electron multiplier detector. Only emitted neutral species are monitored by the mass spectrometry, because surface emitted positive ions are accelerated out of the detection path of the spectrometer, and trapped by the electron containment cage.

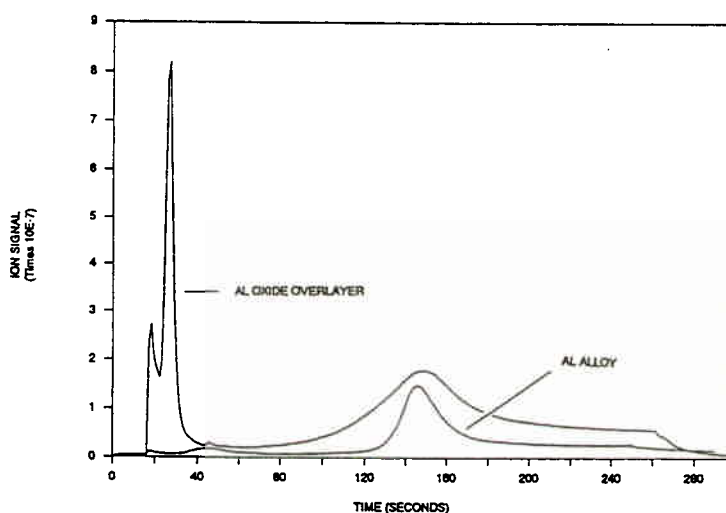


Figure 4 Electron induced desorption spectrum (at 1000 volt electron acceleration) of CO₂ (m/z 44) from a clean 6061 aluminum alloy surface, and from a treated 6061 alloy surface that possessed a 10⁴ monolayer thick coating of oxide, and was exposed to 10 ppm levels of CO₂ in N₂ gas.

RESULTS AND DISCUSSION: As seen in Figure 4, two bulk-bound states of carbonaceous material are observed in the aluminum alloy (6061) used as target material. These states were detected in our instrument as CO (m/z 28) and CO₂ (m/z 44), although only the CO₂ spectrum is shown here, from peaks appearing at 50 and 150 seconds into the EID scan. Upon deposition onto the surface of an oxide coating of approximately 10⁴ monolayers thick, and upon exposure of that modified surface to 1 atmosphere of N₂ gas containing 10 ppm levels of CO₂, we observed a drastic change in the EID spectrum. Two new peaks are introduced by this treatment, appearing at 20 and 30 seconds into the scan. The short appearance times of these peaks lead us to suspect that they represent loosely bound surface carbon.

Results from our EID studies suggest that aluminum purity is perhaps not as important a criteria in target design for high specific activity [¹¹C]O₂, as the amount of material exposed to the beam, and/or the gas plasma during irradiation, since all aluminum surfaces will oxidize to some degree with time and exposure. This build-up in oxide will create a spongy overlayer on the surface which can act as an efficient sink for removal of carbonaceous material from the target gas. Of course, this process will be amplified if the target is frequently opened to air. Accumulated carbon can then

released back into the target gas during proton bombardment, by one or more mechanisms not yet understood. The levels of release should be contingent upon the irradiation conditions, and the degree of carbon saturation of the oxide.

STUDIES CORRELATING TARGET SURFACE AREA WITH TARGET MASS

EXPERIMENTAL PROCEDURE: We investigated the correlation between exposed surface and carrier mass generation by inserting aluminum alloy plugs of various lengths into a 212 cm³ volume cylindrical target. Beam penetration in the unmodified target was calculated to be 27 cm assuming 30% gas density reduction (for a 25 μ A beam) on 10 atmospheres of gas.

Targets were stringently cleaned prior to these studies by repetitively exposing their inner surfaces to gas mixtures of 5% O₂ in neon (10 atm.) during proton irradiations. Cumulative doses of 25 μ A-hr were sufficient to reduce surface bound carbon to low steady-state levels. However, surface bound carbon increased upon re-exposure to target N₂.

RESULTS AND DISCUSSION: Table 1 lists target volumes, exposed surface areas, and measured carrier CO₂ levels from three experiments. In each experiment, 25 μ A of beam was placed on target for 15 minutes. The same 16.5 mil thick aluminum window was used in each instance yielding 13.4 MeV of proton energy on gas. The carrier CO₂ measurement was categorized according to the target gas contribution and other sources. The gas contribution was calculated from target pressure and volume data, and our previous measurements of total carbon content within the target gas. We assumed that all carbonaceous material within the gas was combusted to CO₂ under these circumstances.

TABLE 1

CORRELATION OF TARGET SURFACE AREA WITH CARRIER CO₂ OUTPUT

Target Volume (cm ³)	Surface Area (cm ²)	Carrier CO ₂ Output (nmol)	
		<u>Gas Contribution</u>	<u>Other Sources</u>
212	255	24	38
94	127	12	20
68	102	8	15

Results from these studies suggest that a correlation exists between target surface exposed to beam and carrier contributions arising from sources other than the target gas. Based on our earlier observations made by EID spectroscopy, we must assume that these other sources arise from the release of surface bound carbon from the oxide overlayer when irradiated.

STUDIES ON THE EFFECT OF WINDOW DEFORMATION ON THE SCATTERING AND ENERGY PROFILES OF THE BEAM: POTENTIAL EFFECTS CONTRIBUTING TO TARGET MASS

INTRODUCTION: Recently, we installed a preformed 18.5 mil thick aluminum window, possessing a 5 mm hemispherical deformation, onto our 77 mL volume conical target, but with the deformation placed concave into the target. We did this because pressure and beam induced deformation of our flat aluminum windows would cause them to bow outward beyond the helium cooling axis, which eventually resulted in window failure. We thought that placing a preformed window in a concave geometry would provide additional radial strength to minimize further deformation, and also optimum window cooling thus increasing window lifetime.

The windows were fabricated from 6061 aluminum alloy. The alloy exists in a T_6 state of hardness (the highest level), but can be converted to a T_0 workable state through heating of the alloy for several hours at 500°C. Once in this state, the windows can be deformed over a mandrel with little or no stress added to the surface structure. The alloy automatically reverts back to its original state of hardness over a 48 hour period.

In-direct observations made on [^{11}C]cocaine specific activity suggested that target mass contributions were somewhat reduced with the window placed in a concave configuration. We have yet to verify this directly through CO_2 target mass measurements. Even so, this peaked our interest in what effect window geometry might have on the scattering and energy profiles of the proton beam. These aspects could have significant effects on target surface contributions to mass.

EXPERIMENTAL PROCEDURE: In the beam scattering profile study, we used an optical target fabricated from quartz in the same shape and size as our conical production target. The preformed aluminum windows were sealed onto the front-end of the optical target both in the concave and convex configuration. In both instances, the target was filled to 1 atmosphere with neon gas, and irradiated with a 18 MeV proton beam focussed to a 10 mm spot size. Data was acquired with color video camera interfaced with a digital frame grabber board on a PC computer. This allowed us to collect and overlay beam scattering profiles for the two window geometries.

In the beam energy profile studies, nickel foils (5 cm o.d. x 1 mil thick) were mounted in a test chamber 10 cm behind the beam entry window. This distance was identical to our conical target length. The chamber was filled with 1 atmosphere of helium gas, so gas induced alteration of the beam energy profile could be ignored. The front preformed window was mounted both concave and convex to the nickel foils, and short irradiations were carried out using the same conditions described above. After bombardment, the foils were removed, and cut into 3 mm wide rings for analysis by gamma spectroscopy. Each ring was assessed for relative distributions of ^{55}Co and ^{57}Co activities which were formed from the $^{58}\text{Ni}(p,\alpha)^{55}\text{Co}$ and $^{60}\text{Ni}(p,\alpha)^{57}\text{Co}$ reactions, respectively. Corrections were made to the data for relative abundances of the nickel isotopes, and for detection efficiency of the gamma energies (931 KeV and 122 Kev, respectively) used to measure the cobalt abundances.

Since the proton reactions on nickel exhibit significantly different dependences on energy below 13.5 MeV, this method provides an excellent diagnostic tool for looking at beam energy profile (Kaufman, 1960). Figure 5 illustrates this feature in a correlation of proton energy with the isotope cross section ratio.

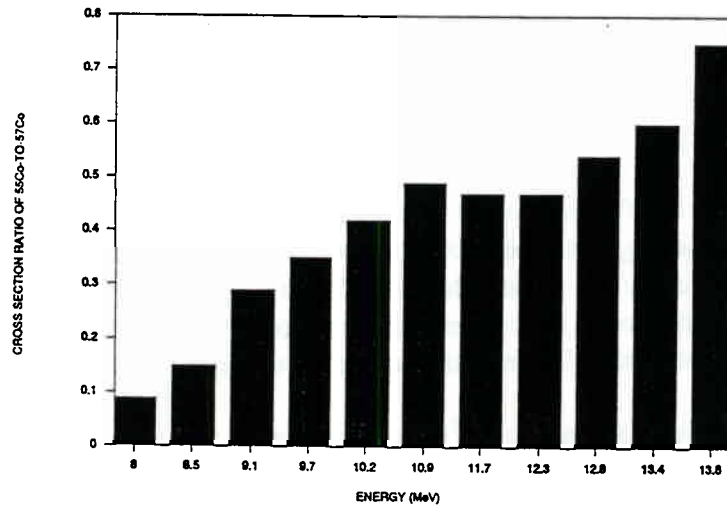


Figure 5 Energy correlation diagram of $^{58}\text{Ni}(p,\alpha)^{55}\text{Co}$ and $^{60}\text{Ni}(p,\alpha)^{57}\text{Co}$ cross section ratios.

RESULTS AND DISCUSSION: Results from the beam scattering studies in the optical target showed no significant differences in beam profile for the two window geometries.

Figures 6 and 7 illustrate the variation of the beam energy, depicted by the ^{55}Co -to- ^{57}Co ratio, as a function of the radial distance from the center axis of the beam, for target windows mounted concave and convex to the target, respectively. The striking feature here is that the beam energy profile is significantly affected by window geometry. We observed much higher beam energies incident on the outer fringes of the nickel foil, when the front target window was mounted concave to the target, than when the window was mounted convex.

One might rationalize that with a higher energy beam incident on the target surface, the Bragg peak would occur deeper within the material and thus have less of an effect on surface release of carbonaceous material entrained within the outer oxide layer. This aspect certainly bears further investigation.

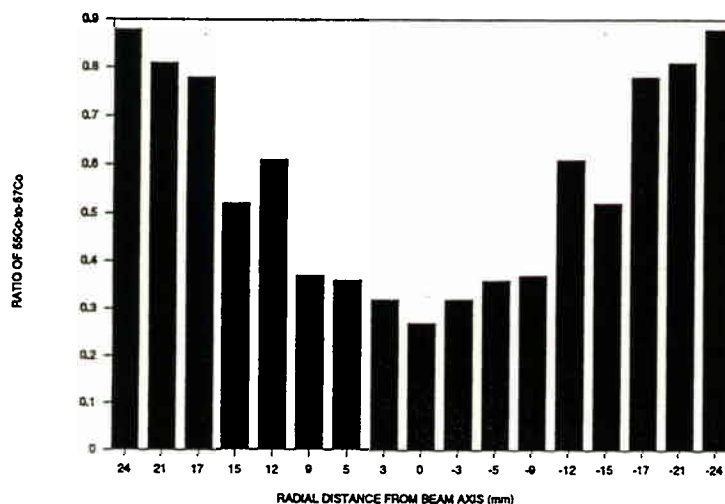


Figure 6 Variation in the proton beam energy, depicted by the ^{55}Co -to- ^{57}Co ratio, as a function of the radial distance from the center axis of the beam, for a concave mounted target window.

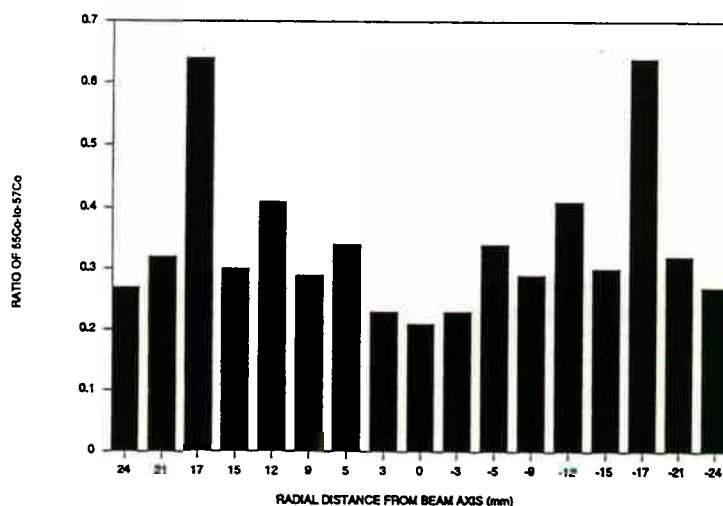


Figure 7 Variation in the proton beam energy, depicted by the ^{55}Co -to- ^{57}Co ratio, as a function of the radial distance from the center axis of the beam, for a convex mounted target window.

SUMMARY

Clearly, the above studies demonstrate that the $[^{11}\text{C}]\text{O}_2$ specific activity will benefit enormously from targets whose size and shape will minimize surface exposure to beam. It goes without saying that smaller volume targets will also minimize gas contributions to mass. In addition, attention to window geometry may have beneficial affects on target surface contributions to mass. Of course, one can only capitalize on this feature if sufficient beam energy is available to expend on a thick window.

Unfortunately, there are practical considerations when trying to achieve high

specific activity [$^{11}\text{C}]\text{O}_2$. We have observed (see Figure 8) that as the amount of carrier mass generated within the target is minimized, the extraction efficiency of carbon-11 activity as [$^{11}\text{C}]\text{O}_2$ decreases from theoretical expectations.

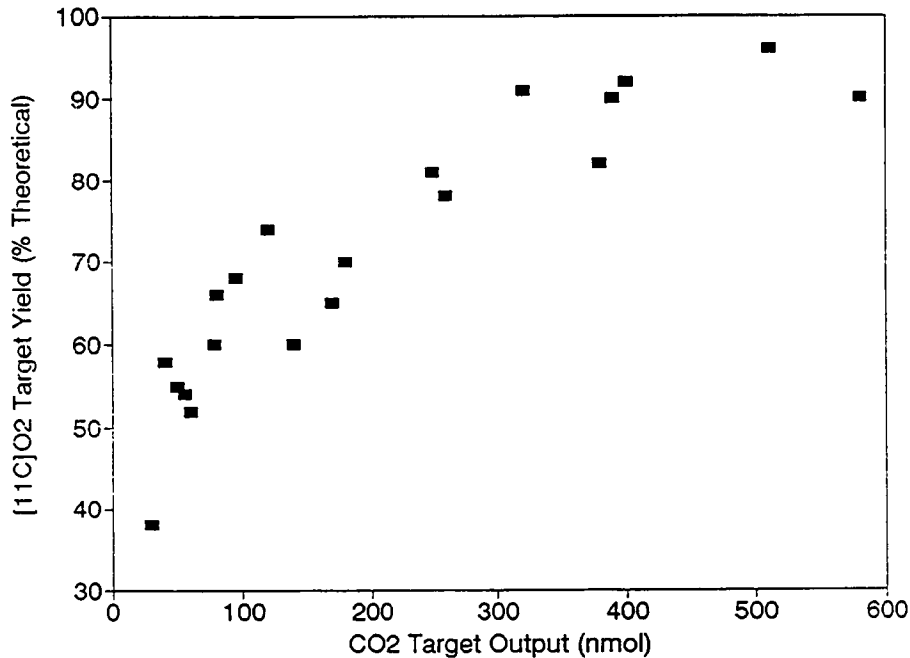


Figure 8. Correlation between target output of carrier CO_2 and the extracted target yield of [$^{11}\text{C}]\text{O}_2$.

This phenomenon appears to occur independent of the nature of the material used to fabricate the target (we have compared identical volume cylindrical targets fabricated from aluminum and nickel), and independent of the size and shape of the target (we have compared cylindrical targets of various volumes with our standard 77 mL conical target). For a lack of a better term, we refer to this phenomenon as a carrier effect. Ultimately, one is faced with the prospect of compromising between [$^{11}\text{C}]\text{O}_2$ specific activity, and the amount of [$^{11}\text{C}]\text{O}_2$ that can be extracted from the target after a reasonable irradiation time.

ACKNOWLEDGEMENT

This research was carried out at Brookhaven National Laboratory under contract DE-ACO2-76CH00016 with the U. S. Department of Energy and supported by its Office of Health and Environmental Research. Research was also supported by the National Institutes of Health under Grant NS-15380.

REFERENCES

- Burns H.D., Dannals R.F., Langstrom B., Ravert H.T., Zemnyan S.E. Duelfer T., Wong D.F., Frost J.J., Kuhar M.J. and Wagner H.N. (1984) (3-N-[^{11}C]methyl)spiperone, a ligand binding to dopamine receptors: Radiochemical synthesis and biodistribution studies in mice. *J. Nucl. Med.* **25**, 1222.
- Czanderna A.W. (ed.) (1975) *Methods of Surface Analysis*, Elsevier Scientific Publishing, New York.
- Dewey S.L., MacGregor R.R., Brodie J.D., Bendriem B., King P.T., Volkow N.D., Schlyer D.J., Fowler J.S., Wolf A.P. Gatley J. and Hitzemann R. (1990) Mapping muscarinii receptor in human and baboon brain using [N- ^{11}C -methyl]- benzotropine. *Synapse* **5**, 213.
- Farde L., Hall H., Ehrin E. and Sedvall G. (1986) Quantitative analysis of D2 dopamine receptor binding in the living human brain by PET. *Science* **231**, 258.
- Goekeler U.K. (1989) Determination of oxygenated hydrocarbons in fuel with oxygen selective detector. *Am. Lab.*, June, 34.
- Hatano K., Ishiwata K., Kawashima K., Hatazawa J., Itoh M. and Ido T. (1989) D2-dopamine receptor specific brain uptake of carbon-11-labeled YM-09151-2. *J. Nucl. Med.* **30**, 515.
- Iwata R., Hatano K., Yanai K. Takahashi T., Ishiwata K. and Ido T. (1991) A semi-automated synthesis system for routine preparation of [^{11}C]YM-09151-2 and [^{11}C]pyrilamine from [^{11}C]methyl iodide. *Appl. Radiat. Isot.* **42**, 202.
- Kaufman S. Reactions of protons with ^{58}Ni and ^{60}Ni (1960) *Phys. Rev.* **117**, 1532.
- Langstrom B. and Lundqvist H. (1976) The preparation of carbon-11 labeled methyl iodide and its use in the synthesis of carbon-11 labeled methyl-L-methionine. *Int. J. Appl. Radiat. Isot.* **27(7)**, 357.
- Pascali C., Pike V.W. and Turton D.R. (1990) The radiosynthesis of NCA [O-methyl- ^{11}C]viqualine through an N-trityl-protected intermediate, as a potential PET radioligand for 5HT re-uptake sites. *J. Label. Compd. Radiopharm.* **28**, 1341.
- Suzuki K., Inoue O., Hashimoto K., Yamasaki T., Kikuchi M. and Tamate K. (1985) Computer-controlled large scale production of high specific activity [^{11}C]RO 15-1788 for PET studies of benzodiazepine receptors *Int. J. Appl. Radiat. Isot.* **36**, 971.
- Watkins G.L., Jewett D.M., Mulholland K., Kilbourne M.R. and Toorongian S.A. (1988) a captive solvent method for rapid N-[^{11}C]methylation of secondary amines: Application to the benzodiazepine, 4'-chlorodiazepam(RO5-4864). *Appl. Radiat. Isot.* **39**, 441.

